In presenting this dissertation as a partial fulfillment of the requirements for an advanced degree from Emory University, I agree that the Library of the University shall make it available for inspection and circulation in accordance with its regulations governing materials of this type. I agree that permission to copy from, or to publish, this dissertation may be granted by the professor under whose direction it was written, or in his absence, by the Dean of the Graduate School when such copying or publication is solely for scholarly purposes and does not involve financial gain. It is understood, that any copying from, or publication of, this dissertation which involves potential financial gain will not be allowed without written permission.

_____
Uliana Danilenko

Analysis of Cocaine Binding Site of Human Dopamine Transporter Using Affinity Labeling and Mass Spectrometry

By

Uliana Danilenko

Advisor: Dr. Joseph B. Justice, Jr.
Department of Chemistry

Approved for the Department by:

_____
Advisor

_____
Dr. Dale Edmondson
Committee Member

_____
Dr. Stefan Lutz
Committee Member

_____
Date
Accepted

_____
Dean of the Graduate School

_____
Date

Analysis of Cocaine Binding Site of

Human Dopamine Transporter Using Affinity

Labeling and Mass Spectrometry

By

Uliana Danilenko
M.S., St. Petersburg State Chemical Pharmaceutical Academy, 2003

Advisor
Joseph B. Justice, Jr., Ph.D.

An Abstract of a Dissertation Submitted to
the Faculty of the Graduate School
of Emory University in Partial Fulfillment
of the Requirements for the Degree of
Doctor of Philosophy

Department of Chemistry
2008

Abstract

The small peptide PLFYM located in transmembrane domain two (TM2) of the human dopamine transporter (hDAT) is suggested to be the labeling site for the irreversible hDAT inhibitor [^{125}I] MFZ 2-24. To locate the [^{125}I] MFZ 2-24 labeling site, hDAT was photolabeled with [^{125}I] MFZ 2-24 and digested with CNBr. The HPLC analysis of the digest showed that one small peptide was labeled. Parnas et al. (2003) demonstrated that [^{125}I] MFZ 2-24 incorporates in transmembrane domains 1 and 2 of hDAT. The possible peptides from the CNBr digest include only two small hDAT peptides from the TM1-2 region, PLFYM and VIAGM, both in TM 2. The secondary enzymatic digests of the small labeled peptide from the CNBr digest of hDAT provided additional information supporting PLFYM being the labeled peptide (Wirtz, 2004).

To further locate the [^{125}I] MFZ 2-24 labeling site, hDAT was photolabeled with [^{125}I] MFZ 2-24 and digested with thermolysin. The digest was separated on HPLC and the fraction corresponding to the labeled peptide collected. Edman degradation of the labeled peptide from the thermolysin digest of hDAT suggested that the second amino acid from the N-terminal was labeled, based on release of radioactivity. Additionally, labeled peptide from a separate thermolysin digest was re-digested with CNBr. The labeled peptide was analyzed by HPLC before and after the CNBr digest. The retention time of the [^{125}I] MFZ 2-24 labeled peptide shifted, indicating that the peptide has a methionine in the sequence. The results from the CNBr and thermolysin digests in relation to the leucine transporter crystal structure (Yamashita et al., 2005) suggest that PLFYM is the labeled region, and F114 or Y115 are the labeled amino acid residues.

The hDAT mass spectrometry coverage and detection limit were examined using a ThermoFinnigan LTQ-FT high resolution mass spectrometer. The peptides from a thermolysin digest were separated on a nanoLC connected to a nanoelectrospray source. Mass spectrometry detection of hDAT peptides from the thermolysin digest resulted in 37 % coverage. The detected hDAT peptides were from the N-,C-terminal regions and the loop regions. A smaller number of peptides were also located in the transmembrane domain regions. This result supports mass spectrometry studies of membrane proteins that indicate the difficulties in detecting peptides from the transmembrane regions of membrane proteins (Wu et al., 2007; Yates et al., 2003). The detection limits for MFZ 2-24 and for the synthetic hDAT peptide FYMELAL were found to be 5 fmol and 10 fmol respectively. Thus the 11.4 fmol of [^{125}I] MFZ 2-24 labeled hDAT peptide left after in-gel digestion and extraction steps of 100 plates of HEK cells is near the detection limit of the instrument.

Analysis of Cocaine Binding Site of

Human Dopamine Transporter Using Affinity

Labeling and Mass Spectrometry

By

Uliana Danilenko
M.S., St. Petersburg State Chemical Pharmaceutical Academy, 2003

Advisor
Joseph B. Justice, Jr., Ph.D.

A Dissertation Submitted to
the Faculty of the Graduate School
of Emory University in Partial Fulfillment
of the Requirements for the Degree of
Doctor of Philosophy

Department of Chemistry
2008

Acknowledgments

I would like to thank my advisor Dr. Joseph Justice Jr. for his support and mentorship for the past five years. He taught me how to be a better scientist and develop critical thinking. He always had advice while at the same time encouraging independent thinking. After working in Dr. Justice's lab for the past five years I feel well prepared for any scientific challenges.

My committee members Dr. Stefan Lutz and Dr. Dale Edmondson always gave me great suggestions during my annual report meetings and encouraged me to look at my research from different prospectives.

I would also like to thank fellow lab members Dr. Sara Wirtz, Dr. Tamara Henderson, Dr. Anh Pham, and Muhsinah Morris for teaching me many techniques and always being there for me in the lab. I was very lucky to have such great colleagues.

I was blessed with many amazing friends at Emory who helped me during the graduate school: Jennifer Sorrells, Ana Alcaraz, Erika Milczek, Cara Mosley, Matt and Rebecca Geballe, Carolyn Leverett and Holly Carpenter.

Most importantly, I would like to thank my family for their support and unconditional love. Thanks to my Mom I always knew that I wanted to be a scientist like her. She is my example of how to be an outstanding scientist and great mother. I want to thank my aunt Galina for supporting me and always cheering me up. I thank my husband Sergei for his patience, understanding and always being there for me.

Table of Contents

List of Figures

Chapter Four: **Discussion**

List of Tables

Chapter One

Introduction

The Problem of Cocaine Abuse

Cocaine addiction is an important health and social problem because cocaine is one of the most abused substances in the USA. According to the National Survey on Drug Use and Health (NSDUH), 34.2 million people in the USA reported lifetime use of cocaine, with 5.6 million annual cocaine users (NIH, 2006). NSDUH also reported that 12.8% of all substance abuse medical admission cases involve cocaine (NSDUH, 2005).

Cocaine is a tropane alkaloid first purified from leaves of the coca plant *Erythroxylum coca* by Dr. Friedrich Gaedcke in 1855. It was initially used for treatment of depression and alcohol and morphine addiction and as a local anesthetic in ophthalmology in the 19th and early 20th centuries (Dackis and O'Brien, 2001). In 1970, cocaine became a controlled substance under the Controlled Substances Act.

There are two forms of cocaine, hydrochloride salt and freebase. Hydrochloride salt can be administered intravenously or by insufflation. Insoluble freebase cocaine and a mixture of freebase with an impurity of ammonium salt (so-called *crack*) are used for inhalation. Widespread recreational use of cocaine with a relatively short half-life of 1 hour has been reported (Huq, 2007). Polydrug use involving combinations of cocaine with alcohol and other psychostimulants is common (Brecht et al., 2008). Cocaine use is associated with alertness, increased energy and motor activity, euphoria, and enhancement of sensation (Preti, 2007).

Various medical and psychological complications including heart attack, stroke, cardiac arrest, respiratory arrest, digestive problems, and alterations in neuronal function have been reported in cocaine users (Brecklin et al., 1999; Dackis, 2005). Severe cocaine

withdrawal symptoms include decreased energy, limited ability to experience pleasure, anxiety, depression, paranoia, hallucinations, and a strong desire to use cocaine again (Gold and Balster, 1996; Kampman et al., 2006).

To date, no effective pharmacotherapy of cocaine addiction exists (Preti, 2007). New, more effective treatments based on the neurochemistry of cocaine are needed. Substitution therapy with dopamine transporter inhibitors and dopamine agonists are among the most promising approaches for cocaine dependence treatment (Preti, 2007; Dackis, 2005).

hDAT Structure and Function

hDAT is a Membrane Protein

Membrane proteins carry out a variety of extracellular and intracellular cell functions, including communication, trafficking, ion transport, signaling, and protein integration/translocation (Speers and Wu, 2007). Transporters, ion channels, and G-protein coupled receptors are among membrane proteins. Membrane proteins occupy approximately 50 % of the volume of all biological membranes and comprise one third of all proteins encoded by eukaryotic genome (Muller et al., 2008; Liu and Rost; 2001). The human dopamine transporter (hDAT) exhibits the general properties of membrane proteins (Giros and Caron, 1993).

The structure of membrane proteins is defined by the interaction of the hydrophobic lipid bilayer with the polar peptide bonds. In order to adapt to the hydrophobic environment, membrane proteins form secondary structures. The majority of

membrane proteins, including the dopamine transporter, form α-helical structures with hydrogen bonds between amide and carbonyl groups, while some proteins from outer membranes of Gram-negative bacteria and a number of proteins of outer membranes of mitochondria and chloroplasts form less common β-barrel transmembrane structures (Speers and Wu, 2007; Tamm et al., 2001). The outer surface of membrane domains formed by amino acid side chains is hydrophobic, permitting interaction with the lipid bilayer, while the functional inside area of membrane proteins can be hydrated and allows the trafficking of water-soluble molecules (Sonders et al., 2005). The transmembrane domains (TMs) usually contain aromatic tyrosines, or phenylalanine residues along with aliphatic leucines, isoleucines, or valines (Coic et al., 2005; Mousson et al., 2001). Tryptophanes are usually located on the membrane interface due to the ability of indole aromatic structures to stabilize the interaction of hydrophobic transmembrane regions with the hydrophilic environment (Muller et al., 2008). Several positively charged amino acid residues interact with negatively charged phospho groups of the bilayer and facilitate the stability of the secondary structure (Chen et al., 2004). Disulfide bond formation between cysteines located in the loop regions also aids the stability of secondary structures of membrane proteins.

Membrane proteins vary in number of spans through the membrane and divide into bitopics with single pass-through membranes and polytopics (Speers and Wu, 2007). For example, the insulin-like growth factor-II/mannose-6 phosphate (IGF-II/M6P) receptor has only one transmembrane domain (Hawkes et al., 2007), while multidrug-resistant protein 1 (MPR1) forms 17 transmembrane regions (Koike et al., 2004).

Membrane proteins are very difficult to study due their low expression levels and solubilization challenges (Midgett and Madden, 2007). This is why the first recombinant eukaryotic atomic structure of the nicotinic acetylcholine receptor was solved only recently (Unwin, 2005). There are almost no high-abundance membrane proteins, and the expression of recombinant eukaryotic membrane proteins is very challenging due to difficulties in proper post-translational modifications; the success rate is only 10%–30% (Midgett and Madden, 2007). Proper glycosylation is important for eukaryotic membrane proteins due to its role in the folding, stability and trafficking (Helenius and Aebi, 2004). Host expression systems for eukaryotic membrane proteins such as *E. coli*, yeast, insect cells, and mammalian cells are available. However, *E.coli* does not allow glycosylation or post-translational modifications, and yeast and insect cells offer non-native glycosylation and non-native lipid environments which means that expressed membrane protein can be nonfunctional (Wagner et al., 2006). While mammalian cells do offer native lipid environments and posttranslational modifications (Tate, 2001), they are technically demanding in handling. Having a host expression system that offers proper post-translational modification is important because it has been shown that mutating out the glycosylation sites of hDAT leads to a decrease in the efficiency of dopamine transport, decreased stability of the transporter, and increased potency of dopamine transporter inhibitors (Li et al., 2004).

Despite expression difficulties, membrane protein structures have been studied by a variety of techniques. The challenge of membrane protein crystallography is in obtaining and purifying sufficient amounts of low-abundance proteins. An additional challenge is selection of the proper detergent to ensure the structure of a protein is the

same as in the lipid bilayer (Matthews et al., 2006). Because of these difficulties, the crystal structure information of only approximately 250 membrane proteins are currently available (Midgett and Madden, 2007). The investigation of intramolecular interactions of membrane proteins with unknown crystal structure can be carried out by variety of techniques including atomic force microscopy, single molecule force spectroscopy, along with mutational studies, mass spectrometry and photoaffinity labeling (Vaughan et al., 2005; Yamashita et al., 2005; Miranda et al., 2005). High-resolution atomic microscopy and single-molecule fluorescence microscopy are also used to identify the oligomerization of membrane proteins and monitor the assembly of the proteins in membrane and conformational changes (Sorkina et al., 2003; Oesterhelt and Scheuring, 2006).

As stated previously, the dopamine transporter shares properties of membrane proteins (Figure 1.4). It is situated on the presynaptic membrane of dopaminergic neurons (Ritz et al., 1987). Its 620 amino acids are organized into 12 transmembrane domains with N- and C-terminals situated intracellularly. Like most integral proteins, the disulfide bond between C180 and C189 in extracellular loop 2 facilitates the secondary structure of the transporter (Chen et al., 2007). The glycosylation sites that are common for this group of membrane proteins are located at N181, N188, and N205 positions (Li et al., 2004).

hDAT is a Member of the NSS Family

The human dopamine transporter belongs to the family of neurotransmitter: sodium symporters (NSS) (Beuming et al., 2006). This family is also called the *sodium- and chloride-dependent neurotransmitter transporter family* (SLC6) according to the

Human Genome Organization nomenclature (Chen et al., 2004). The family employs the Na$^+$ gradient to transport a variety of neurotransmitters. Chloride ion gradients also aid the transport of neurotransmitters back into the cell (Beuming et al., 2006). Neurotransmitters co-transport with sodium ions using their electrochemical gradient. Neurotransmitter sodium symporters are located in the plasma membranes of neuronal and astrogial cells and regulate the concentration of neurotransmitters in the synapse via reuptake of the substrate and by preventing overstimulation of receptors with neurotransmitters released during signal transduction. The uptake of neurotransmitters is one of the mechanisms that ends neurotransmission (Kanner and Zomot, 2008).

The neurotransmitter sodium symporter family includes dopamine (DAT), norepinephrine (NET), serotonin (SERT), γ-aminobutyric acid (GAT), and glycine transporters (Loland et al., 2004). Additionally, the NSS family includes amino acid transporters and bacterial homologues. Recent advances in understanding of the NSS structure are related to the recently solved crystal structure of the bacterial leucine transporter (LeuT$_{Aa}$), a member of the NSS family, from *Aquifex aeolicus* (Yamashita et al., 2005). The sequence identities between prokaryotic LeuT and eukaryotic DAT, SERT, and NET are only 20%, 21%, and 24%, respectively (Beuming et al., 2006). In addition, the structures of eukaryotic transporters have larger N- and C-terminal regions as well as longer loop regions compared to the prokaryotic members of the family (Rudnick, 2007). Despite the low similarities between the eukaryotic and prokaryotic members of the NSS family, the LeuT crystal structure is the relevant information available regarding the family structure (Beuming et al., 2006; Zhou et al., 2007; Huang and Zhan, 2007). The leucine transporter consists of 12 transmembrane domains that are

organized in such way that the binding pocket of the transporter is formed by pseudo-twofold packing of TM1-TM5 and TM6-TM10 superimposed domains (Figure 1.1) (Yamashita et al., 2005). TM1 and TM6 are located close to the leucine binding site, and their residues from unwound regions interact with substrate and ions (Yamashita et al., 2005). Additionally, TM3 and TM8 are participating in the substrate and sodium ion binding. TM1, TM6, and TM8, participating in the substrate binding, are among the most conserved regions among the family. The leucine and sodium ions are located in close proximity to each other when bound to LeuT$_{Aa}$ (Kanner and Zomot, 2008). The molecular structure of hDAT shares similarities with the structure of LeuT$_{Aa}$, like all NSS family members and contains 12 transmembrane segments connected by extracellular and intracellular loops.

The proposed mechanism of transport using LeuT$_{Aa}$ as an example is shown in Figure 1.2. Previous studies of NSSs have suggested that transporters have two gates, one facing the outside and another facing the inside (Chen and Justice, 2000). Only one of the two gates can be open at a time. The crystal structure analysis of LeuT$_{Aa}$ (Yamashita et al., 2005) supports this proposed mechanism. The transporter binds the substrate and sodium ion when it faces the extracellular "outward" conformation with the extracellular gate open. Two charged residues—Arg 30 from TM1b and Asp 404 from TM10—form an extracellular gate (Yamashita et al., 2005). The open outward position is enabled by the localization of TM1 and TM6 in the furthest position from TM3 and TM8. TM1 and TM3 are each formed by two α-helical regions connected by unwound regions, therefore making the TM1b and TM6a regions more flexible. Charged Arg 5 and Asp 369 form the gate facing inward. The extracellular gate is open when the transporter is facing outward,
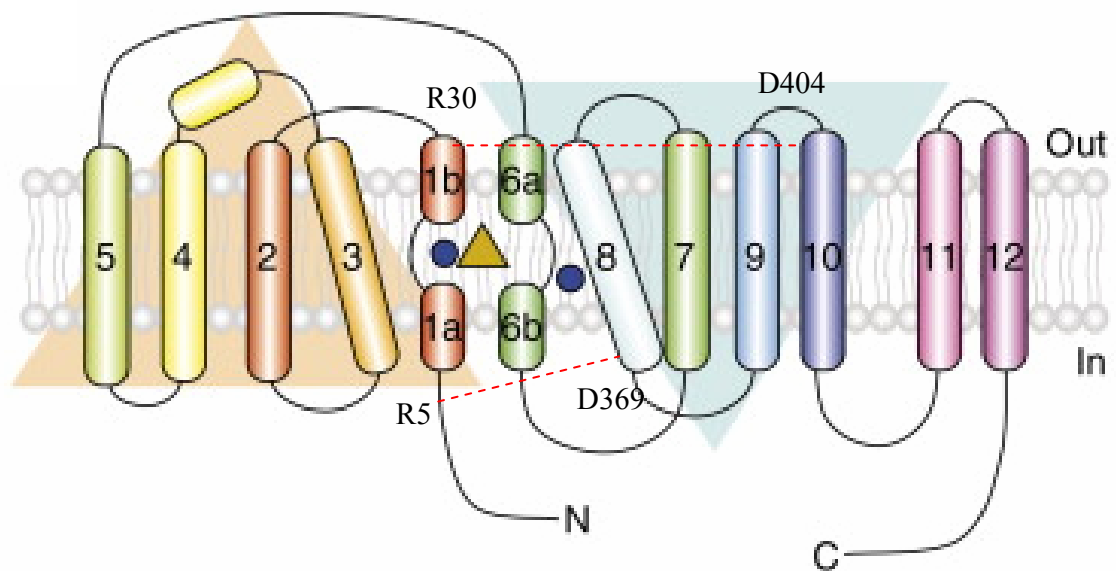
Figure 1.1 The LeuT$_{Aa}$ topology

The leucine transporter forms 12 α-helical transmembrane domains. The leucine molecule is shown as a yellow triangle and the two sodium ions are blue circles. TM1 to TM5 superimpose to TM6 to TM10 by 176.5° (shown in orange and blue triangles, respectively). R30 and D404 form the external gate, and R5 and D369 form the internal gate. (Adapted from Yamashita et al. [2005] and Torres and Amara [2007]).

allowing substrate and sodium ions to access the binding pocket. Substrate and sodium ions bind to the transporter and lead to the closed conformation with substrate and sodium ions trapped in the binding site while the transporter is in the substrate occluding conformation. Following that, the inward-facing conformation of the transporter occurs, when the intracellular gate opens due to the movement of TM1a-TM6b, allowing the release of the substrate and sodium ions (Yamashita et al., 2005).

Despite the fact that some substrates for the NSS family are amino acids and others are biological amines, all members of the family seem to accommodate the differences in substrate nature. For example, aspartate residue containing a carboxy group in the side chain is conserved in TM1 among all biogenic amine transporters and is believed to coordinate both substrate and sodium ions (Rudnick, 2007). Tyrosine residue with an available hydroxyl group that possibly coordinates the substrate carboxy group is conserved in TM3 among all amino acid transporters. Sodium ions are coordinated by the amino acid substrate. This enables the simultaneous transport of both sodium ions and amino acids (Kanner and Zomot, 2008).

Overview of hDAT Function

The main function of DAT is reuptake of dopamine from the synaptic cleft back into the presynaptic terminal (Giros and Caron, 1993; Bannon, 2005). Therefore, DAT regulates the intensity and length of neuronal signal transduction (Mortensen and Amara, 2003; Torres and Amara, 2007). The dopaminergic system is involved in learning, reward-seeking behavior, movement, and emotion (Sotnikova et al., 2006).
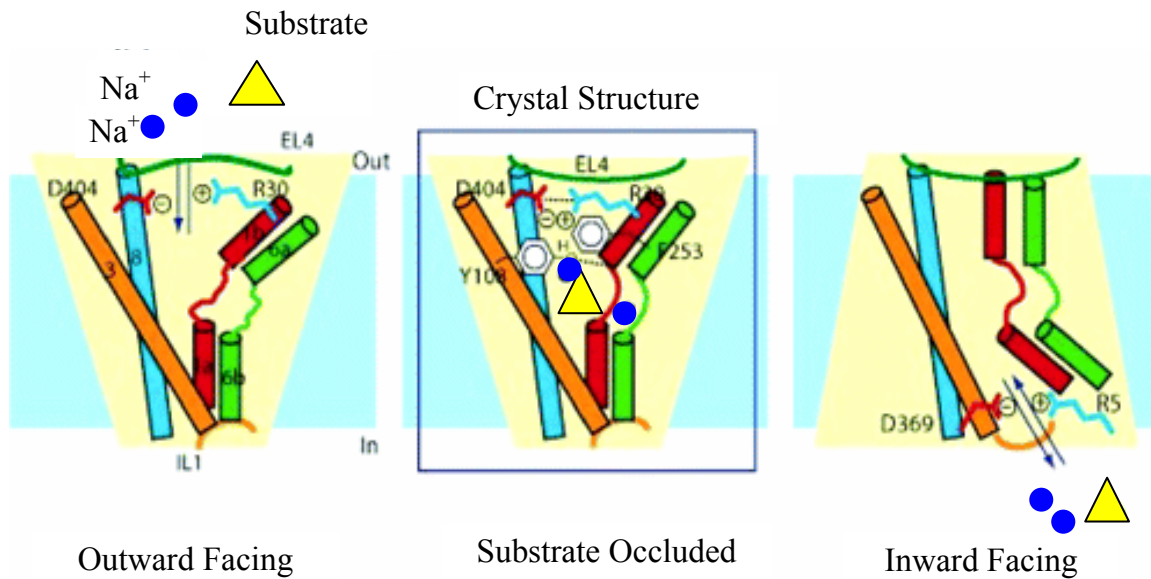
Figure 1.2 Proposed alternating access mechanism of transport of LeuT$_{Aa}$

Substrate and sodium ions bind to the outward-facing conformation of the transporter when the external gates are open and the internal gates are closed. When substrate and sodium ions are bound to the transporter, they are transported to the occluded state when both gates are closed. The third phase of the proposed mechanism is the release of substrate and sodium ions into the intracellular environment by the opening of the internal gate (the transporter is in the inward-facing conformation). The currently available crystal structure of the leucine transporter presents the substrate occluded phase (adapted from Yamashita et al., 2005).

Figure 1.3 shows the neurotransmission in the dopamine synapse. Dopamine is confined to the vesicles with the help of the VMAT2 vesicular amine transporter and then released from the presynaptic neuron (Sotnikova et al., 2006). The neurotransmitter molecules bind to the dopamine receptors of the postsynaptic membrane, leading to the further propagation of the signal and cellular response. DAT is responsible for the uptake of dopamine from the synapse back into the neuronal cell or astroglial cells (Kanner and Zomot, 2008). Recent immunoelectron studies have suggested that DAT is situated not only in the plasma membrane facing the synapse but also at more distant side locations, suggesting the existence of the diffusion of dopamine from the cleft (Nirenberg et al., 1997). The mechanism of DAT dopamine reuptake relies on the co-transport of ions with dopamine. DAT co-transports two sodium ions and one chloride ion. The driving force of the transport is the ion concentration gradient. The gradient is created by plasma membrane $Na^+/K+$ ATPase (Torres et al., 2003; Sotnikova et al., 2006).

Carvelli and colleagues (2004) measured the currents produced by *C. elegans* DAT. Their measurements of the current were greater than predicted in the case of stochiometric transport, suggesting the channel-like properties of DAT (Carvelli et al., 2004). The study showed the increase of single-channel activity in the event of the overexpression of DAT, absence of the channel activity in the knock-out model, and inhibition of the channel activity when DAT inhibitors are present (Carvelli et al., 2004). Other members of the NSS family have been reported to have channel-like activity as well (DeFelice and Goswami, 2007). Single-transporter currents were measured for SERT, DAT, GAT, and NET; however, single-channel events have yet to be observed (Cammack and Schwartz, 1996; Galli et al., 1996; Lin et al., 1996; Carvalli et al., 2004).
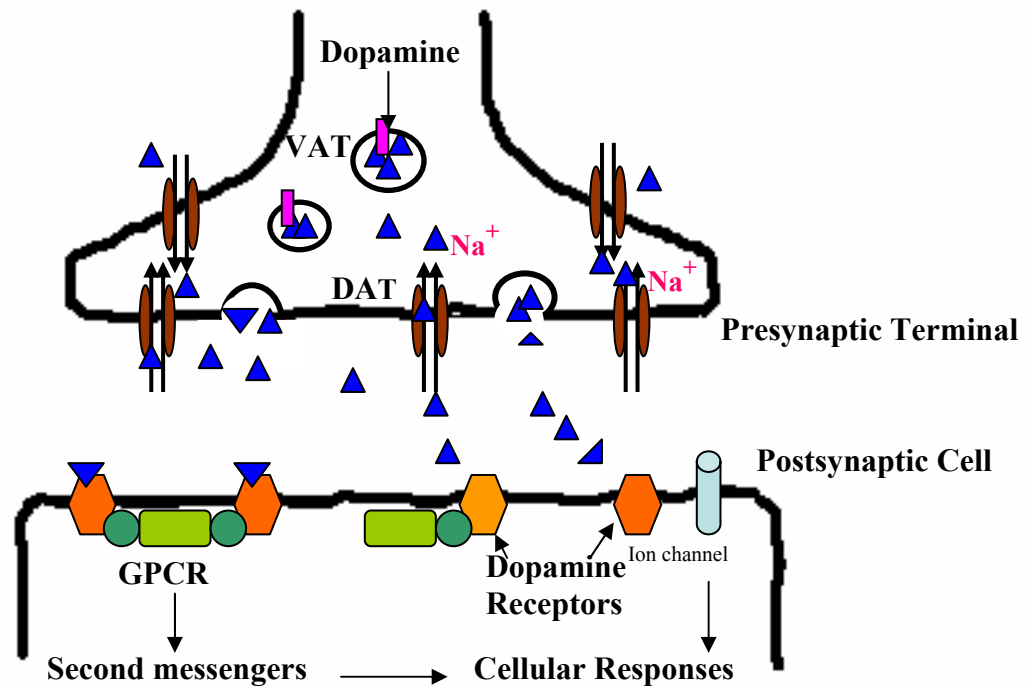
Figure 1.3 Neurotransmission at the dopamine synapse

Dopamine (blue triangles) is stored in presynaptic vesicles. Dopamine releases to the synaptic cleft when vesicles fuse with the presynaptic membrane. Activation of metabotropic G-protein coupled dopamine receptors leads to signal transduction. Following the activation, dopamine is recaptured by the dopamine transporter (adapted from Giros and Caron [1993]).

Regulation of hDAT Function

The function of DAT is modulated by protein-protein interactions, oligomerization, and post-translational modifications (Torres et al., 2003; Torres and Caron, 2005; Maiya et al., 2007). Several approaches have been undertaken to identify the proteome that regulates DAT functioning (Maiya et al., 2007; Torres and Caron, 2005). Maiya et al. (2007) reported co-immunoprecipitation of proteins associated with DAT with the transporter followed by mass spectrometry analysis, which allowed the detection of 20 proteins of different functions that are associated with DAT. The most interesting proteins associated with the dopamine transporter were the voltage-gated potassium channel Kv2.1 and synapsin 1b. Synapsin 1b assists in regulation of GAT function by direct interaction with the transporter and also modulates the gamma-aminobutyric acid (GABA) release (Deken et al., 2000). Synapsin may play an inhibitory role in regulation of DAT transport due to the fact that dopamine uptake increases in synapsin knock-out mice (Bogen et al., 2006).

The yeast two-hybrid system approach was also used to detect the proteins interacting with DAT (Torres and Caron, 2005). The study showed that protein C-kinase-1 and Hic-5 both interact with the dopamine transporter (Torres et al., 2001; Carneiro et al., 2002). C-kinase-1 is suggested to increase uptake activity by increased DAT internalization and is employed in DAT targeting (Torres and Carron, 2005), while the adaptor protein Hic-5 decreases the activity of the transporter by decreasing the amount of DAT in the plasma membrane and also by connecting DAT with the signaling pathway in the cell (Carneiro et al, 2002). To date, a network of different proteins that are associated with the modulation of DAT functions has been discovered. However, the

mechanisms of the actions of many of them on modulating DAT functions have yet to be determined (Maiya et al., 2007; Torres and Amara, 2007).

Oligomerization of DAT may play a role in the modulation of its activity (Mortensen and Amara, 2003; Torres, 2006) and minimization of exposure to an aqueous environment (Muller et al., 2008). The oligomerization of hDAT was detected by measuring fluorescence resonance energy transfer (FRET) between DAT molecules co-expressed with cyan and yellow fluorescent proteins (Sorkina et al., 2003). Evidence was obtained by cross-linking the neighboring wild-type DAT molecules or DAT-lacking cysteines in specified positions of TM4 and TM6. This suggested TM4 and TM6 involvement in formation of the dimer or dimers with two symmetrical dimers facing each other (Hastrup et al., 2001). Torres and colleagues (2003) demonstrated the importance of TM2 leucine repeat in oligomarization using mutational studies. They found that the lack of oligomerization lowers the internalization of DAT (Torres et al., 2003). Dopamine was shown to modulate the oligomerization process by reducing DAT oligomerization at high dopamine concentrations (Chen and Reith, 2008).

Post-translational modifications of DAT include phosphorylation and glycosylation (Foster et al., 2002; Li et al., 2004). Several studies found the phosphorylation sites of DAT (Foster et al., 2002; Granas et al., 2003; Daniels and Amara, 1999). The previous study showed that PKC activation induces N-terminal phosphorylation of DAT in rat striatum (Foster et al. 2002). The protein kinase C down-regulates DAT activity by reducing DAT expression in the plasma membrane (Zahniser and Sorkin, 2004). As stated earlier, glycosylation of DAT is important for transporter trafficking and the dopamine uptake (Li et al., 2004).

Role of hDAT in Human Disease

The dopamine transporter regulates the uptake of dopamine from the synapses. Therefore, DAT plays a role in a number of diseases and in neurotoxicity related to the dopaminenrgic system (Bannon, 2005). For example, neuron loss is associated with Parkinson's disease. Studies have also reported a correlation between low expression of DAT in the midbrain of patients with Parkinson's disease (Harrington et al., 1996). Clinical diagnosis of Parkinson's disease often includes imaging using dopamine transporter inhibitors (Brooks, 2005). Also, DAT gene polymorphism is reported in connection with attention deficit hyperactivity disorder (ADHD) (DiMaio et al., 2003). Higher than normal densities of DAT have been found in untreated ADHD patients (Krause, 2008). Therefore, the common treatment for ADHD is DAT antagonist methylphenidate (Krause, 2008). DAT has also been found to be involved in the mechanism of substance abuse (Torres et al., 2003; Ritz et al., 1987; Kitayama et al., 1992). Cocaine, a dopamine transporter inhibitor, and amphetamine, which acts as a DAT substrate and replaces dopamine, are the two main drugs of abuse involving DAT (Torres et al., 2003). The investigation of the cocaine structure and identification of its binding site can facilitate the progress of the pharmacotherapeutic methods to reduce cocaine addiction by developing medications that compete for the cocaine binding site and simultaneously provide the normal level of the substrate transport.

hDAT Structure Overview

As discussed previously, the dopamine transporter shares structural similarities with the other members of the NSS family (Beuming et al., 2006), such as consisting of

12 TMs connected by extracellular and intracellular loops and 620 amino acids (Figure 1.4). No crystal structure is available for hDAT and little is known about localization of the substrate and inhibitors binding sites of hDAT. To date, the only crystal structure of a NSS family member that has been solved is that of the leucine transporter, LeuT$_{Aa}$ (Yamashita et al., 2005). Since all NSS family members share similar structures, the LeuT$_{Aa}$ structure allows some insight into the possible three-dimensional structure of hDAT (Yamashita et al., 2005).

The leucine transporter structure has been used as a template to construct a model of the putative DAT structure (Indarte et al., 2008). The authors reported the challenges in modeling DAT due to its low similarity with LeuT$_{Aa}$ (only 20%) (Indarte et al., 2008). The DAT model overlapped with the LeuT structure except for TM1b, suggesting a slight change in conformation of bound substrate. However, prolines and glycines are highly conserved between both LeuT and DAT, providing identical unwound regions in both molecules. The backbone residues of unwound regions of TM1 and TM6 directly interact with TM3 and TM8 to form a binding pocket (Yamashita et al., 2005; Indarte et al., 2008).

The putative dopamine binding pocket was investigated. Computational modeling suggested the binding site is situated halfway between TM1 and TM6, near the binding sites for two sodium ions (Indarte, 2008). Backbone carbonyl groups of A77 and V78 from TM1 and of S320 and L321 from TM6 can form hydrogen bonds with an amine group of substrates, and D79 can form a hydrogen bond between its carboxyl group and amino group of substrates (Indarte, 2008). Asp79 of hDAT can additionally facilitate the interaction with one of the sodium ions, replacing the carboxyl group of leucine
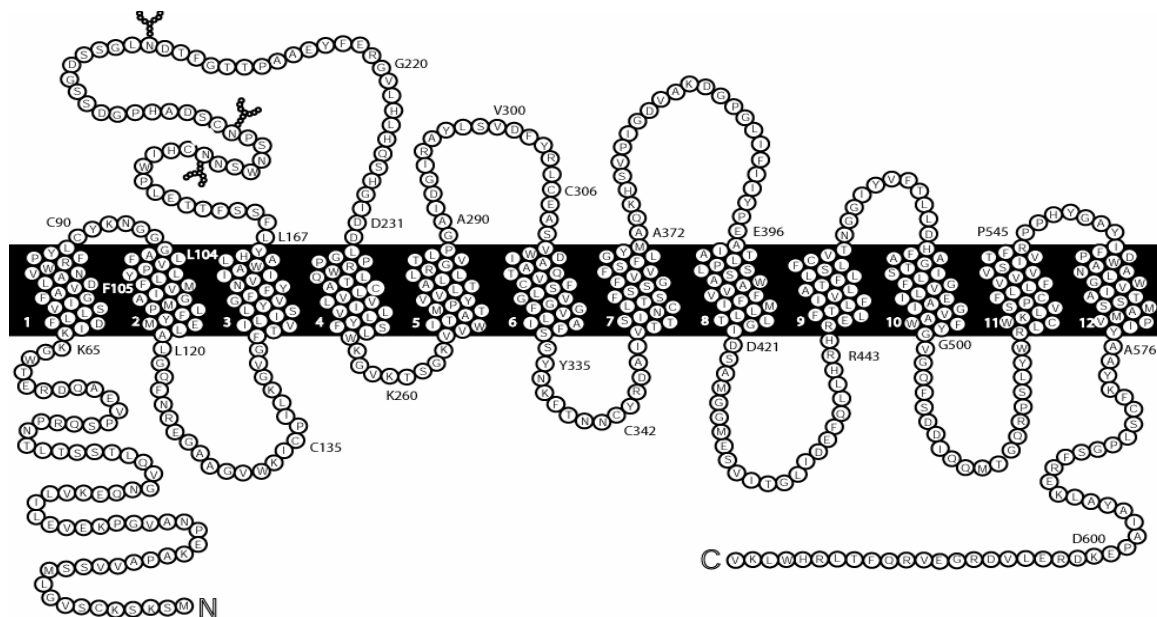
Figure 1.4 Two-dimensional representation of hDAT

hDAT contains 620 amino acid residues packed onto 12 transmembrane domains connected by extracellular and intracellular loops. C- and N-termini are situated intacellularly (adapted from Giros and Caron, 1993).

(Yamashita et al., 2005; Kanner and Zomot, 2008). It is proposed that sodium ions do not directly interact with dopamine because of the lack of the carboxyl group (Indarte et al., 2008). Figure 1.5 shows the proposed amino acid residues of DAT that are interacting with the substrate or situated in the putative DAT binding site (Indarte et al., 2008). The dopamine hydroxyl group can form hydrogen bonds with S421 (TM8) and A422 (TM8). V152 (TM3) and V327 (TM6) contribute to the hydrophobic interactions with the substrate. As reported by Yamashita and collogues (2005), π-π stacking can be facilitated by interactions of substrate with Y156 (TM3), F319 (TM6), and F325 (TM6) (Indarte et al., 2008).

Extensive structure-function mutational studies of hDAT have been carried out to investigate the functional domains and the role of particular amino acid residues in substrate binding (Kitayama et al., 1992; Chen et al., 2001; Uhl and Lin, 2003). Kitayama and colleagues (1992) mutated aspartate 79 from TM1 to alanine, glycine, and glutamine. A sharp decrease in dopamine uptake was reported that correlates with the discussed previously hDAT model suggesting Asp79 is responsible for interaction with the amino group of dopamine (Yamashita et al., 2005; Indarte et al., 2008). Another study showed that E491 (TM10) is important for dopamine binding (Dar et al., 2006). Because TM10 is not expected to participate in the binding site (Yamashita et al., 2005), this finding suggests that residues from TM10 may be part of the extracellular gate or may interact with sodium ion (Dar et al., 2006).

The Ki of dopamine in cells expressing D313N DAT was considerably higher than in wild-type DAT, suggesting the importance of this TM6 residue in substrate binding (Chen et al., 2004). The role of D345 (TM7) and D476 (EL5) for dopamine

binding was reported previously by this group, confirming the importance of aspartate residues for DAT functionality (Chen et al., 2001). Mutation of F155A selectively decreased dopamine activity to a dramatically low level, suggesting the importance of the participation of aromatic phenylalanine residue from TM3 in dopamine binding (Lin et al., 1999).

An endogenous Zn^{2+} DAT binding site formed by His193 (EL2), His375 (TM7), and Glu396 (TM8) was reported (Gether et al., 2001; Norregeerd et al., 1998; Loland et al., 1999). Gether and colleagues (2001) found that the zinc ion acts as a noncompetitive inhibitor of dopamine uptake. Their study also proposes close proximity of EL2, TM3, TM7, and TM8 and correlates with the LeuT crystal structure analysis.

Dopamine Transporter Inhibitors

Mechanism of Cocaine Action

The rewarding effect of cocaine is mainly caused by inhibition of dopamine reuptake from the synaptic cleft via dopamine transporter inhibition and overstimulation of postsynaptic dopamine receptors by excess of dopamine (Ritz et al., 1987; Riddle et al., 2005; Kuhar et al., 1991). The chemical structures of dopamine transporter inhibitors are shown in Figure 1.6. Although the main target for cocaine is the dopamine transporter (Kuhar et al., 1991), it also binds to all monoamine transporters, including SERT and NET, suggesting a complex nature of cocaine dependence (Ritz et al., 1987; Torres et al., 2003; Flippen-Anderson et al., 2003). The ideal treatment for cocaine abuse should have
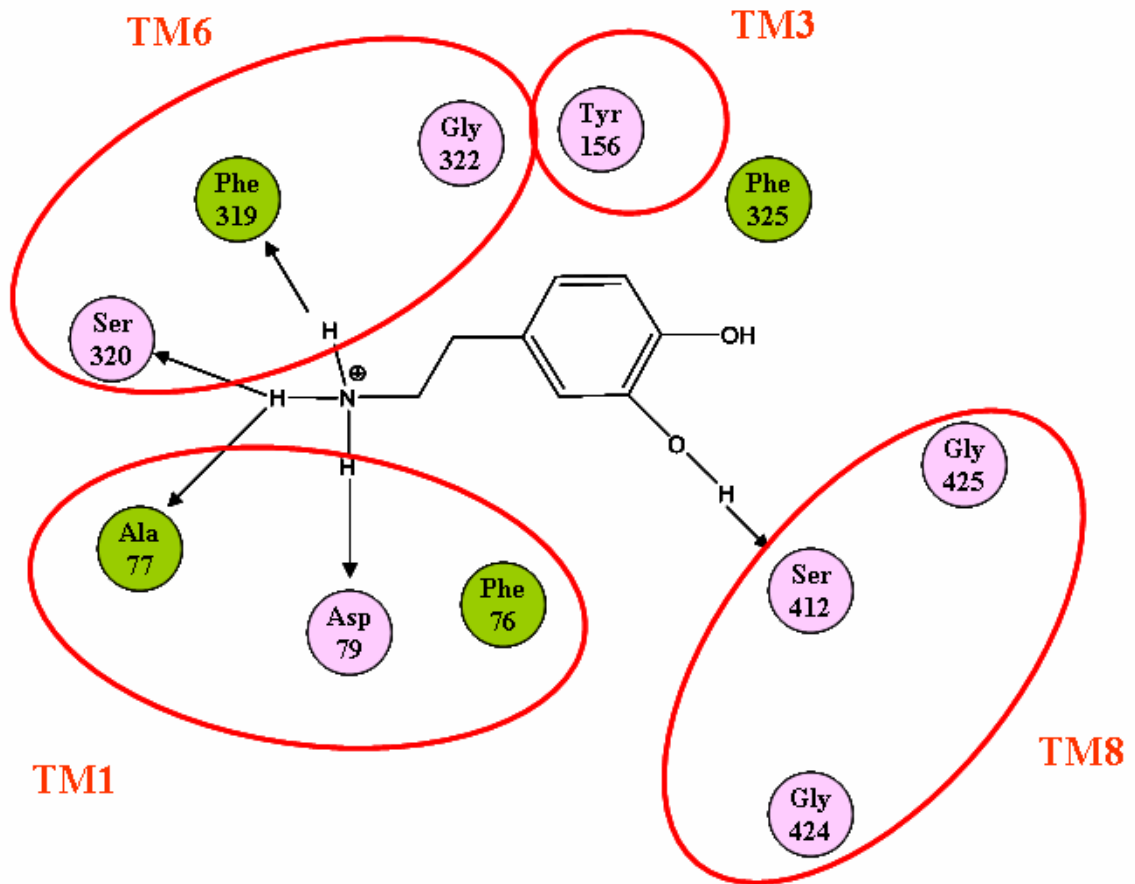
Figure 1.5 Molecular contacts between DAT and bound dopamine

Polar amino acids are shown in pink, hydrophobic in green. Red circles denote the transmembrane domains (adapted from Indarte et al. [2008]).

high affinity to the transporter to compete with cocaine and selectivity and should allow substrate transport (Carrol et al., 1999).

Overview of Different Classes of DAT Inhibitors

Although the DAT inhibitors cocaine, benztropine, mazindol, nomifensine, methylphenidate, and GBR compounds belong to diverse classes of compounds with different structures (Figure 1.6), all these ligands inhibit DAT by binding to hDAT and terminating the dopamine uptake, which increases the concentration of dopamine in the neuronal synaptic cleft (Vaughan, 1998). Structure-activity studies have been performed to investigate the correlation between the structure of the inhibitors and its activity toward dopamine transporters (Carrol et al., 1999; Newman and Kulkarni, 2002; Flippen-Anderson et al., 2002; Newman, 1998).

Cocaine is a tropane alkaloid with two asymmetric centers. The active form of cocaine is R (-) cocaine (Carrol et al., 1991). The nitrogen of the tropane ring is capable of ionic or hydrogen bond formation in the binding site. The carbomethoxy group can participate in the hydrogen bond and the 3β-benzoyl ester group is capable of hydrophobic interactions (Flippen-Anderson et al., 2003). The synthesis of cocaine-based inhibitors is based mostly on the modification of these major functional groups. The potent inhibitors have to retain the stereochemistry of cocaine.

Cocaine analog (-)-2β-Carbomethoxy-3β-phenyltropane (WIN 35,065-2) is a phenyltropane that has a phenyl group in the place of the 3β-benzoyl ester group (Zhu et al., 1998). The affinity of this compound for hDAT is 23 nM (IC_{50}),which is four fold higher affinity compared to the 102 nM affinity of cocaine (Carrol et a., 1991).

Quantitative structure-activity relationship (QSAR) analysis using comparative molecular field analysis (CoMFA) has been performed on numerous cocaine analogs (Zhu et al., 1998). CoMFA correlates the experimental pharmacological activity with electrostatic and special properties of substituting groups with the aim of predicting and choosing the pharmacological properties of newly synthesized compounds (Zhu et al., 1999; Gilbert et al., 2007).

Structure-activity studies also allow researchers to learn more about interactions with the inhibitor in the binding site. For example, introduction of electron-withdrawing fluorine in the para- position of WIN 35,065-2 increases the affinity to hDAT with IC_{50} 13.9 nM (Zhu et al., 1999). Therefore, the fluorine-containing compound WIN 35,428 is widely used in cocaine binding studies due to its high affinity to DAT (Appell et al., 2004; Gulley and Zahniser, 2003). Introduction of any electron-withdrawing atom or group including halogens in the para- position produced more potent compounds compared to cocaine (Zhu et al., 1999). The presence of substitute in position 2 of the tropane ring is required for both potency and selectivity to DAT over SERT and NET (Zou et al., 2001). The variety of studies investigated cocaine-like structures and found a number of potent DAT inhibitors (Newman and Kulkarni, 2003; Carrol et al., 1992; Zhu et al., 1999).

Benzotropine is another analog containing the tropane structure (Newman and Kulkarni, 2003). It is used in the treatment of Parkinson's disease. Several potent and very selective inhibitors of this structure, such as difuoropine, were discovered (Newman and Kulkarni, 2003). Previously, benzotropine analogs were considered not useful as possible cocaine abuse treatments due to their failure to exhibit cocaine-like properties.
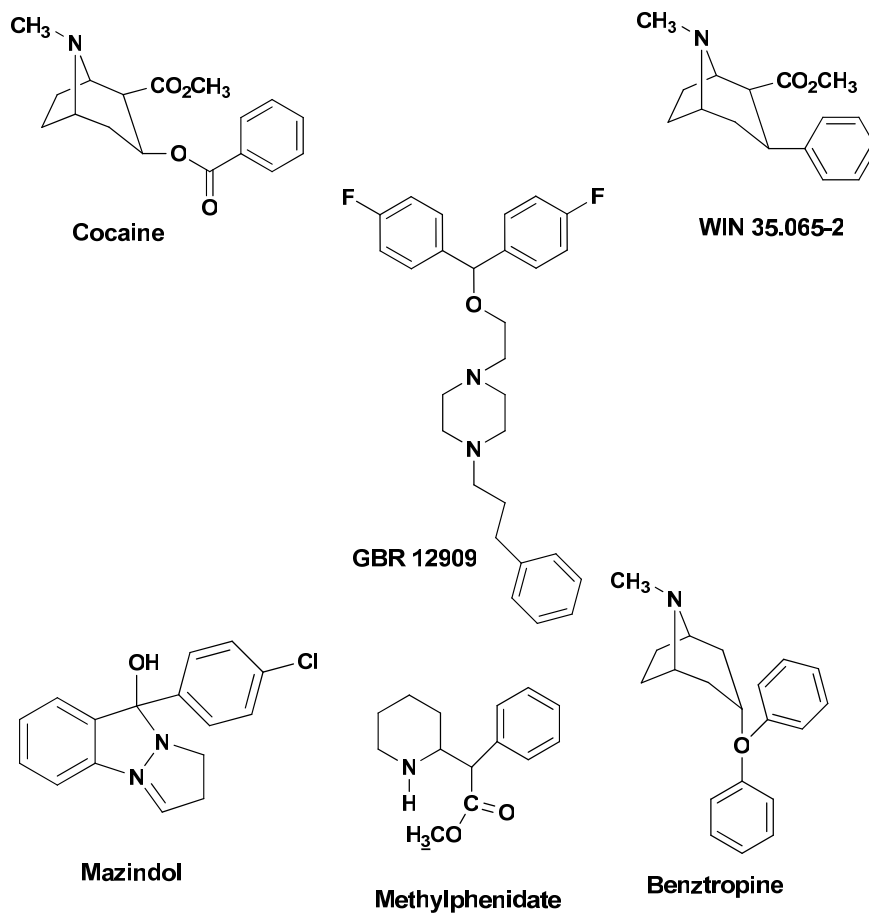
Figure 1.6 hDAT inhibitors (adapted from Carroll et al., 1999)

However, more recent animal studies of large series of compounds showed their promising application in cocaine dependence treatment due their high affinity and low reinforcing effects (Newman and Kulkarni, 2003).

1-{2-[Bis(4-fluorophenyl)methoxy]ethyl}-4-(3-phenylpropyl)piperazine (GBR12909) is a potent DAT inhibitor with a structure different from the tropane-containing structure (Newman and Kulkarni, 2003; Flippen-Anderson et al., 2003). The problem with using the compounds of 1,4-dialkyl-piperazine series is their high lipophilicity, which can be especially challenging when working with membrane proteins (Cao et al., 2001). The major difference of GBR 12909 from the cocaine analog is its slow dissociation when bound to DAT and its exhibition of a slower effect in behavioral studies (Rothman and Glowa, 1995). However, optimization of the structure of GBR compounds allowed synthesis of inhibitors that suppressed self-administration of cocaine in animal models, and had a weaker reinforcing effect than cocaine (Desai et al., 2005).

Investigation of Cocaine Binding Site

Structure-activity relationship studies aim to determine the interactions of DAT with inhibitors. Investigation of the cocaine binding site produces an overwhelming amount of sometimes contradictory information, suggesting possible flexibility of the binding site depending on the inhibitor structure (Newman and Kulkarni, 2003). Many approaches have been undertaken to investigate the cocaine binding site, including affinity labeling, site-directed mutagenesis and X-ray crystallography. These are discussed in more detail in the following paragraphs.

Affinity Labeling

The affinity labeling method allows researchers to obtain information about the binding site and spatial arrangement of the protein of interest. Irreversible ligands react with protein residues situated inside or in close proximity to the inhibitor binding site while their pharmacophores are localized in the cocaine binding pocket (Vaughan, 1998). This method was successfully applied in a number of studies on a number of receptors and transporters such as a nicotinic acetylcholine receptor (Grutter et al., 2002), a human vasopressin receptor (Phalipou et al., 1999), a GABA$_A$ receptor (Jacques et al., 1999), and the ABC multidrug transporter LmrA from *Lactococcus lactis* (Alqwai et al., 2003).

To determine the location of the binding sites of hDAT inhibitors, the hDAT was labeled with variety of photoinducible ligands (Vaughan et al., 1998; Zou et al., 2001; Vaughan et al., 2005). Ligands that have been used for hDAT labeling fall into two groups of dopamine uptake inhibitors: cocaine analogs and GBR 12909 analogs. [^{125}I] MFZ 2-24, [^{125}I] RTI-82 (Zou et al., 2001; Vaughan et al., 2005) and [^{125}I] GA II-34 possess a tropane ring; [^{125}I] AD-96-129 (Dutta et al., 2003) and [^{125}I] DEEP resemble the structure of GBR 12909 (Vaughan et al., 2001; Tomlinson, 2003). Additionally, affinity labeling with isothiocyanate analog MFZ 3-37 was reported (Vaughan et al., 2005). Figure 1.7 shows the chemical structures of hDAT affinity ligands. The majority of these ligands contain an azido group, which is considered one of the most suitable for photoaffinity labeling of reactive polypeptide side chains (Bayley, 1983). [^{125}I] MFZ 3-37 contains an isothiocyanate reactive group, which may react with lysine and cysteine residues (Vaughan et al., 2005).
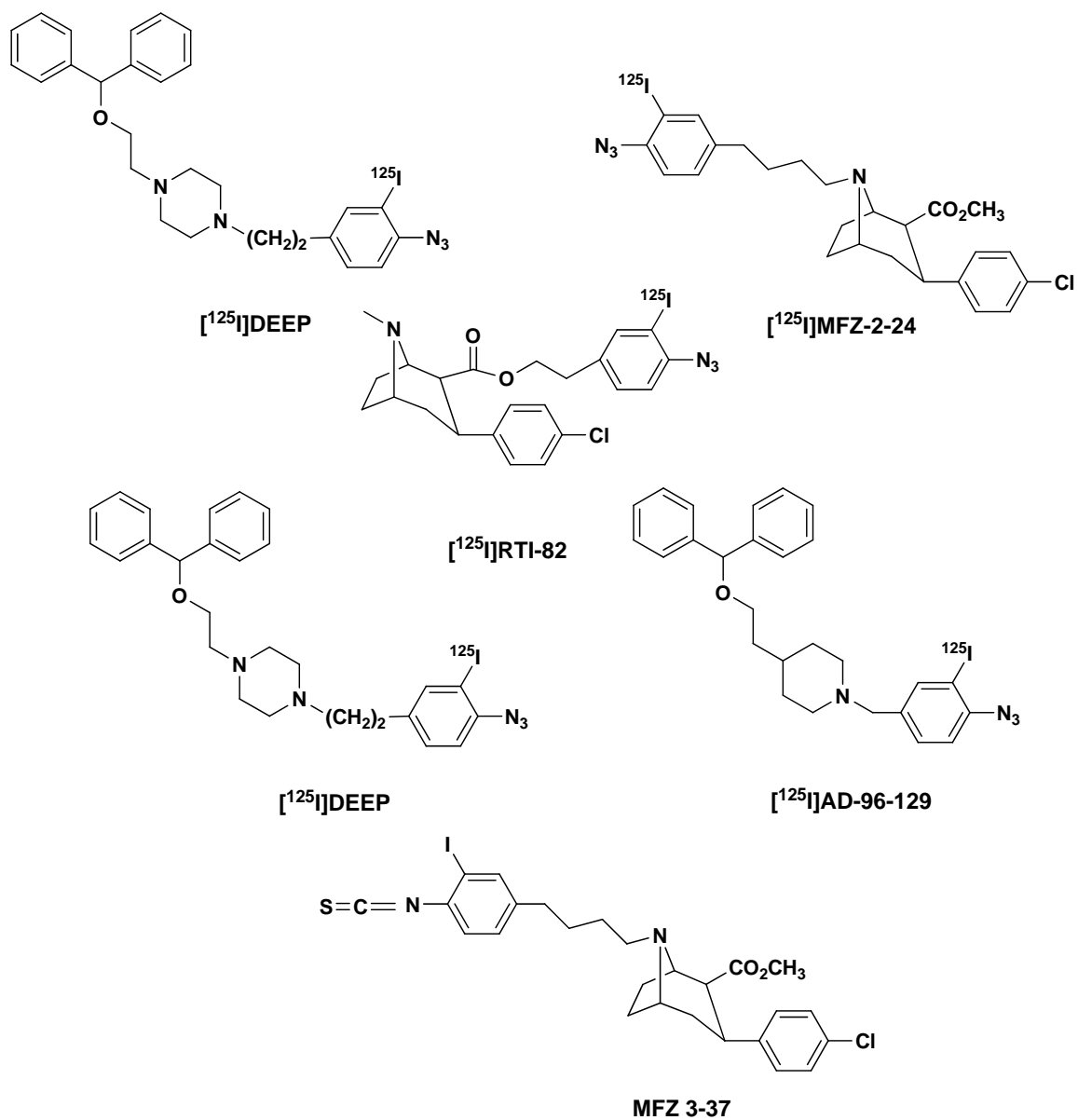
Figure 1.7 Affinity ligands for DAT

All ligands used by Vaughan and colleagues (2001) were photoaffinity labels containing radioactive iodine for tracing. These studies included proteolysis and immunological peptide mapping using antisera to several rDAT sequences distributed throughout the protein. Following the DAT labeling with the ligand and the consecutive proteolysis, the labeled peptides were immunoprecipitated and separated on SDS-PAGE gel (Vaughan et al., 2001; Parnas et al., 2008). With the enzyme cleavage sites and the antiserum known, the results suggested that MFZ 2-24, AD-96, GA-II-34, and DEEP label the TM1-TM2 region. In contrast, RTI-82 and AD 96-129 labeled the TM4-TM7 region. AD 96-129 exhibited dual incorporation in DAT, suggesting the close spatial arrangement of TM1-TM2 and TM4-TM7 regions in DAT (Vaughan et al., 2001; Vaughan et al., 2004).

Recent studies have introduced cleavage sites using mutagenesis. The change in immunoprecipitation of wild-type and mutant DAT were compared, allowing the definition of the RTI-82 labeling region as residues 292-344 in TM6 (Vaughan et al., 2007). Further investigation of the labeling site for either of the labels using HPLC separation, Edman degradation, and mass spectrometry can narrow down the label incorporation site to a singe amino acid residue.

The affinity labels used to study hDAT were the photoaffinity labels and their isothiocynate analogs (Vaughan et al., 2001; Vaughan et al., 2005). The photoaffinity labeling method is based on the formation of short-lived intermediates upon photoactivation (Dorman and Prestwich, 2000). These intermediates could irreversibly react with the residues of macromolecules (Platz M., 1997). The irradiation of precursors used for photoaffinity labeling might generate carbenes or nitrenes (Bayley, 1983).

Because nitrenes prefer interacting with O-H, N-H rather than C-H bonds, the arylazide derivatives were chosen as the preferable compounds to bind to proteins (Bayley and Knowles, 1977). The aromatic azides are relatively stable compounds and often used as photolabeling agents (Harder et al., 1997; Bayley and Staros, 1984; Vaughan et al., 2005). The mechanism of reaction of aryl azides with proteins is shown in Figure 1.8. Under photolysis, an aryl azide forms a singlet aryl nitrene when it loses nitrogen or a triplet azide when intersystem crossing occurs (Kotzyba-Hilbert et al., 1995; Bouchet and Goeldner, 1996; Budyka et al., 1992) (Figure 1.8). Kotzyba-Hilbert and coworkers (1995) showed that the product of the photochemical reaction forms according to the nature of aryl azide derivatives and the nucleophylicity of amino acid residues in the binding site. The mechanism of insertion and H$^\bullet$ radical abstraction followed by coupling is more likely to occur than formation of azepine derivatives in the event of protein photolabeling (Kotzyba-Hilbert et al., 1995).

Comparison of nucleophilicity and the stability of side-chain radicals formed during photoaffinity labeling allow determination of the most reactive amino acid residues. The formation of a stabilized phenoxyl radical for tyrosine, benzylic radicals for tryptophane, phenylalanine, and histidine, as well as thiolate for the cysteine, make the amino acid listed above residues the most likely targets for aryl azide (Kotzybqa-Hilbert et al., 1995). Schwartz and colleagues (1989) reported that cysteine was the most reactive amino acid with phenyl nitrene. Numerous studies report tyrosines and cysteines as the most common sites of photoincorporation (Kotzybqa-Hilbert et al., 1995) The major product of label interaction with Tyr is controversial, while the triplet nitrene might abstract H$\bullet$ either from oxygen or from nearby carbon of the aromatic ring (Kotzyba-
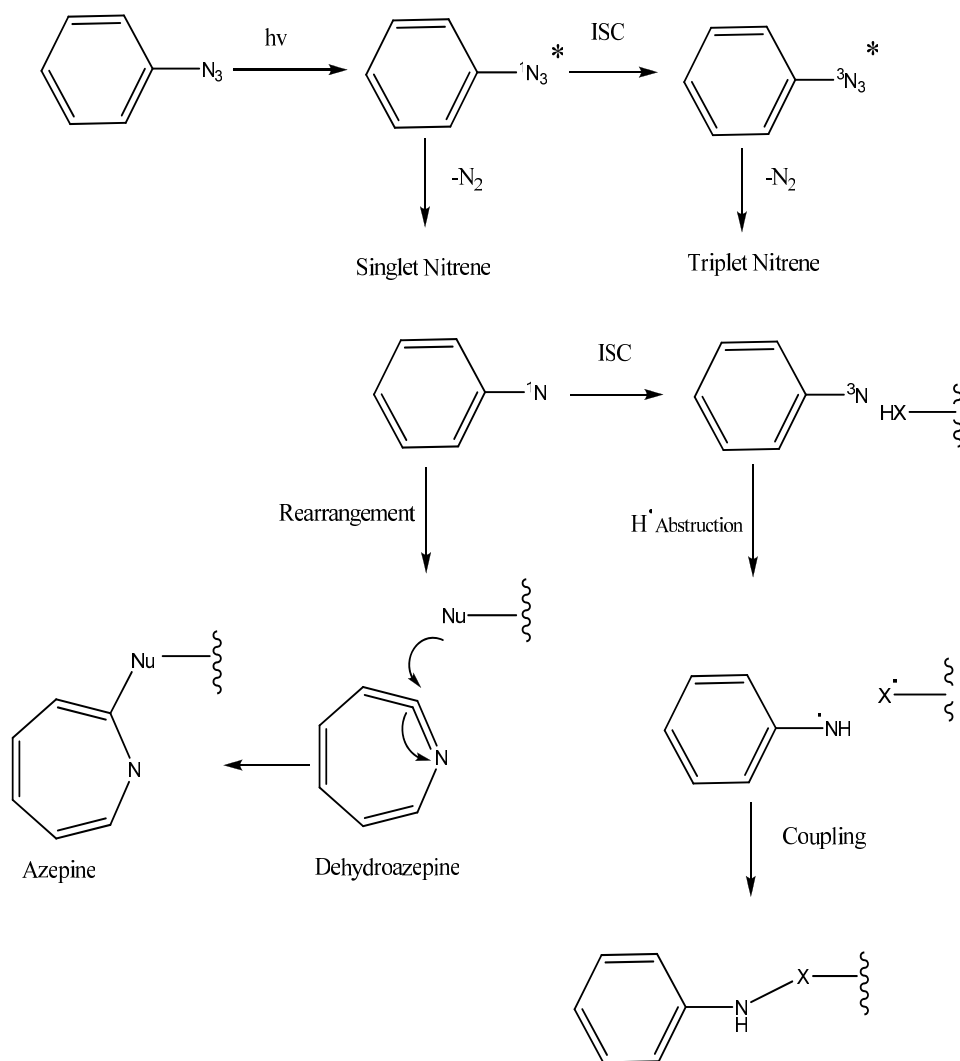
Figure 1.8 Photochemical events during photoaffinity labeling

Following irradiation, an azide forms a singlet excited state. The singlet can lose nitrogen and form a singlet nitrene or can undergo intersystem crossing (ISC) forming triplet azide, which can form a triplet nitrene. The singlet can rearrange and form degydroazepine, which is reactive with nucleophile group of a protein. The triplet niterene abstracts a hydrogen radical from the protein and reacts via free radical mechanism (adapted from Dorman and Prestwich, [2000]; Kotzyba-Hilbert et al.,[1995]).

Hilbert, 1995). Consequently, the obtained products may exhibit different properties, complicating the interpretation of results. Tryptophan and methionine are also among the most frequently labeled amino acids (Kotzybqa-Hilbert et al., 1995).

However, there are several problems recounted when aryl azide compounds are used in photoaffinity binding of hDAT. The introduction of radioisotope tracers such as ^{125}I into the ligand is the convenient method of photolabeling detection (Watt et al., 1989). The majority of compounds applied in hDAT photoaffinity labeling contain iodine in the ortho-position to azide (Vaughan et al., 2001; Vaughan et al., 2005). However, the presence of iodine in the same aryl group leads to a dramatic decrease of labeling efficiency (Watt et al., 1989). This suggests that the amount of labeled DAT may be too low for some applications such as mass spectrometry. However, hDAT can be traced using radioactivity.

Another problem that researchers can face during photoaffinity labeling is nonspecific binding outside or inside the binding site, which might occur when a high concentration of reagent is used or when reactive nucleophylic groups (particularly sulfhydryl groups) are located close to the binding site (Bayley, 1983). However, the addition of the subsequent amount of oxidants and thiols minimizes the nonspecific labeling in photolabeling experiments by quenching the undesired reactions (Bayley, 1983).

To increase the yield of the reaction of the ligand with hDAT, a tropane analog containing an isothiocyanate group was synthesized (Vaughan et al., 2005). Isothiocyanates react with nucleophiles because the carbon of the isothiocyanate group experiences a lack of electron density. Thiols are the primary target for isothiocyanates,

which to a lesser extent also react with amino and hydroxyl groups (Drobinica et al., 1965). The affinity for reaction with isothiocyanates of the cysteine sulfhydryl group is ~1,000 times more than the affinity of the amino group of lysine. It has also been reported that the reactivity of the hydroxyl group is five times lower than the reactivity of the primary amino group (Breier and Ziegelhoffer, 2000). Therefore, cysteines are the primary targets for isothiocyanates (Breier et al., 1996). A study by Breier and Ziegelhoffer (2000) showed that fluorescein isothiocyanate (FITC) acts as an inhibitor on the P-type ATP-ase by reacting with cysteine in its active site. However, FITC transfers during the digest and sequencing from cysteine to the nearby lysine (Breier and Ziegelhoffer, 2000). This suggests that both cysteine and lysine can be labeled with isothiocyanates. The labeling is dependent on the conditions of the experiment.

Photoaffinity labeling is a valuable technique for localization and study of binding sites (Dorman and Prestwich, 2000). Vaughan et al. (2001) suggested that only one amino acid residue is labeled due to the strict spatial orientation of the binding site. The digestion of peptides followed by HPLC, Edman degradation analysis, and mass spectrometry (Figure 1.9) can significantly contribute to determination of the reactive amino acid residue.

Mutagenesis of DAT

A mutagenesis approach to investigating hDAT structure and understanding the interaction of cocaine with dopamine transporters was undertaken (Uhl and Lin, 2003; Kitayama et al., 1992). Various research groups took a close look at the polar and charged amino acid residues, phenylalanines, prolines, and tryptophanes as the most

likely candidates to interact with cocaine or dopamine (Uhl and Lin, 2003). It was suggested that polar amino acid residues can form hydrogen bonds with the nitrogen of the tropane ring and 3β-benzoyl ester group (Flippen-Anderson et al., 2003). Polar residues may also be involved in the interaction with sodium ions. The aromatic residues phenylalanine and tryptophane may interact with the aromatic phenyl ring of cocaine via π-π interaction and assist in the cation-π interaction (Yamashita et al., 2005; Uhl and Lin, 2003). Additionally, prolines may be situated near the binding site due to formation of breaks or kinks in the α-helical structures (Barlow and Thornton, 1988). Mutations of these residues may influence the cocaine binding, provided that these residues are located within the binding pocket.

Substitution of Asp79 to alanine, glycine, and glutamate in TM1 showed reduced affinity of the cocaine analog to DAT (Kitayama et al., 1992). Triple mutation of F98A, P101A, and F105A in TM2 dramatically reduced WIN 35,428 affinity (Chen et al., 2005). F154 mutation resulted in the selectively reduced WIN 35,428 affinity, while mutation of F155 reduced both substrate and cocaine analog binding affinities (Lin and Uhl, 2002). Other mutations in TM4, TM5, EL3, TM6, TM7, EL4, TM8, TM9, and TM11 were reported to reduce cocaine analog affinities, suggesting their direct or indirect interaction with the cocaine binding site (Uhl and Lin, 2003).

Cysteine mutagenesis is an alternative method for mutational studies (Javitch, 1998). The substituted cysteine accessibility method (SCAM) involves the introduction of cysteine reactive residues and assessment of the accessibility of the cysteines to an aqueous environment by reacting cysteines with membrane-impermeable methanethiosulfonate (MTS) regents (Javitch, 1998). If cysteine residue is accessible to

MTS, the residue can be accessed by the substrate or the ligand, enabling evaluation of its role in cocaine binding (Javitch, 1998). Membrane-permeable and membrane-impermeable thiol-reactive MTS reagents were used. Norregaard and colleagues (2003) suggested that Ala 399 may be involved in the cocaine binding site. Following the [3H]CFT binding, the accessibility of A399 (TM8) mutated to cysteine was assessed using the membrane-impermeable [2-(trimethylammonium)ethyl] methanethiosulfonate bromide (MTSET) cysteine-reactive reagent. The study suggested that cysteine in position 399 was not accessible to the MTS reagent in the presence of the cocaine analog and therefore that it may be involved in the cocaine binding site (Norregaard et al., 2003).

Another study investigated the role of extracellular cysteine 135 and cysteine 342 in cocaine binding (Ferrer and Javitch, 1998). The study showed that the binding of cocaine attenuated the reaction with the MTS reagent, which suggests that these two intracellular residues are involved in a conformational rearrangement during ligand binding (Ferrer and Javitch, 1998). A recent cysteine accessibility study showed that cocaine analogs bind the hDAT in the open conformation while enztropine and rimcazole bind a closed hDAT conformation (Loland et al., 2008). The cysteine residue was inserted at the I159C position, whose accessibility depends on whether the extracellular gate is closed or open and assessed by membrane-impermeable [2-(trimethylammonium)ethyl] methanethiosulfonate (MTSET).

Crystal Structure of Leucine Transporter

As previously noted, X-ray crystallography is one the most precise and advanced techniques for studying the structure of proteins and their binding sites. After the

determination of the LeuT crystal structure, the crystal structures of LeuT with the antidepressants desipramine, chloripramine, and imipramine became available (Singh et al., 2007; Zhou et al., 2007). The studies reported the desipramine binding site situated between the external gate and extracellular loop 4 (Singh et al., 2007; Zhou et al., 2007). Asp 401 was reported to interact with bound ligand. Using computational modeling and mutational studies allowed investigation of the putative structure of the desipramine binding site of DAT (Singh et al., 2007; Zhou et al., 2007). However, it is unclear whether the deziapramine and cocaine binding sites overlap.

Mass Spectrometry

Mass Spectrometry of Membrane Proteins

Mass spectrometry is a powerful technique used for identification of proteins, structure analysis, and investigation of posttranslational modifications (Hakansson et al., 2003; Speers and Wu, 2007; Emmet, 2003). Recent advances in mass spectrometry allow detection of low-abundance proteins with high resolution and high sensitivity (Emmet, 2003). The topology of membrane proteins can be predicted by correlating peptides detected using mass spectrometry with their possible topology using a calculation mechanism based on hydrophobicity (Melen et al., 2003). However, the challenges of investigating membrane proteins still remain (Wu and Yates, 2003; Grant and Wu, 2007).

The low abundance of membrane proteins and the difficulties in their purification require special enrichment strategies along with specialized digest conditions (Lu et al., 2008; Speers and Wu, 2007). The general strategies of enrichment techniques involve

removing membrane-associated proteins and delipidation (Speers and Wu, 2007). Solubilization of membrane proteins may be challenging due to the ion-suppressing effect of a number of detergents, including the widely used sodium dodecyl sulfate (SDS) (Loo et al., 1994).

Membrane proteins are separated on two-dimensional or one-dimensional SDS-PAGE gels during the sample preparation. The choice of separation method for low-abundance proteins is complicated, since two-dimensional electrophoresis provides the purity of the sample but some proteins can be lost; in one-dimensional separation, the complexity of the sample may hinder the detection of the protein or peptide of interest (Speers and Wu, 2007). Recent mass spectrometry approaches have suggested using a gel-free methodology based on sample separation using several different chromatography techniques. Combining several layers of column packing material with different properties (based on hydrophobic and hydrophilic interaction and anion exchange) allows better separation of peptide mixtures (Wu and Yates, 2003).

Fourier Transform Ion Cyclotron Resonance (FT-ICR) Mass Spectrometry for Protein Analysis

Fourier transform ion cyclotron resonance (FT-ICR) is the most advanced mass spectrometry technique for studying biopolymers, including proteins and their complex mixtures (Hakansson et al., 2003). Coupled with the electrospray ionization method, FT-ICR provides high accuracy and outstanding resolving power (Bakalarski et al., 2007). The five parts per million (ppm) accuracy is reported as an acceptable mass accuracy for FT-ICR high-resolution analysis, which allows identification of peptides based on their

accurate mass (Tanaka et al., 2001). However, accurate information about the mass is not sufficient for identification of intact proteins because multiple composition matches can occur (Kuehl and Wang, 2007). To reduce the molecular weight of the analyzed species, chemical and enzymatic digests are used, followed by ultra-accurate mass identification of peptides (Nilsson et al., 2002).

FT-ICR mass spectrometry is a very sensitive technique with reported detection limits in the high attomole to low femtomole range (Quenzer et al., 2001; Witt et al., 2003). Quenzer and colleagues (2001) demonstrated detection of 300 amol of vasotocin in artificial cerebral fluid. Witt and colleagues (2003) reported a 5 fmol detection limit for bovine serum albumin digest. The sensitivity of FT-ICR can be affected by ion suppression due to the interference of the volatile compounds with the formation and evaporation of droplets during electrospray ionization (Annesley, 2003; Sterner et al., 2000). Ion suppression occurs when the sample being analyzed contains a high concentration of salt and for complex samples in general. The sensitivity can be increased by using desalting columns and chromatographic separation prior to mass spectrometry (Annesley, 2003).

Tandem Mass Spectrometry in Detection of Proteins and their Post-translational Modifications

Tandem mass spectrometry (MS/MS) is used for identification of proteins as well as for detection of post-translational modifications, including glycosylation, phosphorylation, and ubiquitylation (Peterman and Mulholland, 2006; Miranda et al., 2005).

There are top-down and bottom-up approaches for proteomics analysis (Speers and Wu, 2007; Whitelegge et al., 2006). The *top-down approach* uses mass spectrometry of intact proteins followed by tandem mass spectrometry analysis. This approach is used to study specific proteins of interest as well as their post-translational modifications (Whitelegge at al., 2006). The coverage of the 8kDa *c*-subunit of ATP synthase (AtpH), a membrane protein with two transmembrane domains, was studied using the top-down approach (Zabrouskov and Whitelegge, 2007). Despite the reported successful analyses of some proteins, this approach is limited by high molecular mass, low abundance, and difficulties in purification (Speers and Wu, 2007).

The *bottom-up approach* is based on digestion of proteins followed by analysis of the produced peptides. This approach also allows identification of peptides and post-translational modifications. However, the sequence coverage may be lower than in the top-down approach (Lu et al., 2008; Wu and Yates, 2003). The ability to identify peptides based only on their accurate mass is one of the main benefits of the bottom-up approach (Lu et al., 2008). Miranda and colleagues reported identification of ubiquitylated amino acid residues of DAT by using trypsin and elastase digests followed by mass spectrometry.

Each data acquisition method for tandem mass spectrometry balances the use of high-resolution FT-ICR with ion trap analysis, maximizing the speed of data acquisition and sensitivity. High-resolution FT-ICR and linear quadrupole ion trap (LTQ) analyses can be performed simultaneously. However, acquiring only high-resolution data can limit the number of detected peptides due to the longer scan time needed for FT-ICR (Bakalarski et al., 2007).

Several different approaches have been reported for the identification of post-translational modifications (Bakalarski et al., 2007; Haas et al., 2006; Sorkina et al., 2005). A recent study reported that a combination of a high-resolution FT-ICR scan with several data-dependent MS/MS scans in a low-resolution ion trap was the optimal data-acquisition method when searching for post-translational modifications of phosphopeptides (Bakalarski et al., 2007). This acquisition method was compared to the low-resolution survey and dependent scans and a high-resolution scan followed by a combination of selected ion monitoring (SIM) and low-resolution ion trap analysis (Bakalarski et al., 2007; Haas et al., 2006). Chemical modification of specific amino acid residues can be determined by using the same strategy as that used for the determination of post-translational modifications.

Seiwert and Karst (2007) developed cysteine-reactive N-(2-ferrocenethyl)maleimide (FEM) to determine the number of free and disulfide-bound thiol groups in a protein. β-lactoglobulin was modified with a cysteine-reactive reagent, digested with trypsin, and analyzed on nanoLC-MS. Only peptides with free cysteines exhibited a mass increase consistent with the mass of FEM (Seiwert and Karst, 2007). The methylation sites of the outer membrane protein B (OmpB) of *Rickeettsia prowazekii* were analyzed using high-resolution mass spectrometry coupled with tandem mass spectrometry. The analysis of the acquired MS/MS data was performed using SEQUEST and scoring algorithm for spectral analysis (SALSA) algorithms (Bakalarski et al., 2007; Schiewe et al., 2004). SALSA enables user-defined analysis of MS/MS data. The search parameter can be a specific pattern, an ion fragment formed in the tandem analysis, or a specified mass loss (Chao et al., 2004; Badghisi and Liebler, 2002). The SEQUEST
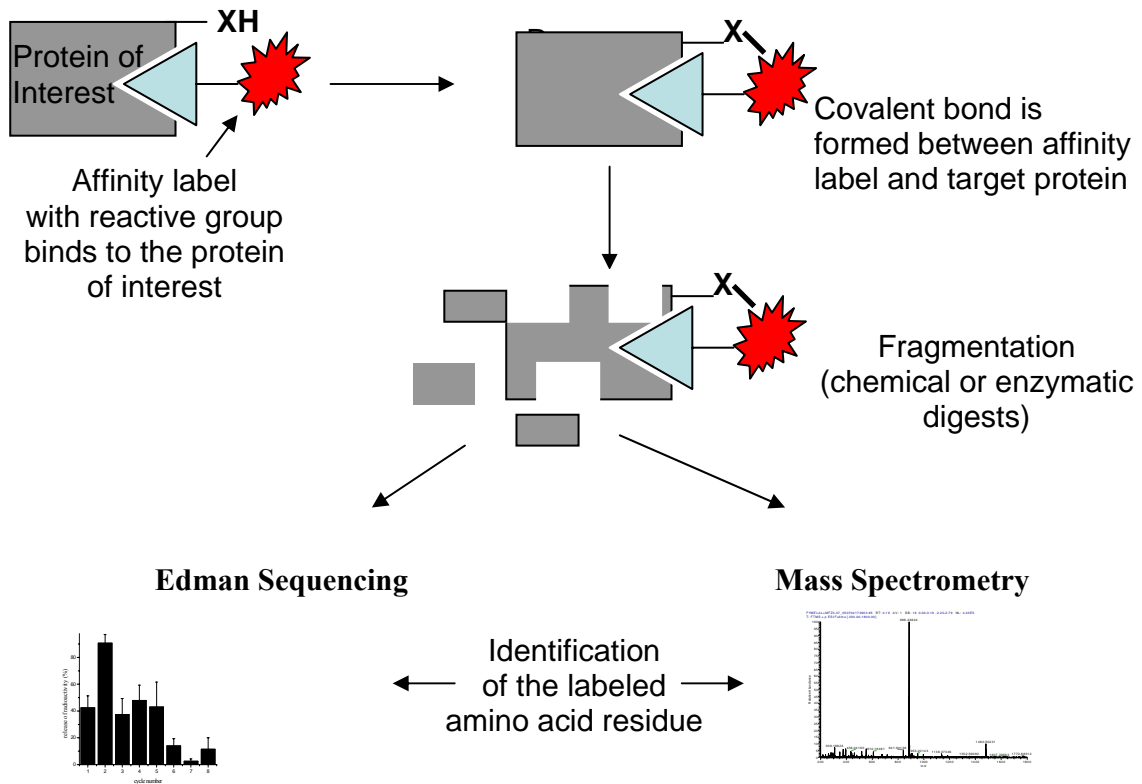
Figure 1.9 Application of affinity labeling, sequencing analysis, and mass spectrometry for the analysis of the binding site of the protein of interest

The labeled target protein is digested and the place of incorporation of the affinity label is detected using HPLC separation followed by Edman degradation or mass spectrometry (modified from Dorman and Prestwich [2000]).

algorithm produces theoretical MS/MS data for peptides from theoretical digest and matches the experimental data with the theoretical data (Zhang et al., 2007). Both algorithms use scoring systems that express the probability of the actual existence of the detected peptide (Schiewe et al., 2004).

This thesis focuses on application of a variety of techniques and developing a methodology to study the dopamine transporter. The ultimate goal of the presented research is to identify the amino acid residues modified by MFZ 2-24 and MFZ 3-37 ligands that irreversibly label hDAT. Based on the performed studies, it is projected that a combination of several affinity labeling techniques with enzymatic and chemical digests, complemented by Edman sequencing and mass spectrometry, can eventually facilitate the identification of the cocaine binding site on hDAT.

Chapter Two

Methods

Cell Culture and Photoaffinity Labeling

Cell Culture Expressing hDAT

HEK cell lines that stably express 3xFLAG-6xHis-hDAT, X5C hDAT, or A90C X5C hDAT were used in this research. Cells were grown on polylysine-treated 150 mm plates (Nunclon delta surface) and 75 mm tissue-treated cell culture flasks (Corning) in a CO_2 water-jacketed incubator (Nuaire, USA) at 37°C with 5% CO_2 content. DMEM/F12 50:50 medium (Cellgro) was supplemented with 10% bovine calf serum, 100 μg/ml penicillin-streptomycin, and 200 mM L-glutamine for all cell lines. Media for wild-type hDAT was additionally supplemented with 0.001% G418.

Membrane Preparation

Plates with cells were washed with filtered KRH buffer (120 mM NaCl, 4.7 mM KCl, 2.2 mM $CaCl_2$, 1.2 mM $MgSO_4$, 1.2 mM KH_2PO_4, 10 mM HEPES, and 10 mM d-glucose, pH 7.4) and with protease inhibitor and subsequently incubated with lysis buffer (1 mM Na_2EDTA, 2mM HEPES) for 10 min at 4°C. Lysed cells were scraped off and centrifuged for 20 min at 16130 rpm at 4°C. After the first centrifugation, membrane pellets were washed with incubation buffer (100 mM NaCl, 50 mM Tris base, pH 7.0) and centrifuged again. The membrane pellets were stored at –40°C (6 plates per pellet).

Photoaffinity Labeling

The membrane pellets were re-suspended in incubation buffer, sonicated for 6 seconds in Heat Systems Ultrasonics model W185, and centrifuged for 20 min at 16130

rpm. The pellets were re-suspended in incubation buffer containing protease inhibitor. Radioactive ligand was added to a 5 nM concentration. The pellets were subsequently incubated for 1 h by shaking on ice in the dark. The sample was transferred into a 5mm dish (Corning) and irradiated with UV light at 254 nm for 4 min using a UV lamp (Upland, USA, model UVG-11). The labeled membranes were centrifuged at 20,000 g for 20 min at 4°C. The pellets were subsequently washed two more times with 1 ml of incubation buffer and centrifuged again at 20,000 g for 20 min at 4°C. The labeled membranes were then incubated with solubilization buffer (1mM EDTA, 150 mM NaCl, 50 mM Tris Cl, 1% Trition, pH 7.4) overnight at 4°C. The pellets were then centrifuged at 31,000 g for 1 hour at 4°C, after which the pellets were discarded. The supernatant contained all the solubilized proteins, including hDAT.

Gel Electrophoresis and Autoradiography

Electrophoresis of hDAT on sodium dodecyl sulfate polyacrylamide gel was performed by the method described by Laemmli (1970). Supernatant containing hDAT was diluted 5:1 with 6X sample buffer (30% glycerol, 70% 50 mM Tris HCl, 0.35 M SDS, 0.6 M DTT, pH 6.8, with 0.001% bromophenol blue) and loaded on the gel. Both 7.5% and 16% SDS-PAGE gels were used. ProSieve Cambrix Color Protein Marker was used for high molecular weight separation on 7.5% gels. A Rainbow Molecular Mass Marker (Amersham) was used for separation of the peptides with low molecular weights on 16% gels. Electrophoresis for the two gels was performed at 70 mA in 1X SDS Electrophoresis buffer prepared from 5X stock solution (pH 8.3) using an Owl Vertical Electrophoresis System. After the electrophoresis, the gel was placed on filter paper and

dried on the gel dryer (BioRad, model 583) for 2 hours at a no more than 80°C. The

dried gel was placed in an exposure cassette (Kodak BioMax MS) with film (Kodak

BioMax MS) and stored at −80°C until developed. The film was developed with a Kodak

developer and fixed with a Kodak fixer in a dark room.   The gel bands corresponding to

labeled hDAT or labeled peptides were excised and subjected to in-gel digest.

In-Gel Chemical and Enzymatic Cleavages

Cyanogen Bromide Digest

The gel bands were rehydrated in 0.1 M NH_4CO_3, cut to fine pieces with a razor,

and placed in eppendorf tubes. A freshly made 1M CNBr solution (Sigma) in 70% TFA

(Pierce) was added to the tubes until it covered the gel pieces (approximately 1 ml in each

eppendorf tube). The tubes were left for 24 hours at room temperature in the dark.

Enzymatic Digests

The TPCK-treated trypsin (Worthington) and thermolysin (Sigma) solutions

containing 1 mg/ml of enzyme in 0.1 M NH_4CO_3 were used to rehydrate the excised gel

bands. After the bands were cut into fine pieces and placed into eppendorf tubes,

additional amounts of enzyme solutions were added. The digest was performed for 24 h

at 37°C.

After the in-gel digest, the excess of solution containing the enzyme or CNBr was

pipetted out and saved. Three consecutive extractions of peptides from the gel were

conducted using 60% (v/v) acetonitrile with 0.1% (v/v) TFA in a sonicating bath

(Branson 1510). 100% ACN with 0.1% (v/v) TFA was used for the fourth extraction. Extraction of peptides formed in the enzymatic digests was handled at room temperature, while extraction of peptides obtained from CNBr digest was performed at 4°C to avoid hydrolysis of the peptides in the presence of TFA. All the extracted fractions were dried down in a speed vac (Eppendorf Concentrator 5301).

High-Performance Liquid Chromatography

HPLC Separation of hDAT Peptides

The dried extractions were dissolved in 200 μL of 60% (v/v) ACN with 0.1% (v/v) TFA and sonicated for 2 hours at room temperature. The sample was filtered using an Ultrafree-MC centrifugal filter device (Millipore) and injected into the HPLC (Hewlett Packard, model 1100). The peptides were separated on a 4.6 mm × 25 cm column (Zorbax) with 5μm C18 packing at 1 ml/min flow rate. The gradient and the solvents used are listed in Table 2.1.

Radioactivity Profile Measurement

Fractions were collected every 1–2 minutes directly into 2 ml eppendorf screw-cap tubes using a fraction collector (Bio-Rad BioLogic BioFrac). Aliquots of each fraction were placed in VWR scintillation vials, and 5 ml of liquid scintillation cocktail (Ultima Gold MVC, Perkin Elmer) was added to each vial. The fractions were counted (Beckman LS 6500) to detect the radioactively labeled peptides. The fractions collected in the eppendorf tubes were used for the Edman degradation experiment.

Time (min)	Solvent A (%) (100 % water, 0.1% TFA), v/v	Solvent B (%) (100 % ACN, 0.1 % TFA), v/v
0	100	0
3	100	0
90	42	58
110	12	88
120	2	98
121	0	100
131	0	100
142	100	0

Table 2.1 The HPLC gradient used to separate peptides obtained from the in-gel digest

A flow rate of 1 ml/min was used. Solvent A was 100% HPLC grade water (Sigma), and Solvent B was HPLC grade 100% ACN. To avoid peptide precipitation in the column, 0.1% TFA was added to each solvent. The solvents were filtered and degassed with He for 15 minutes.

Sequencing of Labeled hDAT Peptides

The Manual Edman Degradation of Labeled hDAT Peptides

The fraction corresponding to the labeled hDAT peptide was dissolved in 50:50 (v/v) water:isopropyl alcohol and applied on PVDF membrane derivatized with arylamine groups (Sequelon-AA kit, Millipore). The membrane was placed on a Mylar sheet and dried at 55°C on a heating block. The mylar sheet with the disk was removed from the heating block, and 100 µl of a freshly made coupling buffer (0.1M 2-(N-morpholino) ethanesulfonic acid) containing 1 mg of 1-ethyl-3-(3-dimethylaminopropyl) carbodiimide (EDAC) in 0.1M MES was added to the disk and incubated for 1 hour at room temperature. The disk was then washed with methanol, acetonitrile, and 25:25:1 (v/v/v) methanol:water:acetic acid. The disk was dried down and subjected to manual sequencing. 500 µl of the coupling reagent (7:1:1:1 (v/v/v)) methanol:water:triethylamine:phenylisothiocyanate (PITC) was added to the 2 ml tube containing the disk, which was then incubated for 10 min at 50°C. After the coupling reagent was removed, the disk was washed five times with methanol. It was subsequently dried on a speed vac, and 500 µl of TFA was added to the disk for 6 min at 50°C. The disk was then washed once with 1 ml of chlorobutane and six times with 500 µl of methanol. The coupling reagent, TFA, and all washes were saved and examined for radioactive iodine on a scintillation counter. The cycles of manual sequencing were repeated. The release of radioactivity was correlated with the labeled amino acid residue.

Chemical Labeling of Synthetic Peptides and Amino Acids

Chemical Labeling with MFZ 3-37

Peptide or amino acid solutions (20 mM) were prepared in methanol. Triethgylamin was added to the solutions at 0.1%. An MFZ 3-37 20 mM solution in methanol was also prepared. The MFZ 3-37 and peptide or amino acid solutions were combined together and incubated for 1 hour on a shaker at room temperature. The reaction mixture was then separated on HPLC. The radioactivity profiles of the collected fractions were counted if tritiated amino acids were used in the reaction.

Examination of C90 as a Potential Labeling Site

3D Modeling of hDAT Using the Spdbv Viewer

A 3D model of TM1 and TM2 hDAT domains was created based on the coordinates of the leucine transporter crystal structure (Yamashita et al., 2005) using the Spdbv viewer (GlaxoSmithKline R&D and the Swiss Institute of Bioinformatics). TM1 and TM2 LeuT$_{Aa}$ domains were represented by ribbon structures. The amino acid residue of interest that corresponded to C90 of hDAT was highlighted. Amino acid residues that corresponded to hDAT were investigated for localization in the 3D structure.

Labeling of hDAT and Mutant hDAT with [^{125}I] MFZ 2-24 and [^{125}I] MFZ 3-37

Wild-type and X5C mutant (provided by Dr. Jonathan Javitch, Columbia University) hDAT in which five out of twelve cysteines (C90, C135, C306, C319, and C342) were

mutated to alanines or phenylalanines were compared. The usual labeling procedure was applied. Membranes containing hDAT were incubated with 5 μM [^{125}I] MFZ 2-24 or [^{125}I] MFZ 3-37 for 1 hour at 4°C. MFZ 2-24 was then irradiated with a UV lamp for 4 min at 254 nm. The membrane pellets were then solubilized, separated on a 7.5% SDS gel, and visualized using autoradiography.

Incubation of hDAT and its Mutants with MTS Reagents

X-A90C, X-A306C, WT, and X5C hDAT mutants were examined. In X-A90C and X-A306C, the same 5 cysteines are mutated out and C90 or C306 are put into the sequence. The labeling levels of WT, X5C, X-A90C, and X-A306C were determined both in the absence and in the presence of the cysteine reactive reagents [2-(trimethylammonium)ethyl] methanethiosulfonate bromide (MTSET) and/or benzyl methanethiosulfonate (MTSBn). The probes reacted with MTS reagents were incubated for 2 min at room temperature with 1 mM MTSET or MTSBn and subsequently incubated with 5 μM [^{125}I] MFZ 2-24 or [^{125}I] MFZ 3-37. 7.5% SDS gel was run. The gel lanes contained wt, wt incubated with MTS reagent(s), X5C, X5C with MTS reagent, X-A90C, X-A90C with MTS reagents, X-A306C, and X-A306C with MTS reagents. The bands corresponding to wild type or mutant were cut out and radioactivity was counted. The lower expression levels of mutant hDAT were taken into account. MTS reagents react with accessible Cys residues and should decrease labeling if Cys residue is at the site of labeling. Thus, the decrease of labeling for one of the Cys mutants indicates that Cys was at the attachment site of the label.

Mass Spectrometry Analysis of hDAT

Sample Preparation

The cell pellets containing hDAT were subjected to the same preparation procedure that was used for the radioactive labeling, but in the mass spectrometry analysis non-radioactive MFZ 2-24 or MFZ 3-37 ligands were used. After the in-gel digestion of the 80-kDa band that corresponded to hDAT on the 7.5% SDS-PAGE gel, hDAT peptides were extracted using 60% acetonitrile with 0.1% TFA solution three times, followed by extraction with a solution of 100% acetonitrile with 0.1% TFA. Thermolysin, CNBr, and trypsin digests were used in the mass spectrometry experiments. The extracted peptides were dried down using a speed vac and combined together. The sample was dissolved in 60% acetonitrile and sonicated for 1 hour at 4°C. HPLC water was then added to the sample to obtain the final 10% concentration of ACN. The sample was injected into an LC-MS system via a 250 μl loop.

Fabrication of In-House LC Nanocolumns

Fused inactivated silica (100–50 μm diameter) was washed with methanol using a pressure bomb under 2000 psi. A 1 μm frit was placed on one end of the fused silica. The Magic C18AQ Beads slurry (Michrom Bioresources Inc.) with a 5 μm particle size and 100 Å pores was suspended in 1 ml of methanol and sonicated for 15 min to ensure a fine distribution of particles in the solvent. Fused silica was filled with the slurry at 2000 psi using a pressure bomb. To assure adequate packing of the material, the column was

then washed with methanol for 30 min. The empty part of the silica tubing was cut, and a 1 μm frit was placed on the other end of the packed column.

Determination of the Mass Spectrometer's Sensitivity to Synthetic Peptides and MFZ 2-24

A series of solutions with different concentrations of FYMELAL synthetic peptide and MFZ 2-24 was made to determine the minimal amounts that could be detected on the nanoLC-MS system. 2.5 to 100 nM solutions were prepared in 60% (v/v) ACN. The solutions were injected using a 2 μL loop on the HPLC column, run on FTMS, and MS/MS-analyzed in an ion trap. The signal intensity was measured. Each run was 20 min long, and each concentration was analyzed in triplicate. 100% ACN with 0.1% (v/v) formic acid was used as a solvent.

Overview of the Mass Spectrometry Experiment

The peptides obtained from the digests were separated on either in-house made or commercially available HPLC columns and analyzed using a nanoelectrospray source on a high-resolution/high mass accuracy LTQ-FT-ICR mass spectrometer (Finnigan, ThermoElectron) that included a linear ion trap (LTQ) front end and a superconducting 7 T magnet inthe back. Simultaneously, MS/MS was performed in the ion trap on the six most intense peaks from the MS run.

The sample was loaded via the 200 μl loop on the in-house column placed inline with an HPLC (Ultimate) and analyzed using the gradient listed in Table 2.1. As the

peptides were eluted from the column, they were electrosprayed into the LTQ FT by a silicatip (New Objective) mounted in the ThermoFinnigan nanospray source.

Alternatively, the sample was loaded on a desalting column (Peptrap, Michrom), washed with 100 μl/min of 90% (v/v/v) water, 10% acetonitrile, and 0.1 % formic acid, and subsequently loaded onto the C18 (Michrom) column for separation. The column was connected directly to the Michrom axial desolvation vacuum-assisted nano capillary electrospray source (ADVANCE).

A variety of gradients were used on the columns. A flow rate of 250 μL/min was used with the standard nanospary source, and 5 μl/min was used with ADVANCE. Solvent A was 100% HPLC grade water (Sigma), and Solvent B was HPLC grade 100% ACN. To avoid peptide precipitation in the column, 0.1% (v/v) TFA was added to each solvent. 100% isopropanol was used in the end of each separation to ensure elution of hydrophobic peptides. The time of analysis ranged from 4 to 6 hours.

A cycle of one full-scan high-resolution mass spectrum (200–4000 m/z) was followed by data-dependent MS/MS spectra ion trap scans of the six most intense peaks observed in the FT scan. The HPLC gradient and the mass spectrometer were controlled by the Xcalibur data system (ThemoFinnigan).

Data Analysis

Pepmap (Bioworks 3.2, ThermoFinnigan) was used to identify peptides from the protein digest separated by HPLC. This program creates an *in-silico* digest of the intact protein and compares theoretical masses of predicted peptides with the ones observed in the experiment. The mass tolerance, the incomplete digest, the character of the disulfide

bonds, and the percentile of the threshold (TIC) are taken into account. Turbosequest (Bioworks 3.2, ThermoFinnigan) was also used. This program searches a combination of the experimental MS and the MS/MS results against the *FASTA* protein databases and theoretical protein digests.

Following the run, the search for hDAT peptides labeled with MFZ 3-37 was conducted using SALSA. SALSA searches for modified peptides in MS/MS scans using specific parameters and reports possible hits and their scores. The searched parameter in this study was the presence of the MFZ 3-37 (595.09 m/z) ion in the MS/MS stage. SALSA picked all the first-stage ions that produced 595 m/z ions in the second (MS/MS) stage. The parent ions generating a 595 m/z product ion were ranked by a scoring algorithm. The highest-ranking ions were compared to peptides from a thermolysin digest of hDAT.

hDAT Affinity Purification

Western Blot Analysis

3xFLAG-6xHis-hDAT was separated on a 7.5% gel on an electrophoresis apparatus. The gel, blotting paper (Whatman), and polyvinylidene fluoride (PVDF) membranes were soaked in transfer buffer (40 mM Tris base, 39 mM Glycine, 10% methanol). The gel was placed on top of the membrane between two pieces of blotting paper and was transferred at 11 V for 2 hours on a BioRad semidry blotting apparatus. The membrane with the transferred proteins was rinsed with methanol and washed with TTBS buffer (125 mM NaCl, 25 mM Tris HCl, pH 8.0, 0.1% Tween 20) for 5 min.

Blocking buffer (5% dried milk in TTBS) was applied for 30 min at room temperature. The membrane was then washed with TTBS three times for 5 min at room temperature. Primary antibody against the FLAG epitope (Sigma) was applied at 1:10,000 dilution. The antibody was diluted in blocking buffer. The PVDF membrane was incubated with the antibody mixture for 1 hour at room temperature with shaking. Following incubation with primary antibodies, the PVDF membrane was washed for 10 minutes with TTBS at room temperature. This procedure was repeated three times. A secondary antibody, directed toward the primary antibody, containing a phosphatase-conjugated IgG (Pierce) was diluted 1:10,000 in blocking buffer. The membrane was incubated with the secondary antibody solution for 1 hour at room temperature. After the incubation with the secondary antibodies, the membrane was washed for 10 min with TTBS at room temperature. This procedure was repeated three times. The PVDF membranes were developed using NBT/BCIP (Pierce). The development was stopped by rinsing the membrane with distilled water.

hDAT Purification Using FLAG M2 Affinity Chromatography

Solubilized 3XFLAG-6xHis-hDAT was diluted in FLAG binding buffer (50 mM Tris, 150 mM NaCl, 105 glycerol, 1% Triton) and incubated with the FLAG M2 affinity gel (SIGMA) column. Following the incubation, the column with attached hDAT was washed five times with 1 ml FLAG binding buffer, and 3XFLAG-6X-His-hDAT was eluted with 0.1 M glycine.

Purification of Labeled hDAT Using MFZ 3-37 Antibodies

hDAT was labeled with [^{125}I] MFZ 2-24 as described above. The solubilized hDAT was digested with thermolysin (2 mg/ml) in solubilization buffer for 24 hours at 37°C. Soybean protein (2 mg) was added to each 1 ml of the digest. Labeled hDAT peptides were purified using a MFZ 3-37 antibody column. As a purification procedure, 500 μl of UltraLink Immobilized NeurAvidin Protein (Pierce) was placed in a 2 ml disposable gravity column (Talon, Clontech) and equilibrated with 2.5 ml of binding buffer (0.1 M phosphate, 0.15 M NaCl, pH 7.2). Biotinylated monoclonal MFZ 3-37 antibodies (provided by Dr. Jonathan Javitch, Columbia University) were diluted in half with binding buffer and applied to the column for overnight incubation at 4°C. The column was then washed with 5 ml of binding buffer. Thermolysin digest solution was added to the column, which was then incubated for 30 min at room temperature. The column was washed with 5 ml of binding buffer. The antigen was eluted with 60% ACN, 0.1% TFA since the normally recommended elution buffer was not able to dissociate the formed antigen-antibody complex. All the eluted fractions and washes were collected and analyzed using HPLC and a radioactivity counter.

Chapter Three

Results

Analysis of [^{125}I] MFZ 2-24 Labeled hDAT

hDAT was labeled with [^{125}I] MFZ 2-24 and digested using CNBr, thermolysin, or a combination of these two digests performed consecutively. The peptides produced in the digests were separated on HPLC. The radioactivity profiles of the peptides labeled with [^{125}I] MFZ 2-24 were obtained. In addition, the reactions of synthetic hDAT peptides with the MFZ 2-24 analog provided an estimate for the retention time of the peptides of interest. The effect of the label on peptides and single amino acids was also assessed. An Edman degradation study was performed to determine which amino acid residues were labeled.

WIN 35,428 Protection Experiment

hDAT was labeled with the photoaffinity label [^{125}I] MFZ 2-24 both in the presence and in the absence of hDAT inhibitor WIN 35,428, enabling analysis of the relation between MFZ 2-24 and the cocaine binding site. Solubilized hDAT was then separated on 7.5% SDS-PAGE gel (Figure 3.1). The observed band between 80 and 125 kDa corresponded to hDAT labeled with [^{125}I] MFZ 2-24 in the absence of an inhibitor. In contrast, the addition of WIN 35,428 prior to the ligand produced no band corresponding to the labeled hDAT on 7.5% SDS gel, indicating that [^{125}I] MFZ 2-24 and WIN 35,428 share the same binding site.

CNBr Digest of [^{125}I] MFZ 2-24 Labeled hDAT

hDAT labeled with [^{125}I] MFZ 2-24 was chemically digested with 1 M CNBr in 70% TFA solution. The produced peptides were separated on 16.5% SDS-PAGE gel. hDAT peptides labeled with [^{125}I] MFZ 2-24 migrated to the 2.5–6.5 kDa region (Figure 3.2). The radioactive band was removed from the gel and the peptides were extracted and analyzed on HPLC to obtain the radioactivity profile (Figure 3.3). Only one main peak at 79 min was detected. It was attributed to the [^{125}I] MFZ 2-24 labeled peptide formed after the CNBr digest. The labeled peptide had the same retention time as PLFYM reacted with MFZ 3-37 (Figure 3.9).

To evaluate the stability of [^{125}I] MFZ 2-24, the ligand was tested under the same conditions as those of the actual digest (Figure 3.4). The majority of the label did not decompose after 24 hours of exposure to 1 M CNBr in 70% TFA. It exhibited an 84 min retention time, which matched the retention time of the control sample containing the label incubated in 100% acetonitrile. Only a small amount of the label decomposed under the harsh CNBr/TFA conditions, producing a 65 min peak, which was likely the product of decomposition.

Thermolysin Digest of [^{125}I] MFZ 2-24 Labeled hDAT

A thermolysin digest of [^{125}I] MFZ 2-24 labeled hDAT was separated on HPLC, and a radioactivity profile of the run was obtained (Figure 3.5). The initial profile of the thermolysin digest yielded 73 min and 78 min peaks. However, it was noticed that when separating such a complex mixture, the retention times of peptides may shift. Both the 73 min and the 78 min peaks were re-separated on HPLC using the same gradient. The 73

without WIN 35,428   with WIN 35,428
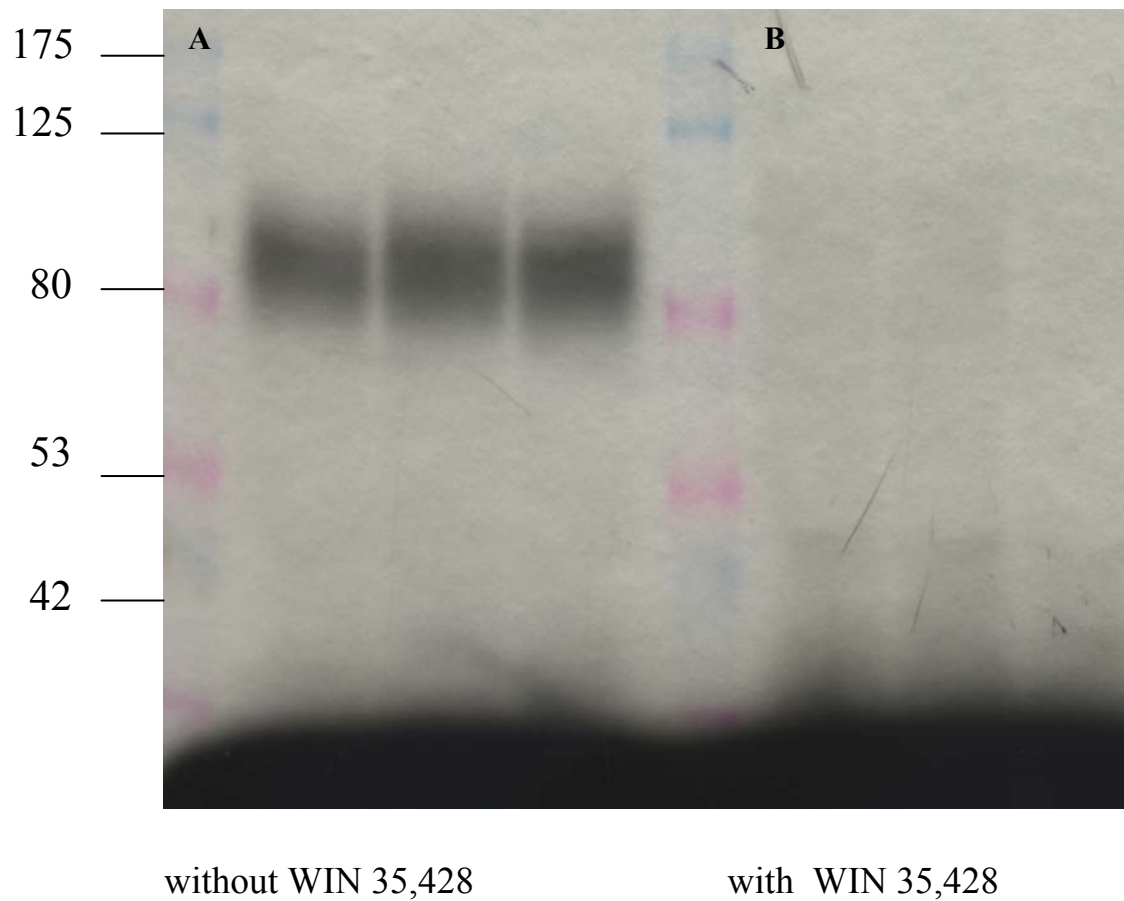
Figure 3.1 Autoradiograph of 7.5% SDS-PAGE separated [^{125}I] MFZ 2-24 labeled

intact hDAT in the presence and in the absence of the WIN 35,428 inhibitor

A. Intact hDAT labeled with [^{125}I] MFZ 2-24 corresponds to the band between 80 and

125 kDa. B. [^{125}I] MFZ 2-24 does not label hDAT in the presence of the WIN 35,428

inhibitor.
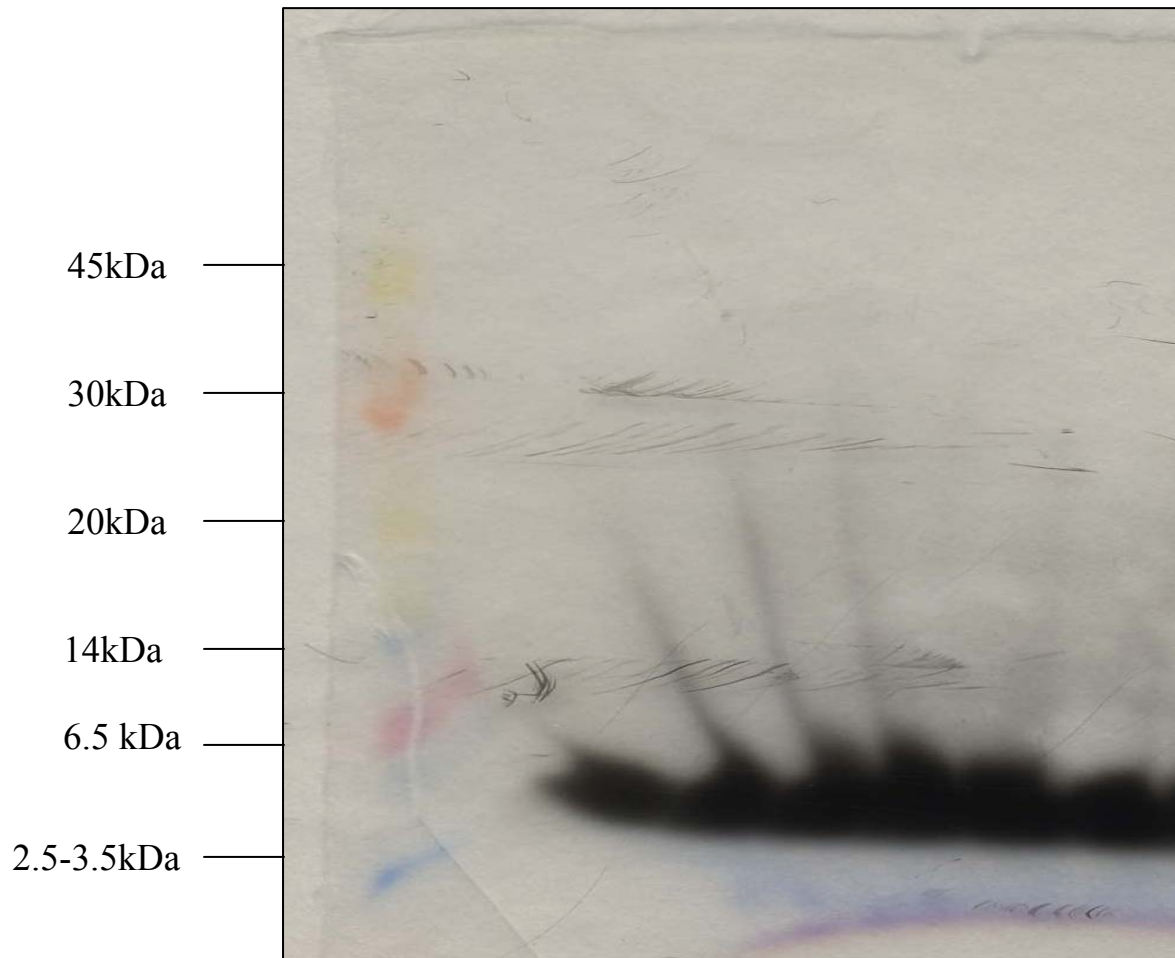
Figure 3.2 Autoradiograph of 16.5% SDS-PAGE separated CNBr peptide labeled with [125I] MFZ 2-24

hDAT labeled with [125I] MFZ 2-24 was chemically digested with CNBr and separated on a 16.5% gel. The labeled peptide migrated at 2–6 kDa.
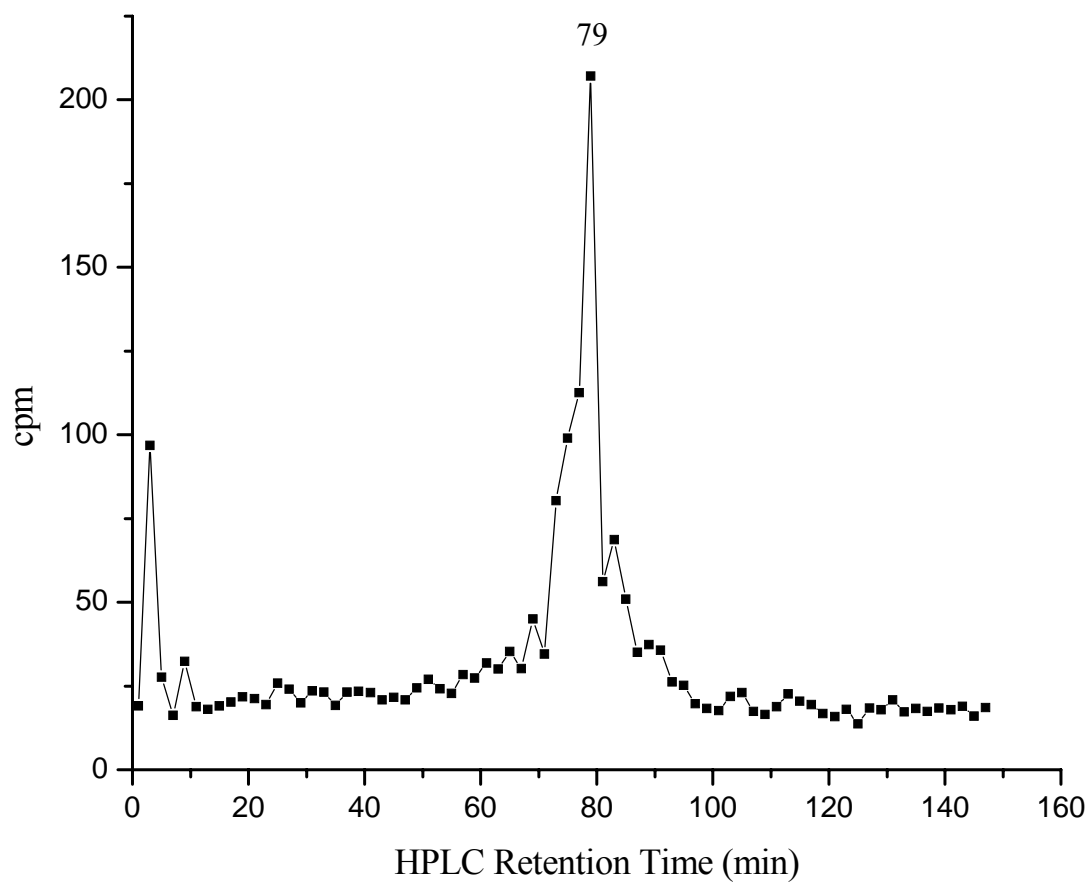
Figure 3.3 Radioactivity profile of CNBr digest of [¹²⁵I] MFZ 2-24 labeled hDAT

The major peak of radioactivity was observed at 79 min, which was likely a [^{125}I] MFZ 2-24 labeled peptide formed after the CNBr digest.
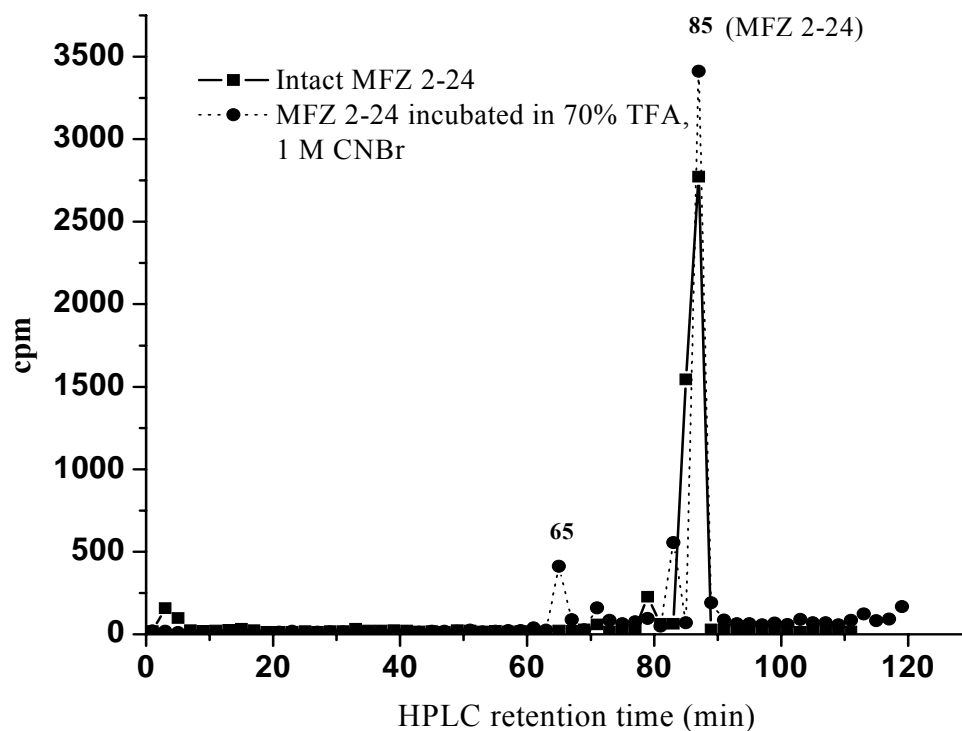
Figure 3.4 Stability of [^{125}I] MFZ 2-24 under the conditions of the CNBr digest

[^{125}I] MFZ 2-24 was incubated in a solution containing 1 M CNBr in 70% (v/v) TFA for 24 hours at room temperature. The radioactivity profiles of HPLC runs showed a major 85 min peak for both the control and the label incubated in the CNBr solution. However, exposure to harsh conditions led to insignificant decomposition of the ligand corresponding to the 65 min peak.

min peak shifted to 63 min, and the 78 min peak shifted to 72 min (Figure 3.6). These 63 min and 72 min peaks are likely the actual retention times for the labeled peptide produced in the thermolysin digest.

Figure 3.7 shows the radioactivity profile of the secondary CNBr digest of the labeled 63 min peptide obtained from the thermolysin digest. The fraction corresponding to the 63 min peak was incubated with 1 M CNBr in 70% TFA for 24 hours and subsequently separated on HPLC. As a result, the radioactivity peak shifted to 77 min, indicating that the initial 63 min peptide contained methionine. The increase in the retention time was attributed to the increased influence of the label on the retention time of the shorter labeled peptide.

Edman Degradation Analysis of the [^{125}I] MFZ 2-24 Labeled hDAT Peptide

A radiolabeled hDAT peptide obtained from a complete thermolysin digest was analyzed by the manual Edman degradation technique (Figure 3.8), performed by U. Danilenko and Dr. T. Henderson. The 63 min peptide was attached to a Sequelon-AA disk via the C-terminal end. It was subsequently exposed to reagents, which removed one N-terminal amino acid residue during each cycle. The radioactivity was monitored after each cycle. The second cycle produced the largest and statistically different ($p < 0.01$) radioactivity release, as compared to the other cycles. The experiment was repeated 7 times; 8 cycles were performed in each experiment. The release of radioactivity during the second Edman degradation cycle indicated that the second amino acid of the peptide was labeled.
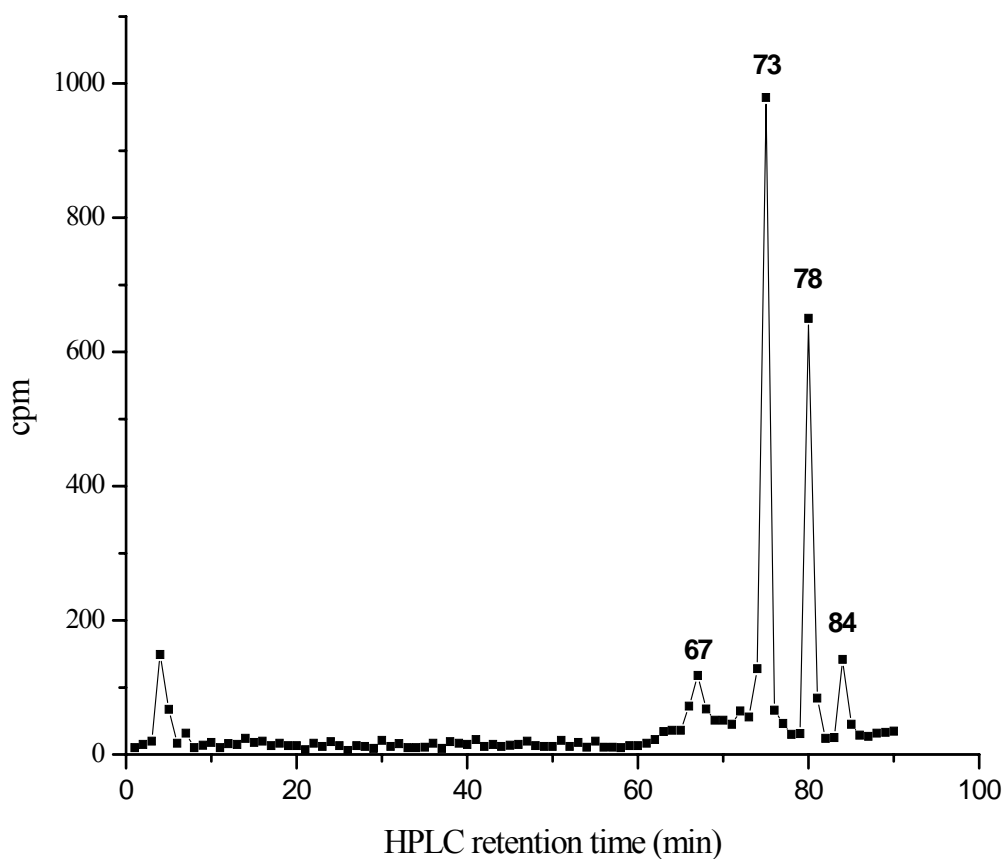
Figure 3.5 Radioactivity profile of the thermolysin digest of [^{125}I] MFZ 2-24 labeled hDAT

[^{125}I] MFZ 2-24 labeled hDAT was digested with 1 mg/ml thermolysin for 24 hours at 37°C. The digest mixture was separated on HPLC. Two major radioactivity peaks at 73 min and 78 min were produced. However, it was noticed that due to the high concentration of peptides in the sample, the retention times may be shifted compared to the true retention times.
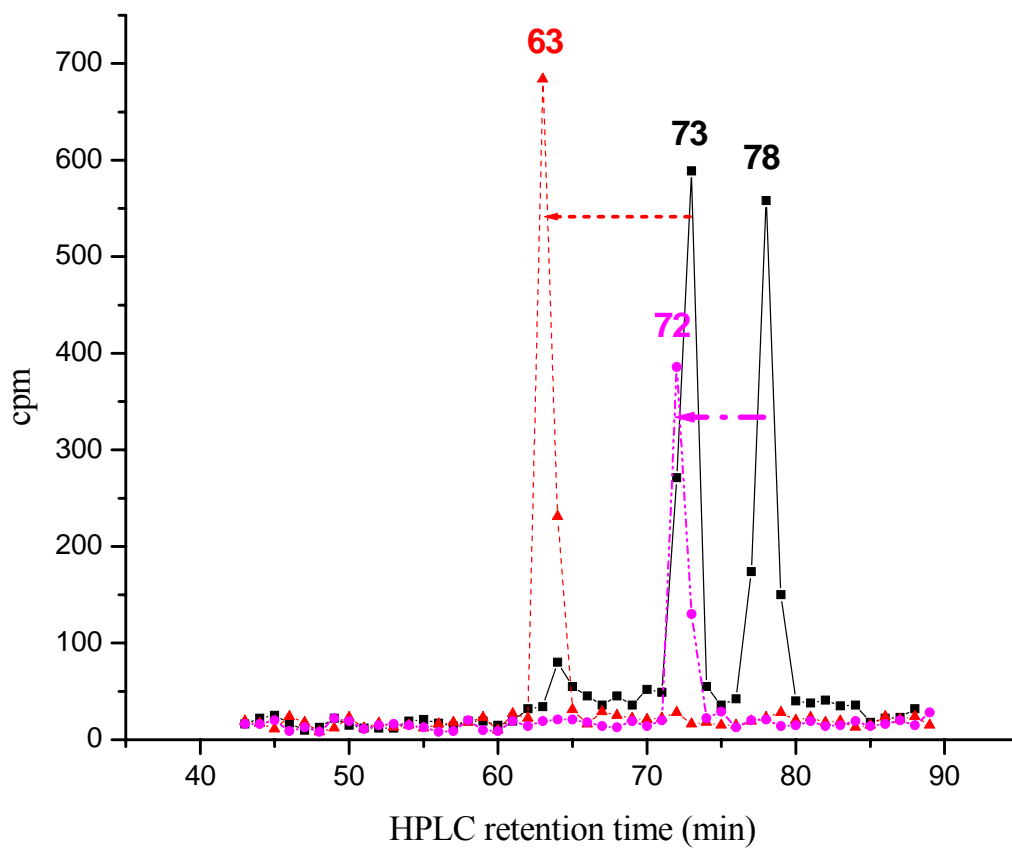
Figure 3.6 Radioactivity profile for re-runs of the 73 min and 78 min peaks

The 73 min and 78 min peaks were individually separated on HPLC to establish the true retention times for the labeled thermolysin peptides. The initial 73 min peak shifted to 63 min, and the 78 min peak shifted to 72 min. These 63 min and 72 min peaks are considered the true retention times for the thermolysin peptides.
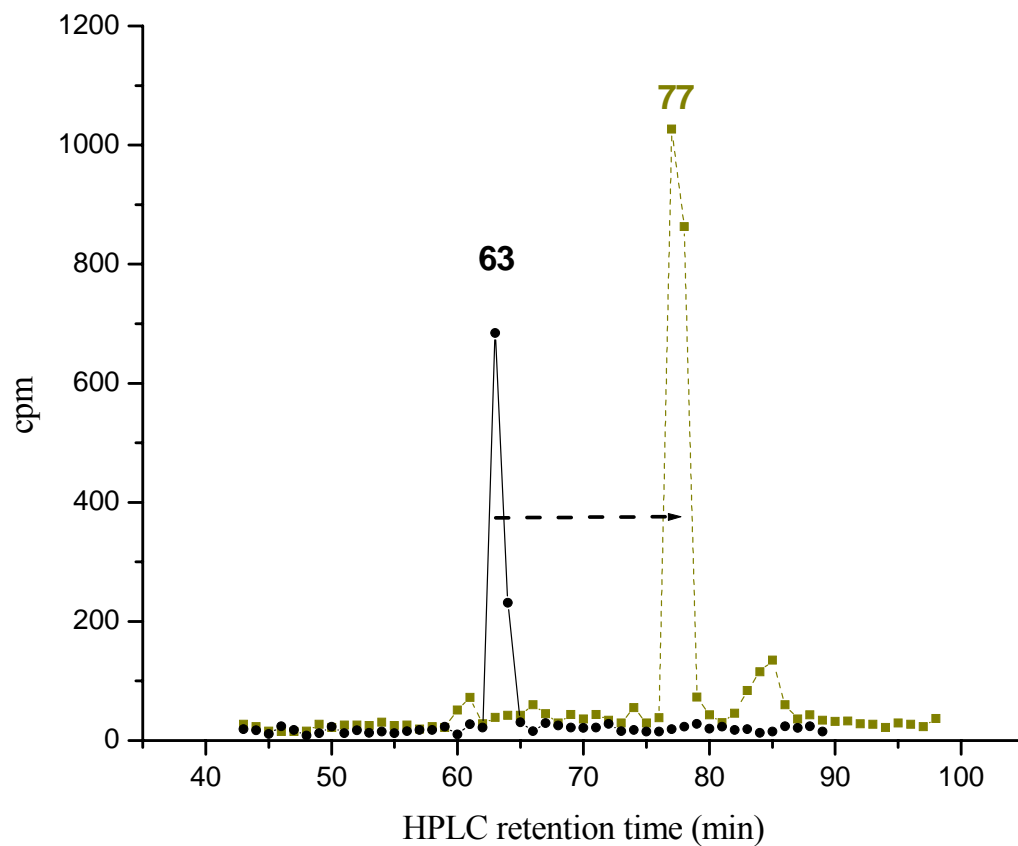
Figure 3.7 Radioactivity profile for the CNBr-digested [¹²⁵I] MFZ 2-24 labeled peptide from the thermolysin digest

The CNBr digest of the peptide corresponding to the 63 min peak shifted the retention time of the labeled peptide to 77 min.
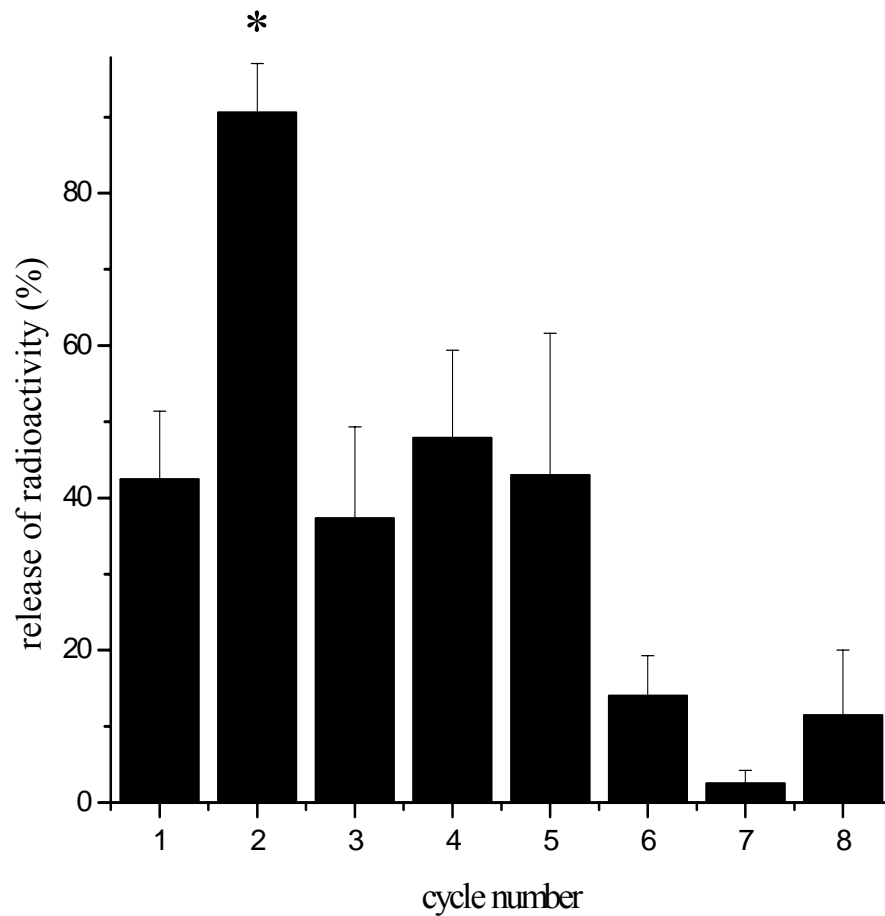
Figure 3.8 Edman degradation of the peptide obtained from the thermolysin digest of hDAT labeled with MFZ 2-24

A major release of radioactivity was observed at the second cycle of the Edman degradation analysis, demonstrating that the second amino acid residue was labeled. The experiment was performed 7 times. The second cycle was statistically different from the rest of the cycles ($p < 0.01$). The arylamine disk was counted after 7 cycles.

Effect of the Label on the Retention Time of Peptides and Amino Acids

To confirm the retention times of the labeled peptides obtained in the CNBr and enzymatic digests, suspected synthetic peptides and amino acids were reacted with both radioactive and non-radioactive versions of MFZ 2-24. Several attempts to react peptides with the label-containing azido group were made both in solution and in solid state. However, due to the low yield of the reaction, the products were never detected with the UV detector during HPLC separation of reaction mixtures. The products also could not be detected by counting the radioactivity profile of the reaction mixtures containing [^{125}I] MFZ 2-24. Therefore, the isothiocyanate analog of MFZ 2-24 was used to obtain higher yields of the products. Isothiocyanates are commonly used in chromatographic techniques to visualize amino acids during HPLC separation. Isothiocyanate reacts with amino groups of lysines, arginines, and a free N-terminal amino group of peptides or amino acids. Up to 90% yields were reported for the products when using the isothiocyanate analog. The retention time of the reaction product of the peptide with MFZ 3-37 should be similar to the retention time of the product of the reaction with MFZ 2-24. Synthetic peptides were reacted with an excess of MFZ 3-37 and subsequently separated on HPLC. Tritiated amino acids were used in reactions with isothiocyanate due to the difficulty of the product detection with the UV detector. Fractions were collected every 1 min and counted on a scintillation counter.

The peptide of interest, PLFYM, was reacted with MFZ 3-37 (performed by Dr. Sara Wirtz; data not shown). Controls for MFZ 3-37 and PLFYM were performed to obtain their UV traces and to detect the retention times. The 90 min peak corresponded to the excess of free MFZ 3-37. The unlabeled peptide had a retention time of 51 min. The
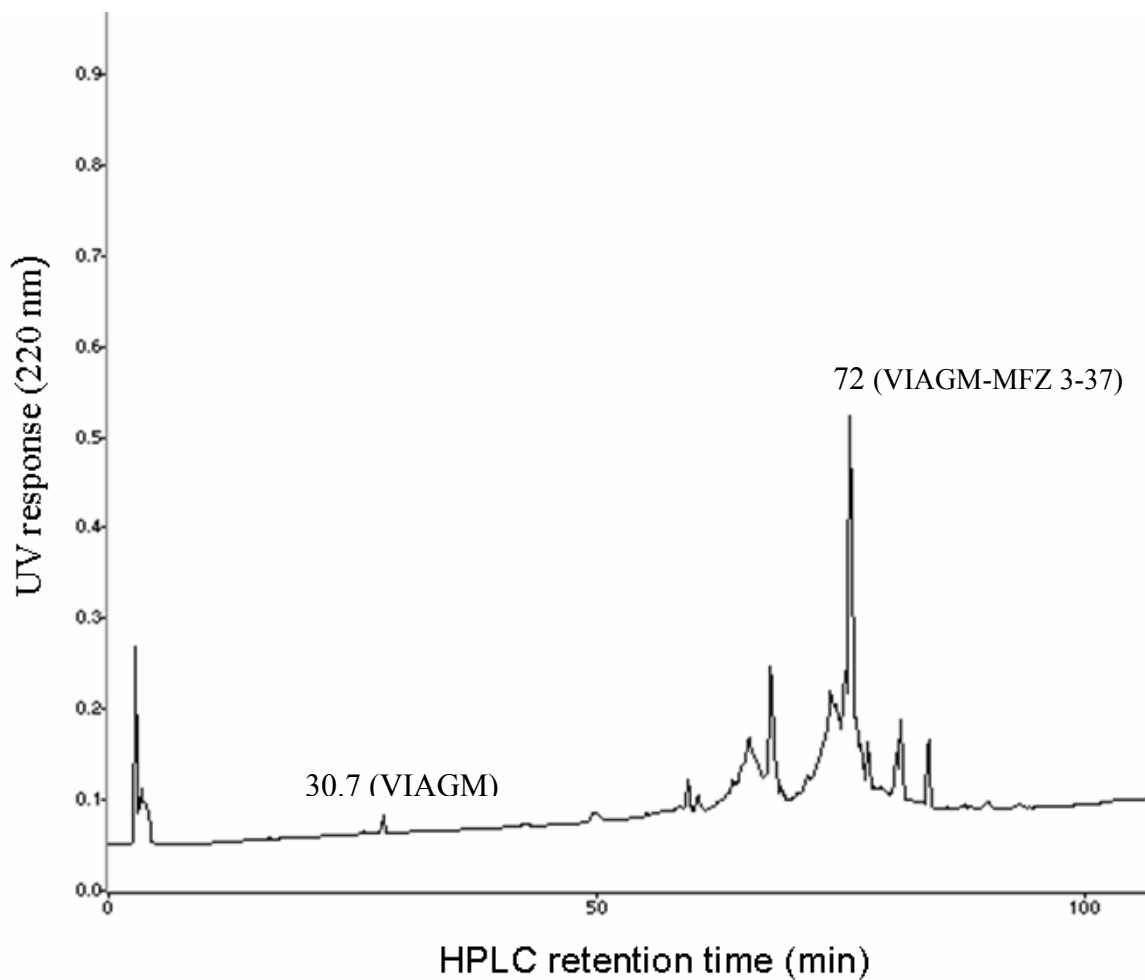
Figure 3.9 HPLC chromatogram of MFZ 3-37 reacted with VIAGM

The peak at 30.7 min is VIAGM. This result was confirmed by mass spectrometry analysis of the fractions corresponding to the 72 min peak.
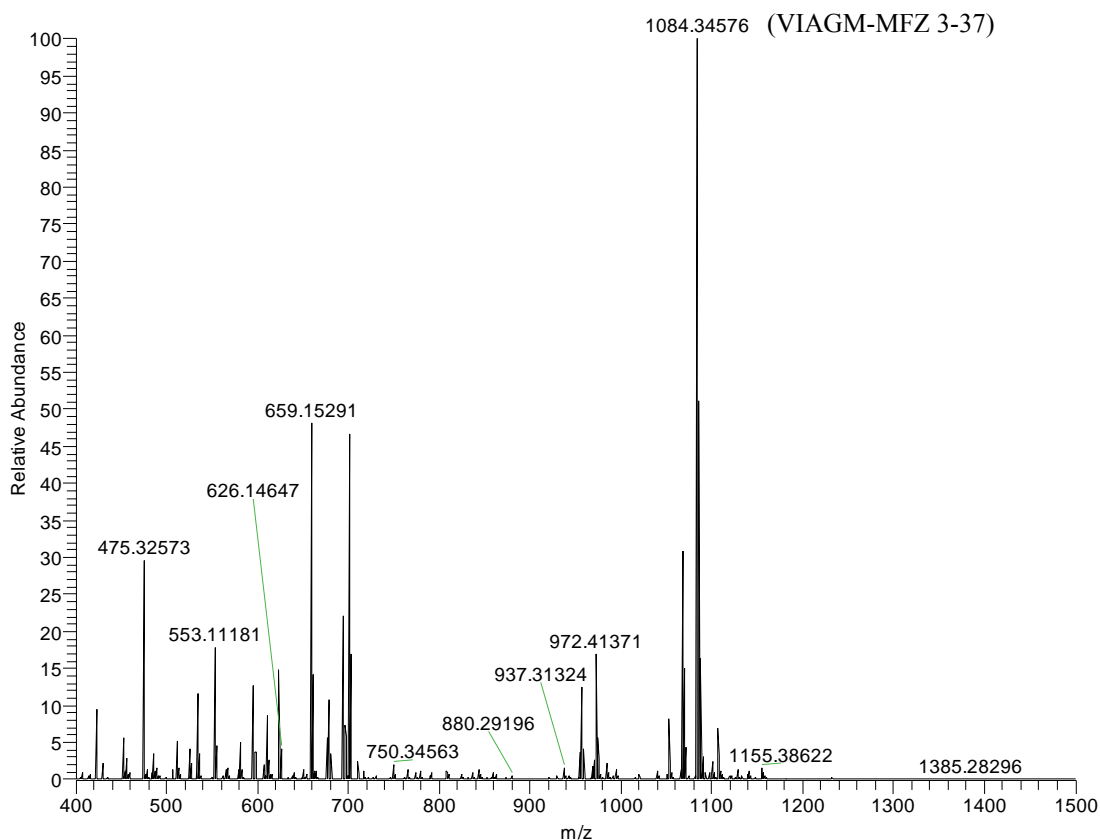
Figure 3.10 Mass spectrometry analysis of the product of the reaction of synthetic VIAGM peptide with MFZ 3-37

The reaction mixture was separated on HPLC and the fractions corresponding to the peaks were collected and subsequently analyzed by mass spectrometry. VIAGM labeled with MFZ 3-37 has a mass of 1084.34576 m/z (theoretical M+H$^+$ 1084.32985 m/z; -1.72 ppm accuracy) and retention time of 72 min. Screening of other fractions showed that several side products were formed.
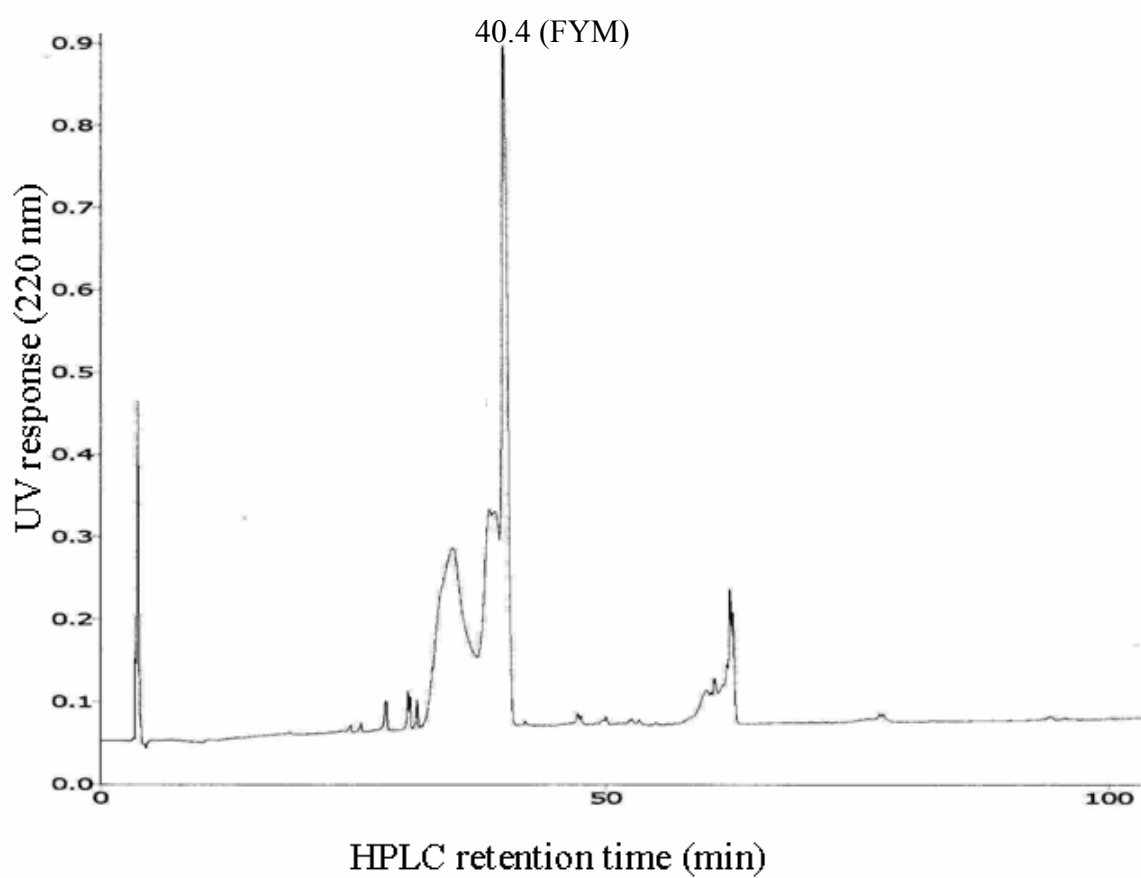
Figure 3.11 HPLC chromatogram of synthetic hDAT TM2 peptide FYM

The peptide produced the peak at 40.4 min.
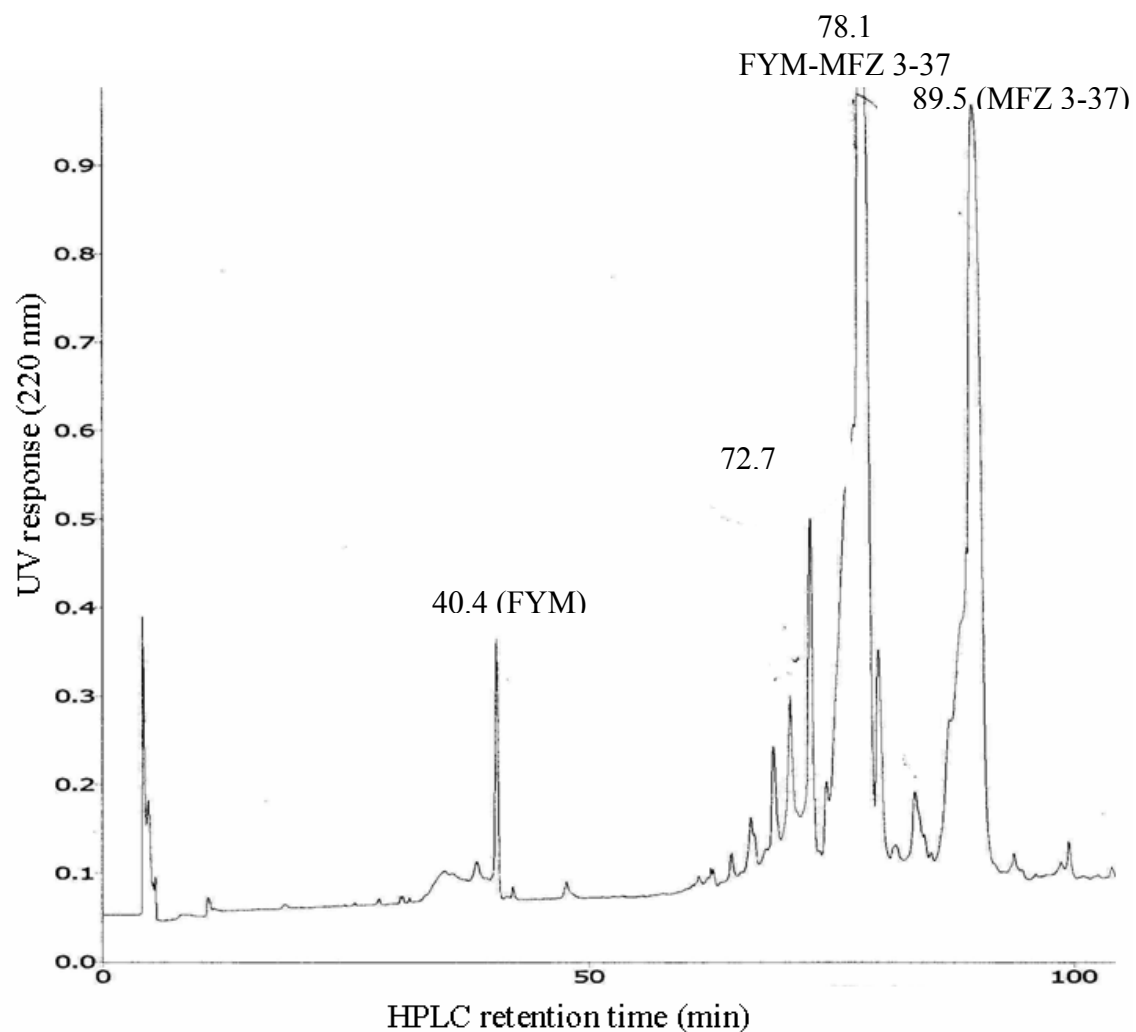
Figure 3.12 HPLC chromatogram of MFZ 3-37 reacted with synthetic FYM peptide

The peak at 40.4 min is FYM and at 89.5 min is the free MFZ 3-37. Two new peaks were produced in the HPLC analysis at 72.7 min and 78.1 min. Mass spectrometry analysis of the fractions corresponding to those peaks confirmed that the 78.1 min peak is the product and the 72.7 min peak is a side product.
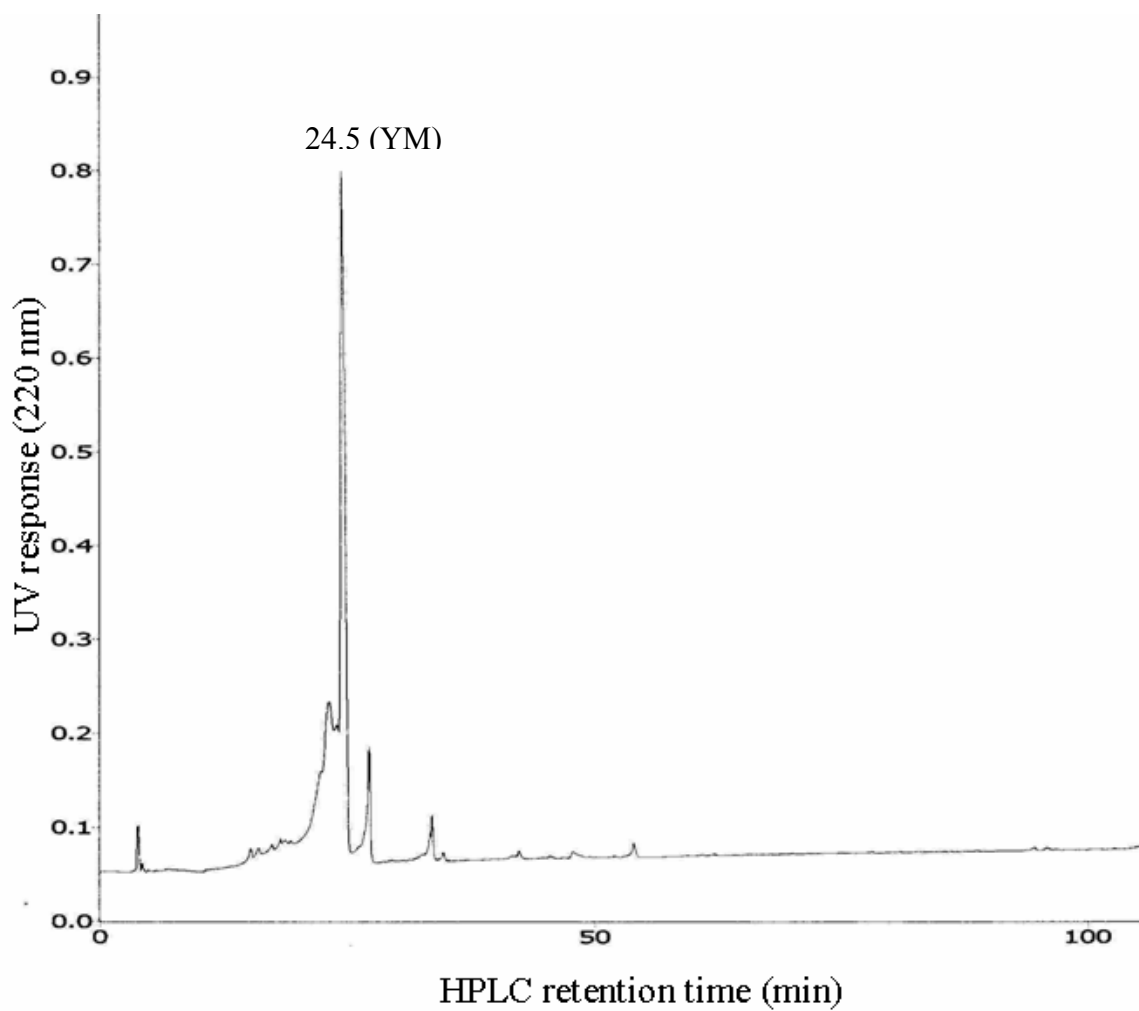
Figure 3.13 HPLC chromatogram of synthetic hDAT TM2 peptide YM

The peptide produced the peak at 24.5 min.
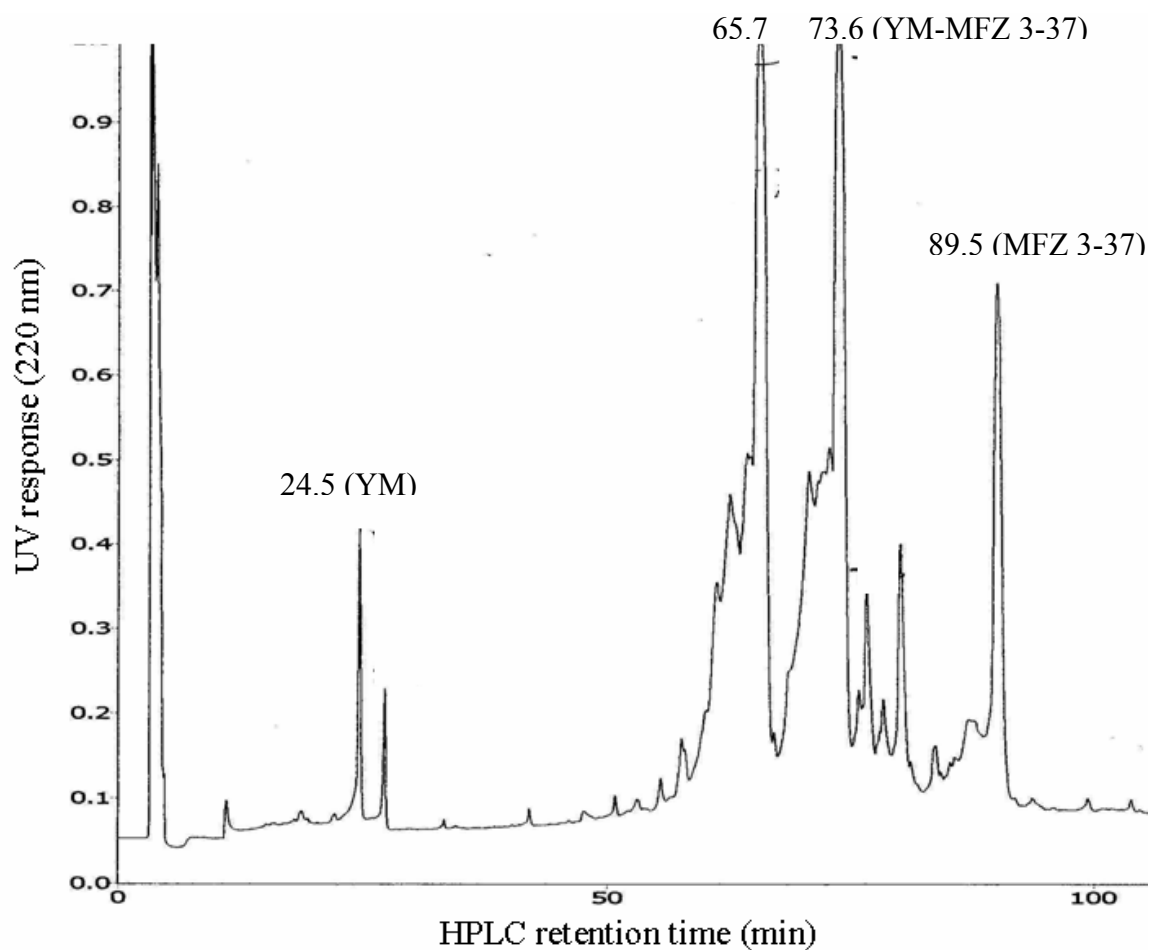
Figure 3.14 HPLC chromatogram of MFZ 3-37 reacted with YM

The peak at 24.5 min is YM and at 89.5 min is the free MFZ 3-37. Two new peaks were produced by HPLC analysis at 65.7 min and 73.6 min. Mass spectrometry analysis of the fractions corresponding to the 65.7 min and 73.6 min peaks confirmed that the 78.1 min peak is the product and the 72.7 min peak is a side product.
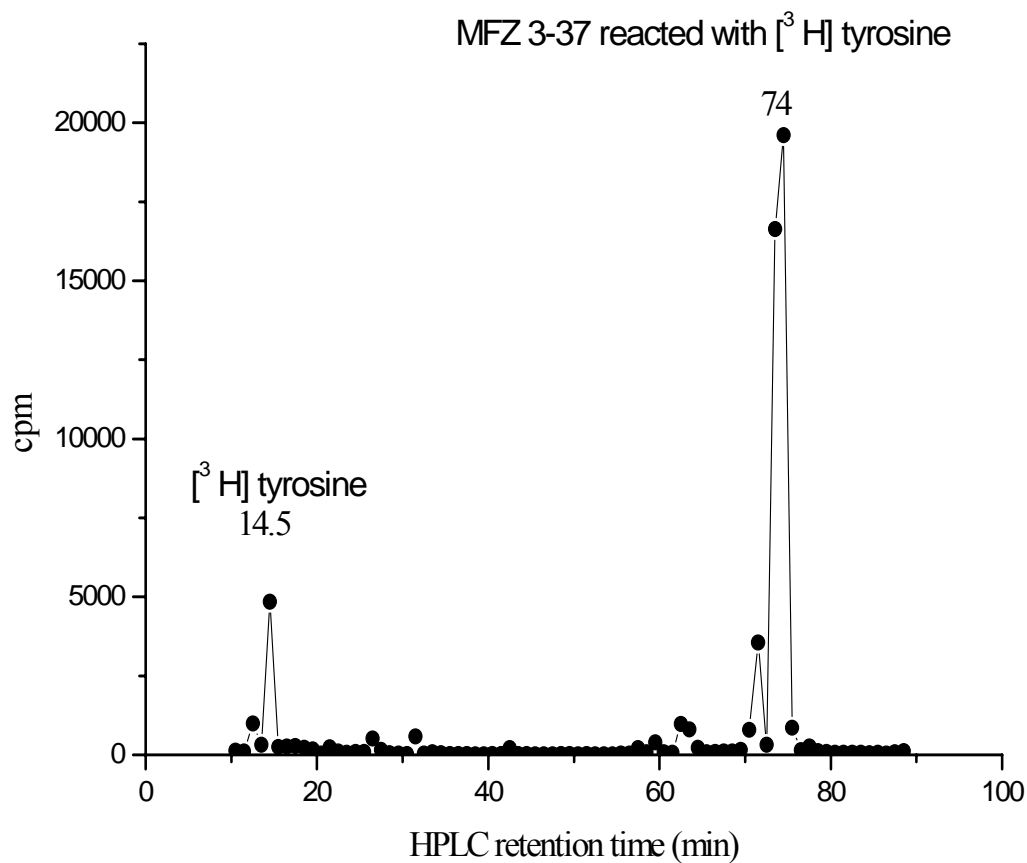
Figure 3.15 Radioactivity profile of MFZ 3-37 reacted with [^{3} H] tyrosine

The 14 min peak is [^{3} H] tyrosine, as confirmed by the control experiment, and the 74 min

peak is the product of the reaction. The label shifted the retention time of tyrosine by 59.5

min. MFZ 3-37 has retention time of 89.5 min.

Peptide/ Amino Acid	HPLC RT (min.)	HPLC RT of Peptide/Amino Acid Labeled with MFZ 3-37	Change in RT (min)
PLFYM*	51.4	79	27.6
FYM	40.4	78.1	37.7
VIAGM	30.7	72	41.3
YM	24.6	73.6	49
[^{3}H] W	26.5	80.5	54
[^{3}H] M	6.5	62.5	56
[^{3}H] Y	14.5	74	59.5
[^{3}H] F	17.5	81.5	64

Table 3.1 Summary of the HPLC retention times for synthetic peptides, amino acids, and products of their reactions with MFZ 3-37

Synthetic peptides and amino acids were reacted with MFZ 3-37. The effect of the label on HPLC retention was assessed. Synthetic FYM, VIAGM, and YM were labeled with MFZ 3-37 and separated on HPLC. Fractions corresponding to the product were collected and analyzed by mass spectrometry to confirm the formation of the product. Tritiated amino acids were reacted with MFZ 3-37 and separated on HPLC. Fractions were collected every 1 min, and radioactivity was counted. *Reaction of MFZ 3-37 with PLFYM was performed by Dr. S. Wirtz.

new product peak had a 79 min retention time that corresponded to the 79 min retention time of the labeled hDAT peptide produced from the CNBr digest. The change in the retention time was 28 min.

VIAGM had a retention time of 30.7 min (not shown). Reaction of VIAGM with MFZ 3-37 produced several products. The fractions corresponding to the peaks were collected and subsequently analyzed by mass spectrometry. The product with 1084 m/z was detected in the fraction corresponding to the 72 min retention time (Figure 3.10). The label had a much larger effect on the VIAGM retention time (41 min shift) than on the retention time of the product of the reaction with PLFYM (Table 3.1).

FYM was reacted with MFZ 3-37 and separated on HPLC, and the new product peaks were analyzed by mass spectrometry. Two new peaks at 78.1 min and 72 min corresponded to the products with and without iodine (Figure 3.12). The retention time for FYM was 40.4 min (Figure 3.11).

Figure 3.14 shows the results of HPLC separation for the reaction of YM with MFZ 3-37. Two new peaks appeared at 68 min and 73.6 min. The 73.6 min peak was the product. The YM retention time of 24.6 min was confirmed by running a control (Figure 3.13). The label attachment changed the retention time of the peptide by 49 min.

To further investigate the effect of the label on the retention time, single amino acids were reacted with MFZ 3-37. Table 3.1 summarizes the retention times, which were 17.5 min, 6.5 min, 14.5 min, and 26.5 min for [3H] phenylalanine, [3H] methionine, [3H] tyrosine, and [3H] tryptophan, respectively. Addition of MFZ 3-37 changed the retention times by 64 min, 56 min, 59.5 min, and 54 min, respectively. An example

radioactivity profile (that for the reaction of [^{3}H] tyrosine with MFZ 3-37) is shown in Figure 3.15. The summary of the effect of the label on the retention times of peptides and single amino acids is presented in Table 3.1. The change in retention time is dependent on the properties of the particular peptide or amino acid. The label affects amino acids more significantly than it does the larger peptides (Table 3.1). However, the peptides contribute more significantly to the properties of the product.

Analysis of Cysteine 90 hDAT Mutant

Previous immunoprecipitation studies pointed to TM1 or TM2 as the sites of photoincorporation of MFZ 2-24 (Vaughan et al., 2005). To determine the sites of MFZ 2-24 and MFZ 3-37 incorporation, cysteine mutants obtained from Dr. Javitch's group were used (Ferrer and Javitch, 1998). The specific object of interest in this research was Cys90, since it is located at the top of TM1. To investigate the importance of C90 for the MFZ compounds, the X5C hDAT was studied. X5C is formed by mutation of five cysteines—C90, C135, C306, C319, and C342—to alanines or phenylalanines. In addition to WT and X5C, X-A90C and X-A306C hDAT were tested, in which wild-type cysteines were placed back one at a time. The labeling levels of WT, X5C, X-A90C, and X-A306C were determined both with and without the cysteine reactive reagents [2-(trimethylammonium)ethyl] methanethiosulfonate bromide (MTSET) and benzyl methanethiosulfonate (MTSBn). Information about the labeling levels can lead to better understanding of the effects of C90 on labeling and help locate the site of label incorporation.
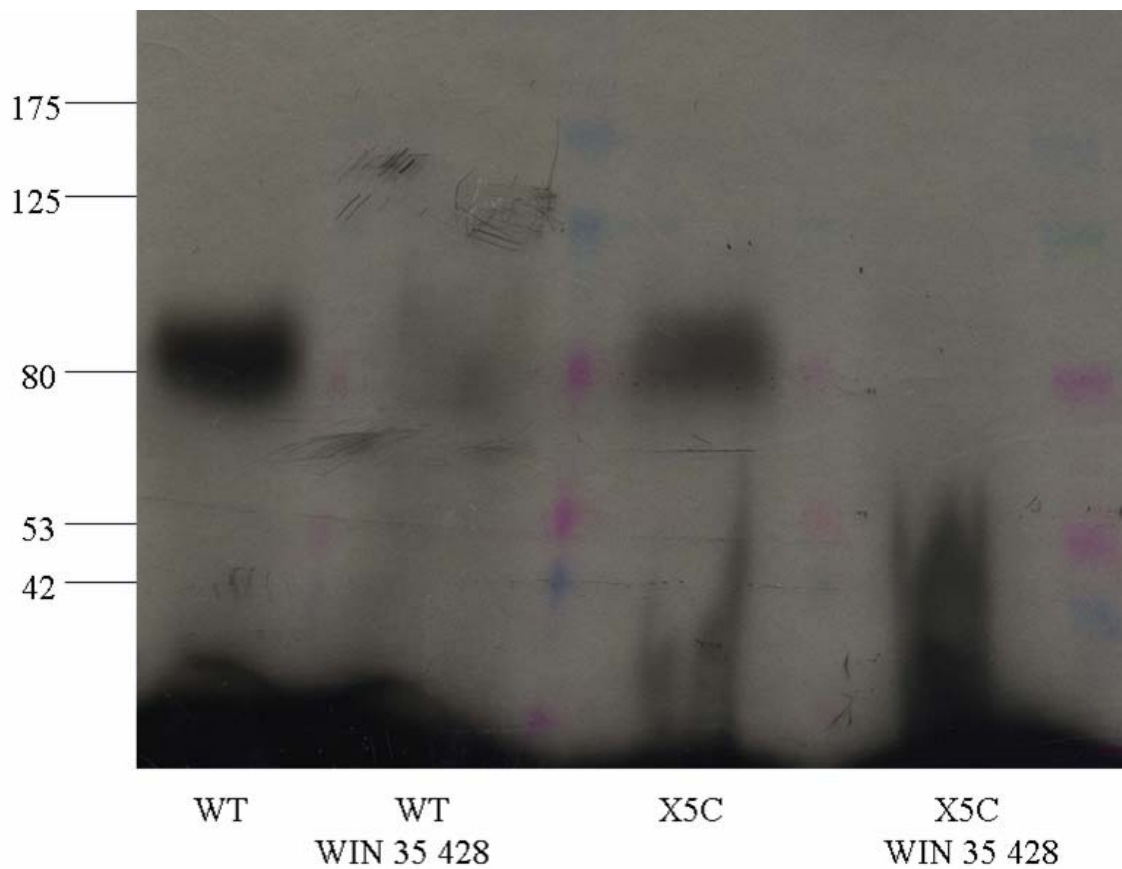
Figure 3.16 Autoradiograph of 7.5% SDS-PAGE separated [^{125}I] MFZ 2-24 labeled wild-type and X5C hDAT in the presence and in the absence of the WIN 35,428 inhibitor

Wild-type and X5C hDAT labeled with [^{125}I] MFZ 2-24 corresponded to the bands between 80 and 125 kDa. [^{125}I] MFZ 2-24 did not label hDAT in the presence of the WIN 35,428 inhibitor.
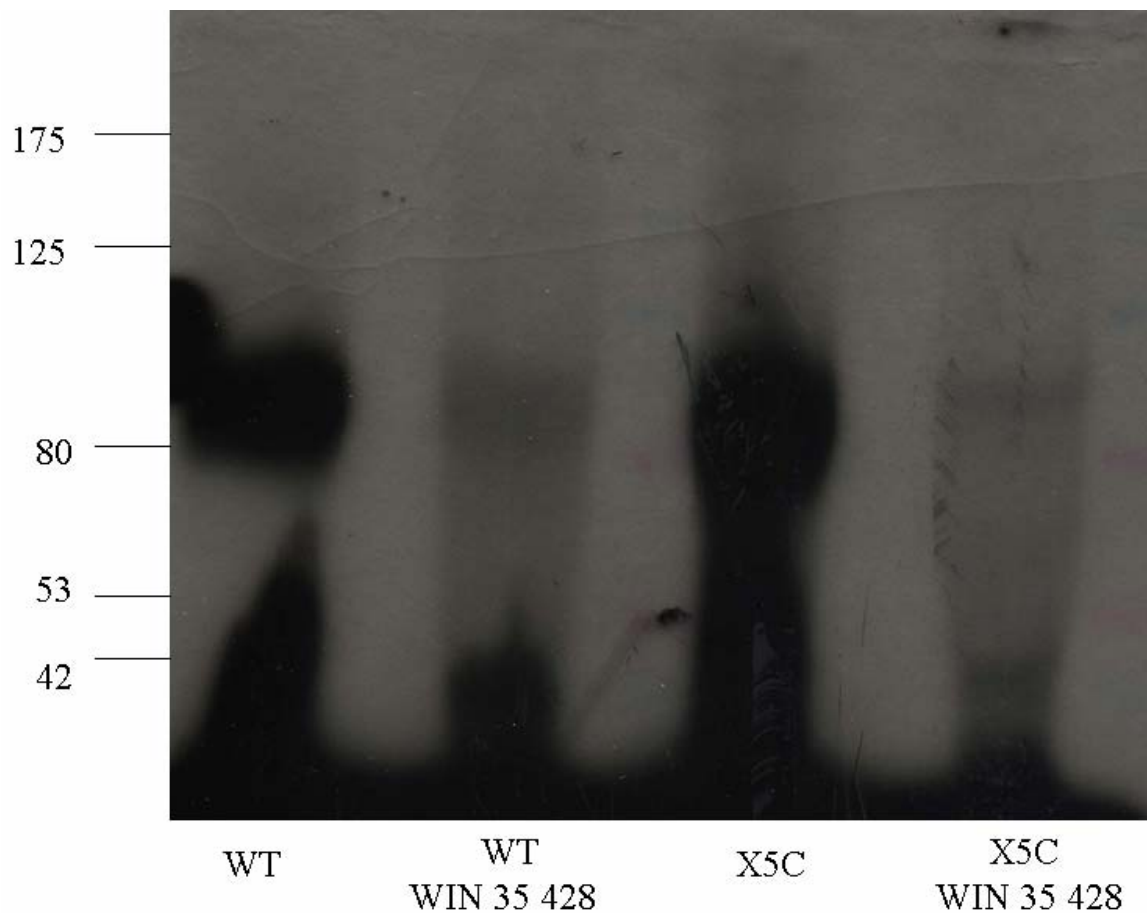
Figure 3.17 Autoradiograph of 7.5% SDS-PAGE separated [^{125}I] MFZ 3-37 labeled wild-type and X5C hDAT in the presence and in the absence of the WIN 35,428 inhibitor

Wild-type and X5C hDAT labeled with [^{125}I] MFZ 3-37 corresponded to the bands between 80 and 125 kDa. [^{125}I] MFZ 3-37 exhibited a low level of nonspecific labeling in the 80 to 125 kDa region in the presence of the WIN 35,428 inhibitor.
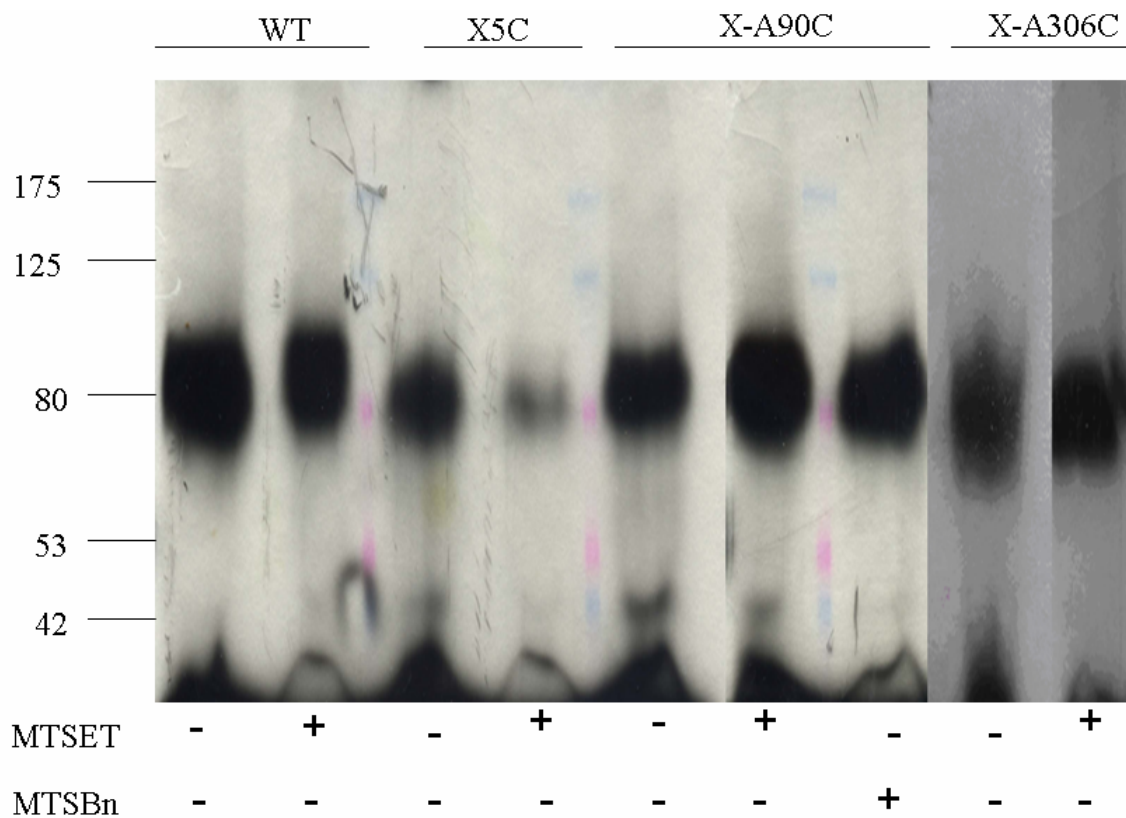
Figure 3.18 Autoradiograph of 7.5% SDS-PAGE separated [^{125}I] MFZ 2-24 labeled wild-type, X5C, X-A90C, and X-A306C hDAT in the presence and in the absence of MTS reagents

The usual labeling procedure was used to label wild-type, X5C, X-A90C, and X-A306C hDAT mutants with [^{125}I] MFZ 2-24 in the presence and in the absence of MTS reagents. Labeled hDAT was separated on a 7.5% SDS gel. Bands corresponding to the labeled hDAT were cut out and counted on a scintillation counter.

Affinity Label ing of Wild-Type (WT) and X5C hDAT

[^{125}I] MFZ 2-24 labels both wild-type (WT) hDAT and X5C hDAT at the same level, once the X5C expression level of 50% from WT is taken into account (Ferrer et al., 1998) (Figure 3.16). The WT and X5C hDAT were labeled with [^{125}I] MFZ 2-24, separated on a 7.5% SDS gel, and visualized using autoradiography. Simultaneously, the cocaine analog WIN 35,428 was added to the WT and X5C membrane preparations and subsequently labeled with [^{125}I] MFZ 2-24 to determine whether [^{125}I] MFZ 2-24 is linked to the binding site of X5C hDAT and to assess nonspecific labeling. The observed band between 80 and 125 kDa corresponded to WT and X5C hDAT labeled with [^{125}I] MFZ 2-24 in the absence of the inhibitor. The results confirmed that [^{125}I] MFZ 2-24 has the same binding site as the inhibitor WIN 35,428. The bands were excised from the gel and counted on a scintillation counter. The experiment was repeated three times.

Figure 3.17 shows the autoradography of WT and X5C hDAT labeled with [^{125}I] MFZ 3-37 in the presence and in the absence of the cocaine analog WIN 35,428. The labeled hDAT was separated on 7.5% SDS gel. The bands corresponding to 80–125 kDa are [^{125}I] MFZ 3-37 labeled WT and X5C hDAT. Low levels of nonspecific labeling for WT and X5C hDAT were observed in the presence of the cocaine analog.

Role of C90 in hDAT Photoaffinity Labeling with [^{125}I] MFZ 2-24

To further investigate the role of C90 in hDAT photoaffinity labeling with [^{125}I] MFZ 2-24, mutants of X-A90C, X-A306C, WT, and X5C hDAT were examined. The same 5 cysteines are mutated out in X-A90C and X-A306C, and C90 or C306 are put back in the sequence instead of them. Membranes containing WT, X5C, X-A90C,
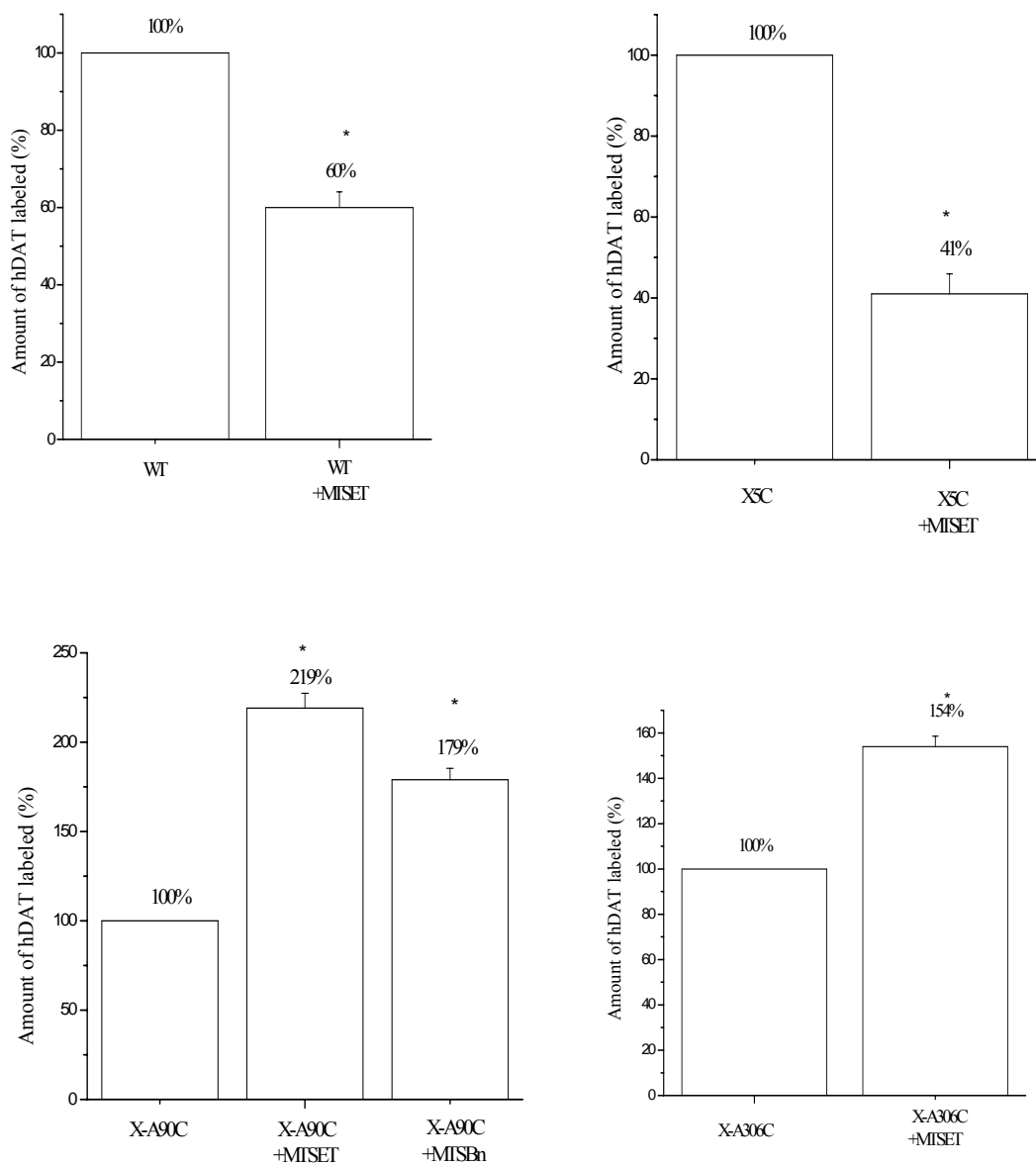
Figure 3.19 Effect of MTS reagents on [^{125}I] MFZ 2-24 labeling

WT, X5C, X-A90C, and X-A306C hDAT mutants were labeled with [^{125}I] MFZ 2-24 in

the presence and in the absence of MTS reagents. The bands corresponding to the labeled

hDAT were counted on a scintillation counter. The increase or the decrease in labeling in

the presence of MTS reagents was presented as a percentage of the controls (WT, X5C,

X-A90C, or X-A306C hDAT). Labeling of WT and X5C hDAT decreased in the

presence of MTS reagents and increased for X-A90C and X-A306C when the same MTS

reagents were used. Data are mean±s.d. from three different experiments (n=3).

* indicates statistical significance (Student's t-test; p<0.05).
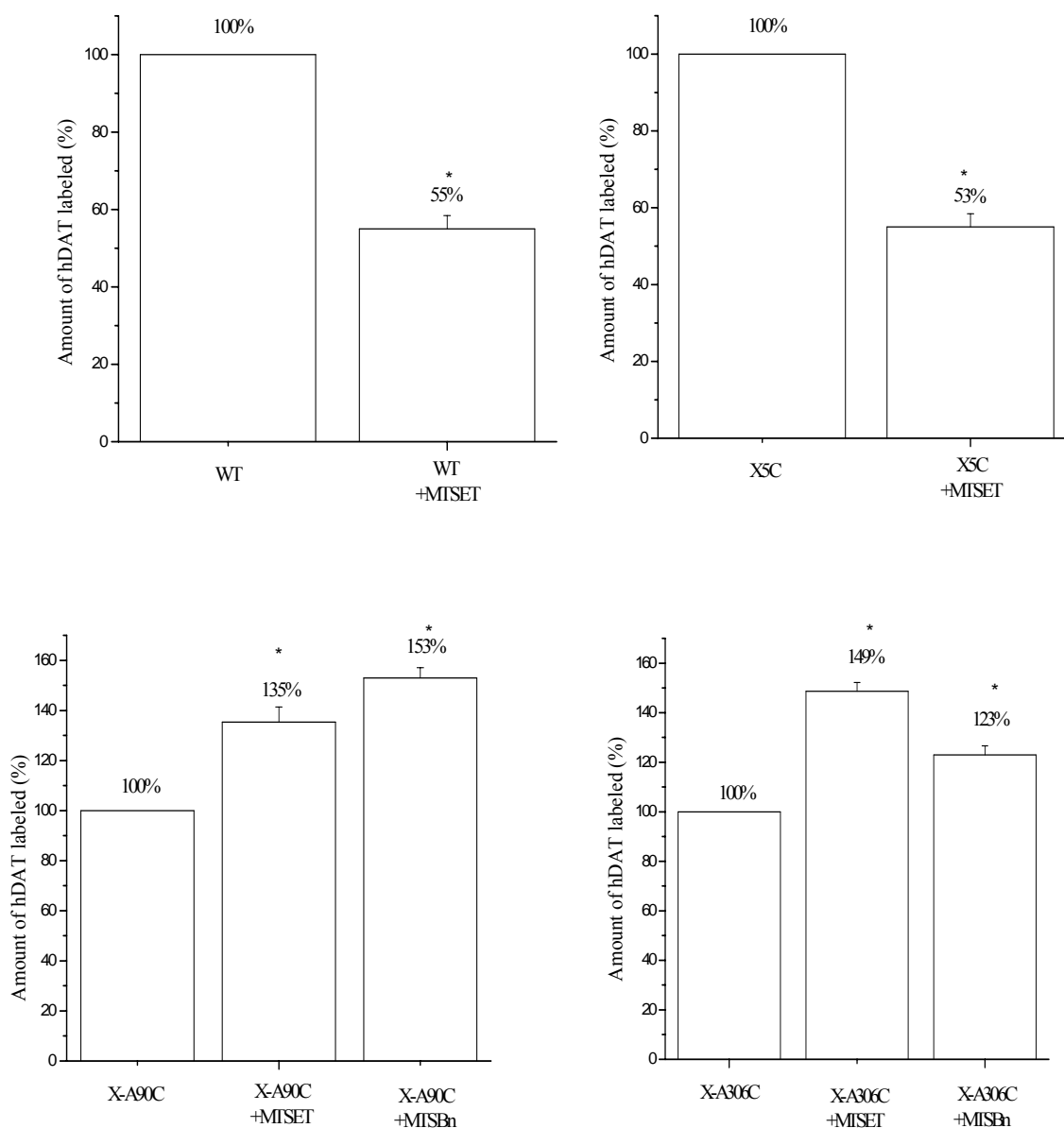
Figure 3.20 Effect of MTS reagents on [^{125}I] MFZ 3-37 labeling

WT, X5C, X-A90C, and X-A306C hDAT mutants were labeled with [^{125}I] MFZ 3-37 in

the presence and in the absence of MTS reagents. The bands corresponding to the labeled

hDAT were counted on a scintillation counter. The increase or the decrease in labeling in

the presence of MTS reagents was presented as a percentage of the controls (WT, X5C,

X-A90C or X-A306C hDAT). Labeling of WT and X5C hDAT decreased in the presence of MTS reagents and increased for X-A90C and X-A306C when the same MTS reagents were used. Data are mean±s.d. from three different experiments (n=3).

* indicates statistical significance (Student's t-test; p<0.05).

and X-A306C hDAT were incubated with 5 μM [^{125}I] MFZ 2-24 for 1 hour at 4°C and then UV irradiated. The labeling levels of WT, X5C, X-A90C, and X-A306C were determined both with and without the cysteine reactive reagents MTSET and/or MTSBn. The membrane pellets reacted with MTS reagents were incubated with 1 mM MTSET or MTSBn for 2 min at room temperature and subsequently incubated with MFZ 2-24. The membrane pellets were then solubilized, separated on 7.5% SDS gel, and visualized using autoradiography (Figure 3.18).

Figure 3.19 shows the relative labeling levels for WT, X5C, X-A90C, and X-A306C labeled with [^{125}I] MFZ 2-24 in the presence and in the absence of MTSET or MTSBn. Interestingly, WT and X5C labeled in the presence of MTSET exhibited decreases to 60% and 41%, correspondingly. However, X-A90C and X-A306C showed a significant increase in labeling when reacted with MTSET or MTSBn. X-A90C hDAT labeling increased to 219% when reacted with MTSET and to 179% when reacted with MTSBn. X-A306C was used as a control. The [^{125}I] MFZ 2-24 labeling levels also increased in the presence of MTSET, to 154%.

Role of C90 in hDAT Affinity Labeling with [^{125}I] MFZ 3-37

[^{125}I] MFZ 3-37 labeling levels in the presence of MTS reagents were also tested (Figure 3.20). The labeled hDAT mutants were separated on 7.5% SDS gel and visualized using autoradiography. The bands corresponding to the labeled hDAT were cut from the gel and counted on a scintillation counter. The labeling levels for WT and the mutants without the MTS reagents present were used as the full scale (100%). The [^{125}I] MFZ 3-37 labeling levels of hDAT mutants reacted with MTS reagents were

expressed in percents relative to the controls. The [^{125}I] MFZ 3-37 labeling levels of WT and X5C decreased to 55% and 53%, respectively, when the pellet containing hDAT was exposed to the MTSET reagent prior to labeling. However, X-A90C labeling increased to 135% when the mutant was reacted with MTSET and to 153% when reacted with MTSBn. The X-A306C control exhibited the same tendency as X-A90C, and reaction with MTSET and MTSBn increased the labeling to 149% and 123%, correspondingly.

Mass Spectrometry Analysis of hDAT

Mass spectrometry was used to identify the labeled amino acid residue. Preliminary investigation showed that the sensitivity of the mass spectrometry method was sufficient for the detection of small quantities of peptides and possibly of the labeled peptides. Studies were performed to determine the detection limits for the label and hDAT peptides using standard and ADVANCE (Michrom) nanospray sources. A comparison of these two sources was also performed. Several nanoLC-MS runs made it possible to identify the hDAT peptides.

Attempts to detect MFZ 2-24 labeled hDAT peptides obtained from CNBr or thermolysin digests were not successful due to the insufficient amounts of labeled peptides. This difficulty originated from a very low yield of the reaction with MFZ 2-24. The main focus of the study was transferred to identifying the amino acid residue that reacted with the isothiocyanate analog MFZ 3-37. After several unsuccessful attempts to detect the MFZ 3-37 labeled peptide, it was concluded that the product was likely
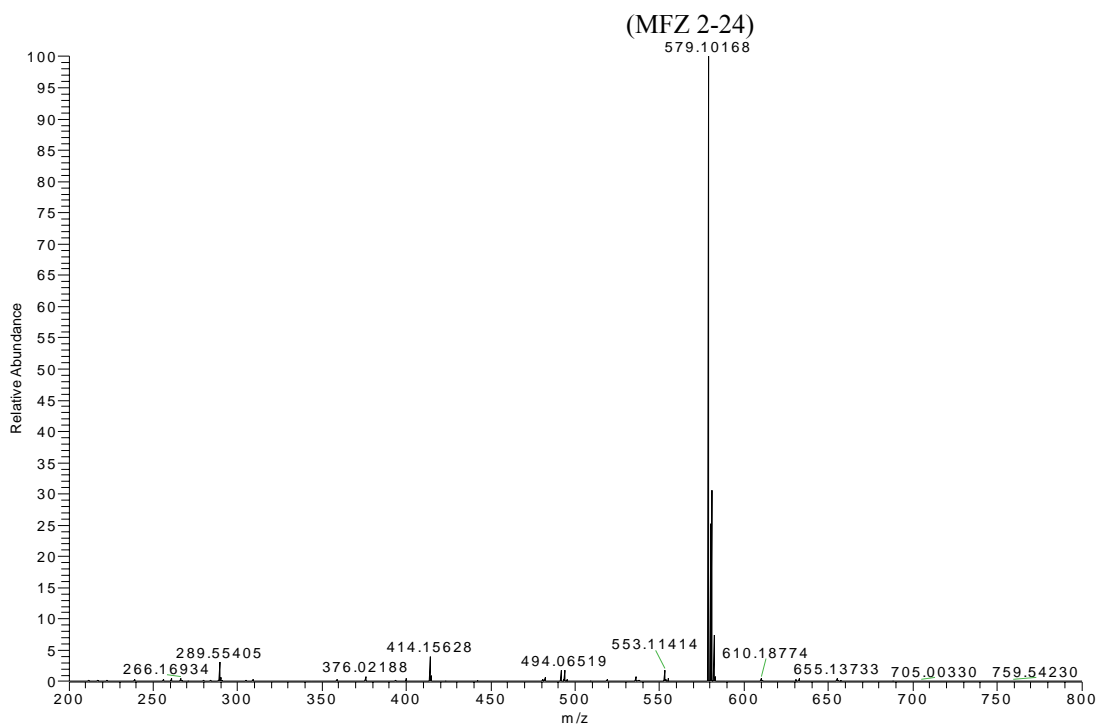
Figure 3.21 Mass spectrum of MFZ 2-24

An electrospray ionization source was used to detect the 579.10168 m/z peak (theoretical

$M + H^+$ 579.10182 m/z) corresponding to the MFZ 2-24 mass. The mass was obtained

with an accuracy of 0.26 ppm.
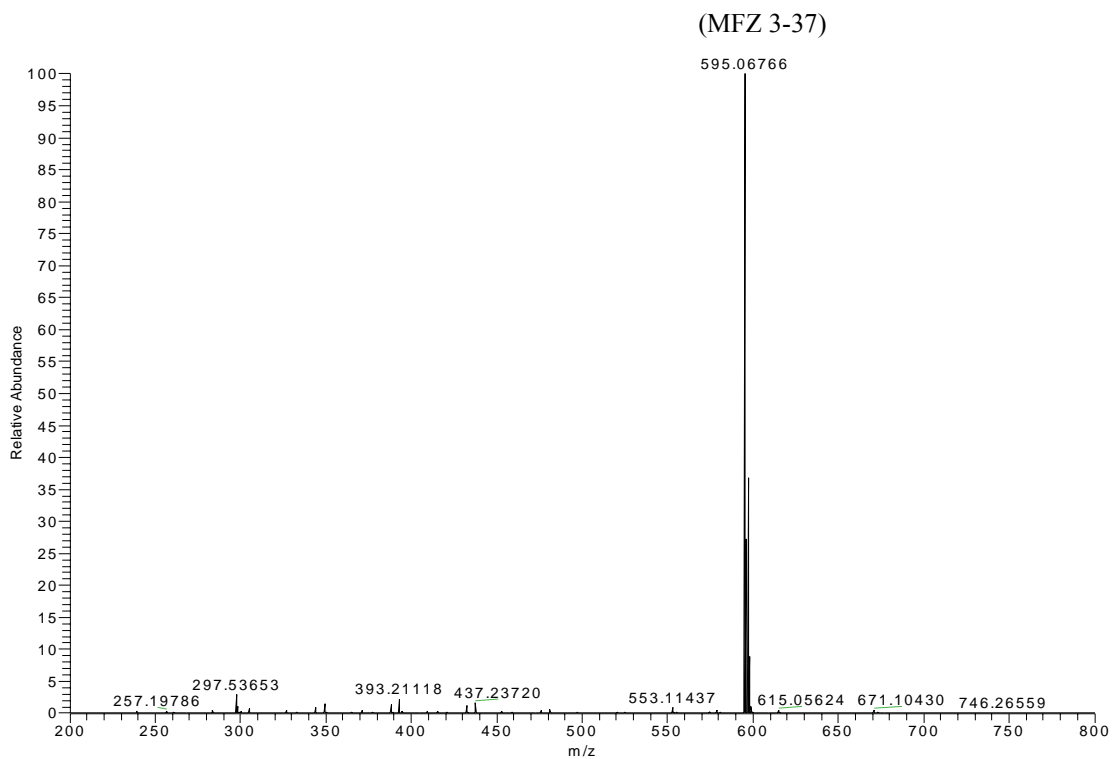
Figure 3.22 Mass spectrum of MFZ 3-37

An electrospray ionization source was used to detect the 595.06766 m/z peak (theoretical

$M+H^+$ 595.06775 m/z) corresponding to the MFZ 3-37 mass. The mass was obtained

with an accuracy of 0.16 ppm.
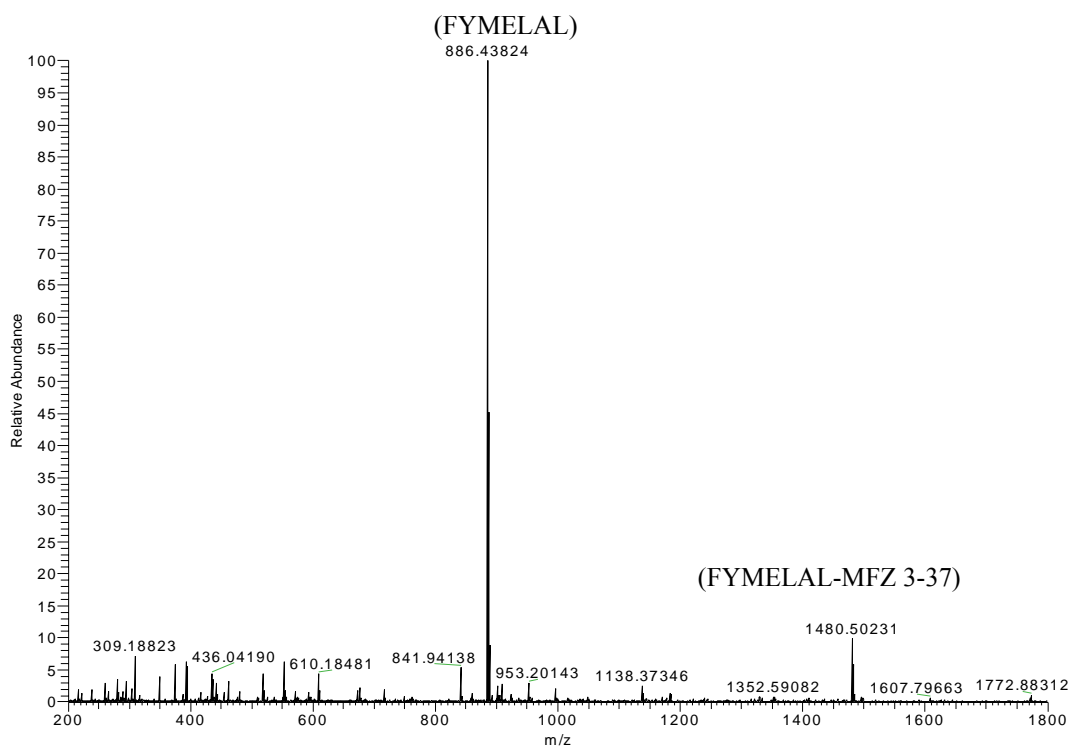
Figure 3.23 Mass spectrometry analysis of the product of the reaction of synthetic FYMELAL peptide with MFZ 3-37

Synthetic FYMELAL peptide was reacted with MFZ 3-37, and the reaction mixture was analyzed by mass spectrometry. The 1480.50231 m/z peak (theoretical M+H$^+$ 1480.49838 m/z; accuracy 2.65 ppm) corresponded to the MFZ 3-37 reaction product, and the 886.43824 m/z peak (theoretical M+H$^+$ 886.43790 m/z; accuracy 0.44 ppm) was the excess of synthetic FYMELAL.
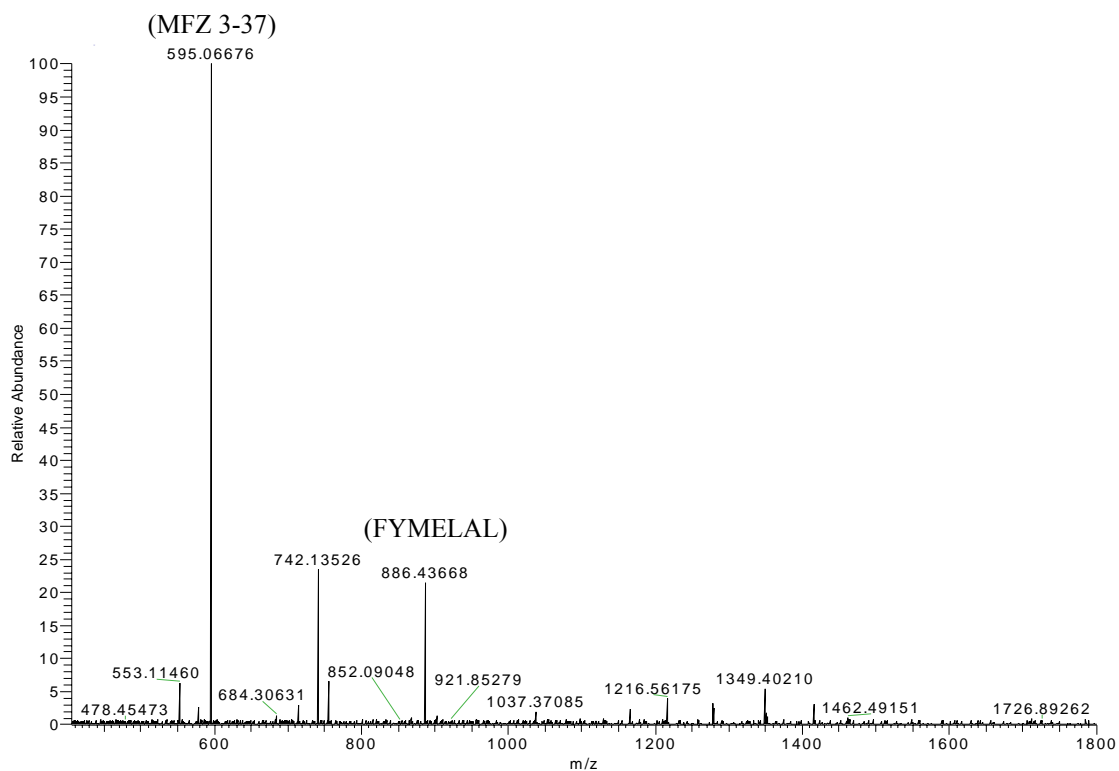
Figure 3.24 MS/MS analysis of the product of the reaction of MFZ 3-37 with synthetic FYMELAL peptide ion

Synthetic FYMELAL peptide was reacted with MFZ 3-37, producing the 1480 m/z product. The second-stage analysis was performed on the 1480 m/z product ion. MS/MS of the 1480 m/z produced peptide and MFZ 3-37 ions. The 595 m/z was the most intense ion, which can be used to search for the parent ion in the actual runs of labeled hDAT digests.

unstable. Further stability studies of the product of synthetic peptide reaction with MFZ 3-37 were performed. Additionally, attempts to purify hDAT prior to mass spectrometry analysis using FLAG and MFZ 3-37 columns were initiated to obtain cleaner samples for mass spectrometry analysis.

Mass Spectrometry Analysis of MFZ 2-24 and Synthetic Peptides

Initial mass spectrometry analyses of the ligands and synthetic peptides were performed. An electrospray ionization source was used to ionize MFZ 2-24 (Figure 3.21) and MFZ 3-37 (Figure 3.22). The 595.06766 m/z and 579.10168 m/z peaks corresponded to MFZ 3-37 and MFZ 2-24, respectively.

To simulate the search for the labeled peptide in the actual hDAT run, synthetic hDAT FYMELAL peptide was reacted with MFZ 3-37 and analyzed by mass spectrometry. The product of the reaction of synthetic FYMELAL peptide with MFZ 3-37 corresponded to the 1480.50231 m/z peak (Figure 3.23). The 886.43824 m/z peak was FYMELAL, and the 595.06766 m/z peak was the excess ligand. The second-stage analysis of the 1480 m/z product lead to its decomposition, with the formation of a 595 m/z peak corresponding to MFZ 3-37 and a less intense 886 m/z peak of FYMELAL peptide (Figure 3.24). The MFZ 3-37 peak had the highest intensity in the MS/MS analysis of the reaction product and was used as a marker in the search for the labeled hDAT peptide.

Sensitivity of FT-ICR Mass Spectrometer

To estimate the amount of hDAT sufficient for identification of the labeled peptide by mass spectrometry, the detection limits for MFZ 2-24 and synthetic FYMELAL were determined in FT and ion trap. Two nanospray sources were more sensitive than the standard source when larger amounts of peptide were analyzed. Each concentration was analyzed three times (n=3), and these were compared. The in-house built source and a new ADVANCE (Michrom) source recently introduced to the market were tested.

Five femtomoles of MFZ 2-24 was the smallest amount detected in both the FT (Figure 3.25) and the ion trap (Figure 3.26). The detection limit was 10 fmoles for synthetic peptide FYMELAL when a standard nanospray source was used (Figure 3.25). The ligand ionized significantly better than the peptide, which is reflected in its steeper calibration curve compared to the one for the peptide (Figure 3.25).

The ADVANCE source allowed the detection limit of 5 fmoles of FYMELAL, which is only twice the sensitivity for a standard nanospray source. However, when larger amounts of peptide were analyzed, the ADVANCE source was up to 8 times more sensitive (Figure 3.27), indicating that ADVANCE is the most promising source for the detection of hDAT peptides.
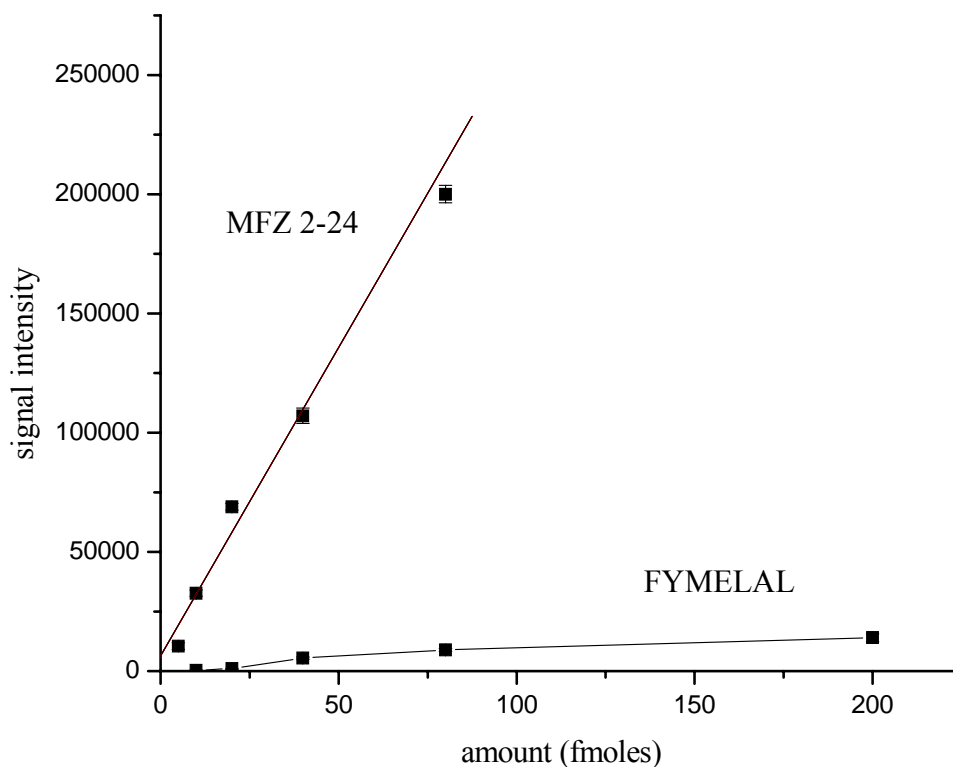
Figure 3.25 Sensitivity study of the high-resolution MS analysis of MFZ 2-24 and synthetic FYMELAL using a standard nanospray source

MFZ 2-24 and synthetic hDAT peptide FYMELAL were used as control samples to evaluate the dependence of signal intensity on the amounts of analyzed material using high-resolution FT-MS. Additional information about the limit of detection for synthetic FYMELAL and MFZ 2-24 was obtained. Detection limits of 10 fmoles for synthetic FYMELAL and less than 5 fmoles for MFZ 2-24 were obtained. Each concentration was analyzed three times (n=3).
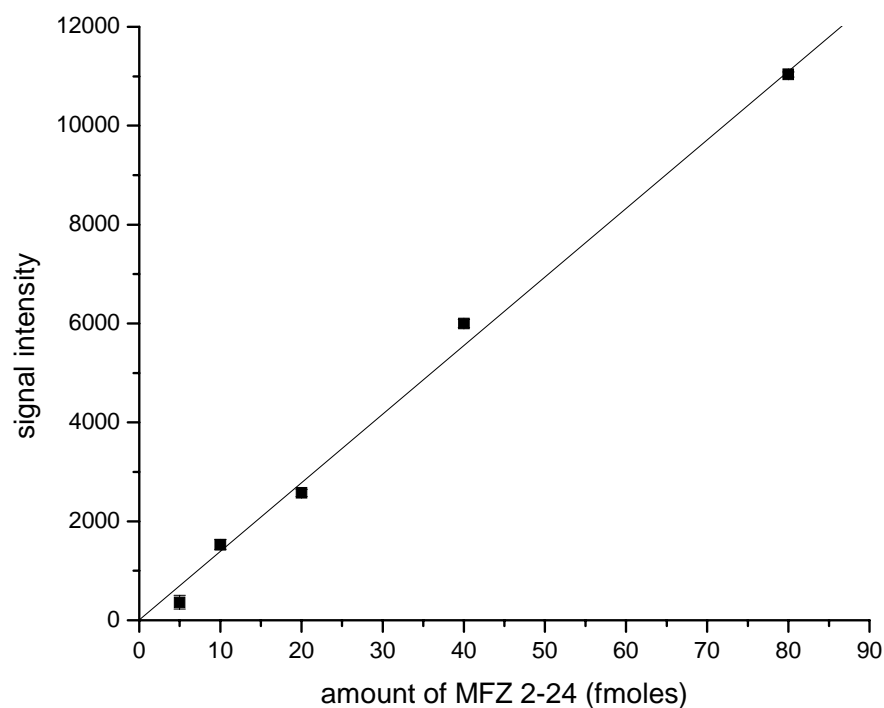
Figure 3.26 Determination of the sensitivity of the second-stage MS analysis of MFZ 2-24

Second-stage analysis of the 579.10168 m/z MFZ 2-24 peak produced several peaks, including a major 551 m/z peak. The intensity of the 551 m/z peak produced from MS/MS analysis of MFZ 2-24 was measured. The second-stage MS/MS signals were detected in the ion trap. Five fmoles of MFZ 2-24 were detected. Measurements for each concentration were performed three times (n=3).
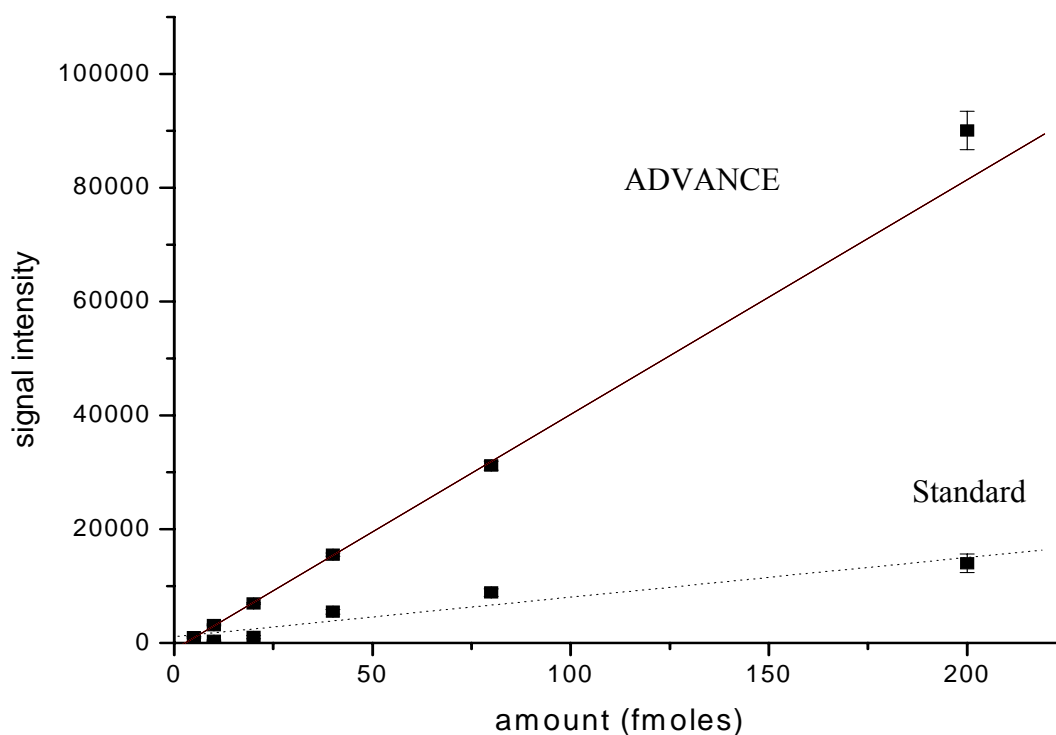
Figure 3.27 Determination of the sensitivity of high-resolution MS analysis of synthetic FYMELAL using standard nanospray and ADVANCE sources

Synthetic hDAT peptide FYMELAL was used as a control sample to evaluate the correlation between signal intensity and the amounts of analyzed material using high-resolution FT-MS. A standard nanospray source was compared to the ADVANCE source. A minimum of 5 fmoles of synthetic FYMELAL was detected using ADVANCE; the minimum was 10 fmoles using a standard source. The ADVANCE source was up to 8 times more sensitive than the standard source when larger amounts of peptide were analyzed. Each concentration was analyzed three times (n=3).

Mass Spectrometry of 3XFLAG-6XHis-hDAT

Figure 3.28 shows an example of a nanoHPLC chromatogram obtained during one of the analyses of the hDAT thermolysin digest. The analyzed digest is a very complex mixture of peptides and requires extended separation using a long 360 min gradient. A 100 μm column was packed with C18, 5 Å slurry using a pressure bomb and connected to a standard nanospray source. Solvent A was water with 0.1% formic acid, solvent B was acetonitrile with 0.1% TFA, and solvent C was isopropanol with 0.1% formic acid added. Ninety percent of solvent A was run for the first 20 min of the gradient, followed by a gradual increase of the concentration of solvent B up to 100% at 240 min at a 5 μl/min flow rate. Pure solvent C was used for the following 80 min of the run to ensure complete elution of the hydrophobic peptides from the column.

The hDAT peptide coverage obtained from multiple nanoLC-MS runs is presented in Table 3.2. The peptides were separated on the in-house fabricated nanoHPLC and analyzed by a nanoelectrospray source on Thermo Finnegan LTQ-FT to obtain high-resolution mass spectra. Simultaneously, MS/MS on the six most intense peaks from the MS run was performed in the ion trap. Bioworks software (Thermo Scientific) was used to examine and identify the observed hDAT peptides. The detected hDAT peptides were from extra- and intra-cellular loops as well as from the C- and N-terminals and transmembrane domains. However, peptides from the TM1-TM2 domain region were not observed. This may be due to the high hydrophobisity of the transmembrane domains.
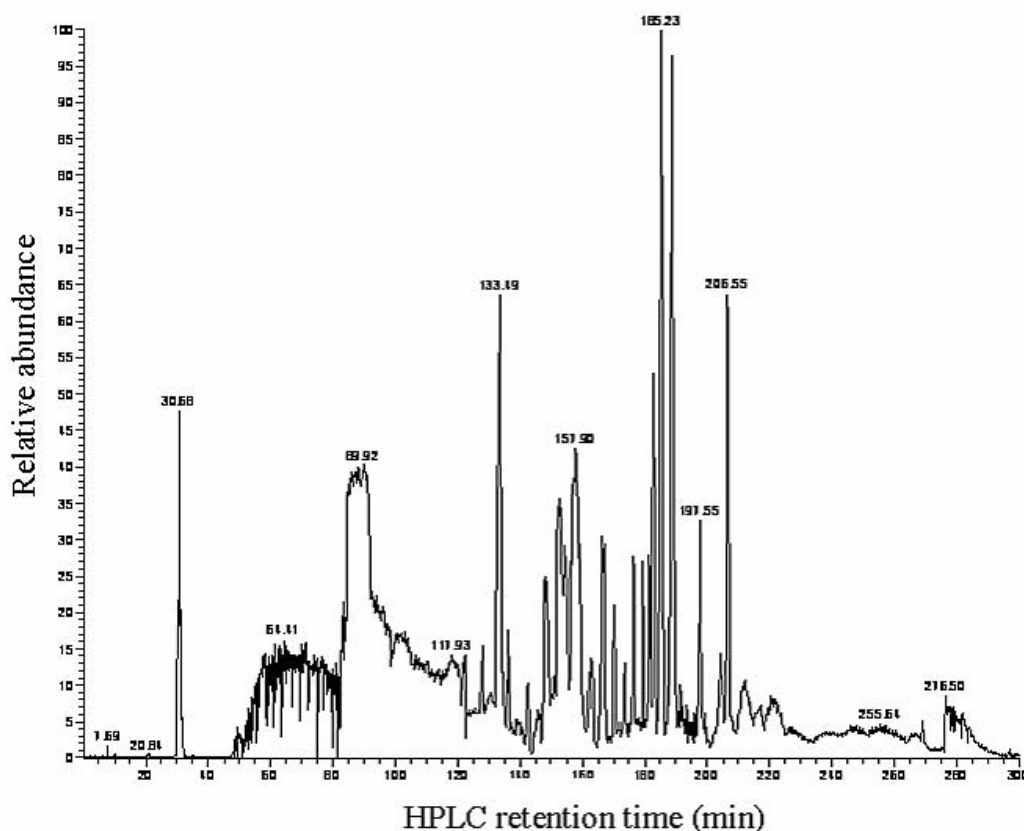
Figure 3.28 HPLC chromatogram of the thermolysin digest of hDAT

Solubilized hDAT was separated on a 7.5% SDS gel. The band corresponding to hDAT was cut out and an in-gel thermolysin digest was performed. Peptides were extracted from the gel using 60% ACN, combined together, and dried down. The extracted peptides were dissolved in 20% ACN and separated on the in-house packed C18 column connected to a standard nanospray source. The figure shows an example of the HPLC chromatogram obtained during the experiment. The analyzed sample was very complex, which is reflected in the chromatogram. Following the HPLC separation, peptides were analyzed on an FT mass spectrometer and the top six ions from each scan were subjected to second-stage MS analysis. A summary of hDAT peptides detected in five successful runs is shown in Table 3.2.

Peptide	Localization on 3XFLAG-6XHis hDAT
MGGSHHHHHHGMASMTGGQQMGRDLYDDDDKVPKDP≠	His tag
VWWNSSTPSVPMSKSKCSVGLMSSVVAPAKEPNA*	His tag and N-terminal
LMSSVVAPAKEPNAVGPKEVEL*	N-terminal
LILVMEQNGVQLTSSTLTNPRQSP≠	N-terminal
FFYNVIIAWALHYL*	TM3
VGFFYNVIIAWA*	TM3
LHLHQSHGIDDLGPPRWQ*	EL2 TM4
LHLHQSHGIDDLGPPRWQLTACLV*	EL2 TM4
VLTALLLRG≠	TM 5
FGVLIAFSSYNK≠	TM6 IL3
IVTTSINCLTSFSSGFV*	TM7
FIIYPEAIATLPLSSAWAV*	EL4
LIFIIYPEAIATLPLSSAWA≠	EL4 and TM8
LPLSSAWAVVFF*	TM8
IDSAMGGMES*	IL4
IQQMTGQRPS≠	IL 5
VTFRPPHTGAYIFPDWANALGW≠	EL 6
VPIYAAYKFCSLPGSFREKLAYA*	C-terminal
LPGSFREK≠	C-terminal
LAYAIAPEKDRELVDRGEVRQ*	C-terminal

Table 3.2 hDAT Peptides found in LC-MS runs of hDAT thermolysin digests

Peptides marked with a number sign (#) were detected in two 60-plate runs, analyzed by TurboSequest, and supported by the *b*, *y*, and *a* series of ions. Three 18-plate runs were analyzed by PepMap software based on the exact masses of the proteins. Peptides detected in these runs are marked with an asterisk (*).
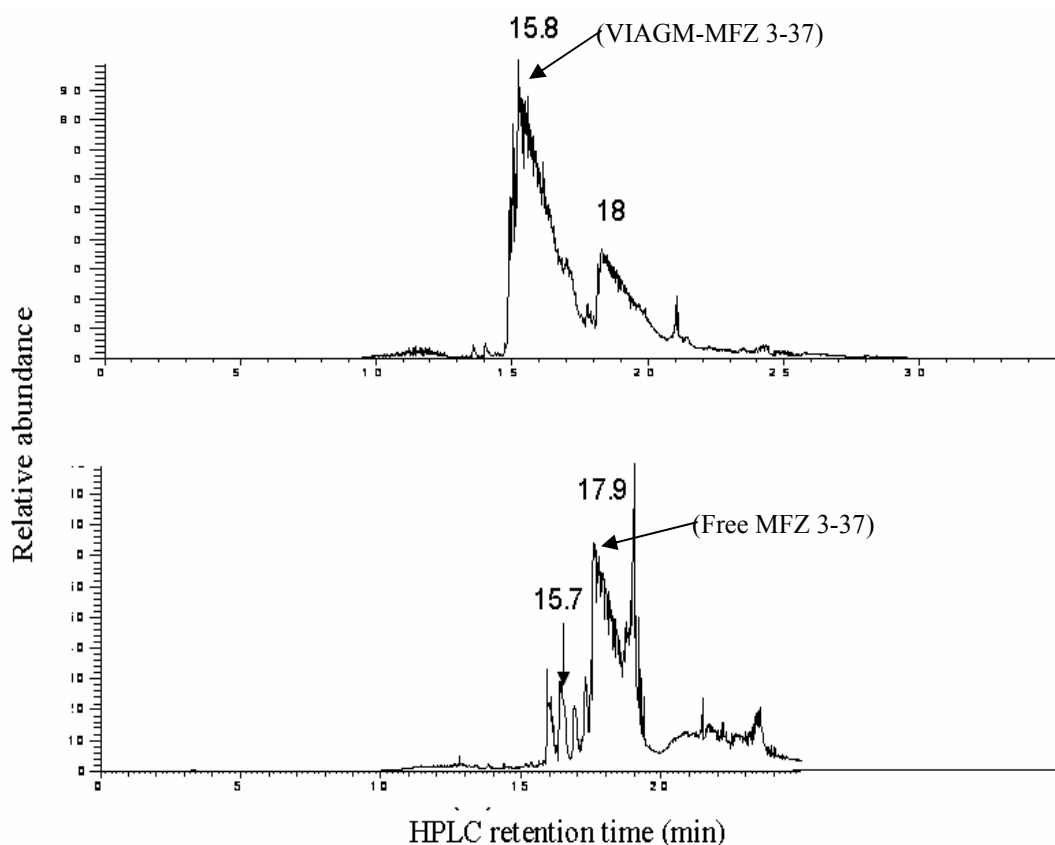
Figure 3.29 Comparison of HPLC analysis of MFZ 3-37 reacted VIAGM before and after incubation at 37°C for 24 hours

A synthetic VIAGM peptide was reacted with MFZ 3-37, and the reaction mixture was analyzed on nanoHPLC-MS. The initial reaction mixture contained the majority of the product of the reaction of MFZ 3-37 with VIAGM. After a 24-hour incubation at 37°C, the same conditions as those used for thermolysin digest, decomposition of the product and an increase in the amount of free MFZ 3-37 were observed. The 15.7 min and 15.8 min peaks corresponded to MFZ 3-37 reacted with VIAGM, and the 17.9 min and 18 min peaks corresponded to the free MFZ 3-37 label. Relative amounts of the components in the mixture were estimated using signal intensities in mass spectra.

Stability of MFZ 3-37 Reacted with hDAT Peptides

hDAT was labeled with MFZ 3-37, digested with thermolysin, and analyzed via nanoLC-MS using the same setup as that employed for the detection of hDAT peptides. Following the run, the product was searched for the 595 m/z ion of MFZ 3-37. The parent ions generating the 595 m/z ion were ranked using a scoring algorithm. The highest-ranking ions were compared to peptides from the thermolysin digest of hDAT. Several false positives were found. However, none of the suspected labeled peptides contained the cysteine or lysine residue required for reaction with MFZ 3-37. Consequently, the stability of the product of the reaction of MFZ 3-37 with peptides was questioned.

To further investigate this issue, synthetic VIAGM was reacted with MFZ 3-37. The reaction mixture was divided into two equal parts. The first part was analyzed using nanoLC-MS immediately after the reaction was stopped (Figure 3.29). The second part was subjected to the conditions used in the thermolysin digest. The reaction mixture was incubated at 37°C for 24 hours in incubation buffer. The initial HPLC separation showed that the majority of the product of the reaction of MFZ 3-37 with VIAGM at 15.8 min was present in the sample. The intensity of the signal corresponding to the product was 2.62×10^8 when analyzed on FT-MS. However, the peak at 18 min corresponding to the free MFZ 3-37 dramatically increased after 24 hours of incubation, indicating decomposition of the product. The 15.7 min peak of MFZ 3-37 reacted VIAGM corresponded to only 2.56×10^7 signal intensity in mass spectrometry analysis. Therefore, only ~10% of the initially formed MFZ 3-37 reacted with VIAGM was left after 24 hours of incubation at 37°C. This suggests that the MFZ 3-37 labeled peptide in the hDAT

thermolysin digest run may be decomposed due to several days of processing, including the solubilisation, the digest, and extractions.

hDAT Purification

Attempts to purify and concentrate hDAT for mass spectrometry analysis using column purification were made. To confirm the expression of 3xFLAG-tagged hDAT in HEK293 cells, Western blot analysis was performed. 3XFLAG-6XHis-tagged hDAT was separated on a 7.5% SDS-polyacrylamide gel, electrotransferred to a nitrocellulose membrane, and assessed by Western blot using anti-FLAG antibodies (Figure 3.30). 3XFLAG-6XHis-hDAT corresponded to the band between 80 and 125 kDa.

3XFLAG-6XHis-hDAT labeled with [^{125}I] MFZ 2-24 was solubilized from HEK293 membranes and purified on the FLAG column. The fraction containing purified 3XFLAG-6XHis-hDAT eluted from the column was separated from the fraction that did not bind to the column on 7.5% SDS-polyacrylamide gel. An autoradiograph of the gel was obtained, and the band corresponding to [^{125}I] MFZ 2-24 labeled hDAT was excised from the gel and counted with a scintillation counter. The relative percentages of hDAT loss, purified hDAT, and hDAT that did not bind were calculated. The experiment was repeated 3 times. Only about 12% of 3XFLAG-6XHis-hDAT was recovered (Figure 3.31). Such a low recovery rate was attributed either to the loss of the 3XFLAG tag by the majority of the expressed hDAT or to weak interaction between the 3XFLAG tag and the FLAG antibodies on the column.
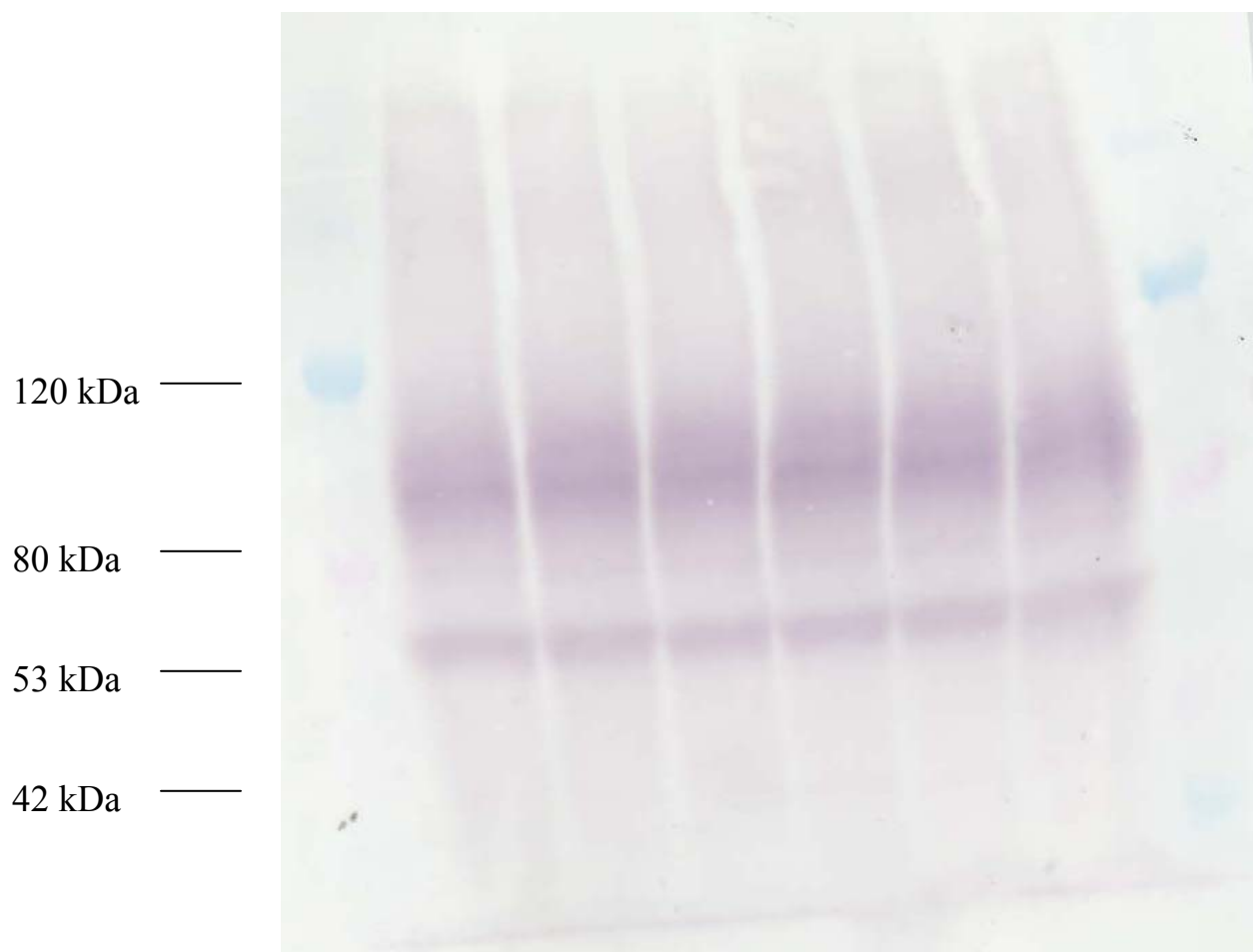
Figure 3.30 Western blot analysis of HEK cells expressing hDAT lysate using the FLAG antibodies

3XFLAG-6XHis-hDAT was separated on a 7.5% SDS gel and transferred to the nitrocellulose membrane. Primary FLAG antibodies were used. The signal was detected by chemiluminescence. Molecular weight markers are indicated. 3XFLAG-6XHis-hDAT corresponded to the band at 80–125 kDa.
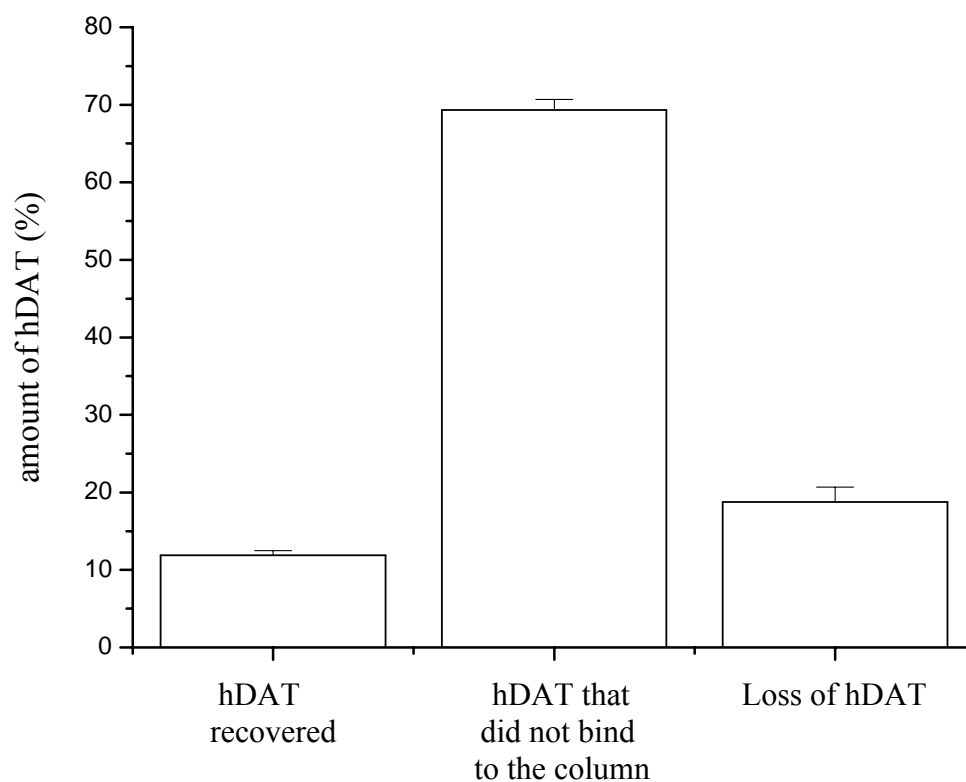
Figure 3.31 Purification of 3XFLAG-6XHis-hDAT using the FLAG column

3XFLAG-6XHis-hDAT labeled with [^{125}I] MFZ 2-24 was purified on the FLAG column. The relative percentages of the hDAT loss, purified hDAT, and hDAT that did not bind were calculated. The experiment was repeated three times. Only ~12% of 3XFLAG-6XHis-hDAT was recovered.

Chapter Four

Discussion

Introduction to the Discussion

Three different approaches to studying hDAT and the cocaine binding site of hDAT have been used in this dissertation. Radioactive labeling of hDAT with [^{125}I]MFZ 2-24 was followed by gel separation and then in-gel thermolysin or CNBr digests. The hDAT peptides formed in the digests were extracted and separated on the HPLC. The radioactivity profiles of the runs allowed determination of the retention times for the radioactively labeled hDAT peptides. When necessary, secondary digests were performed with cyanogen bromide or chymotrypsin to investigate the possible changes of the retention time of the labeled peptide. Such changes would suggest that specific CNBr or chymotrypsin cut sites are present in the peptide. The initial CNBr digest enabled identification of the labeled peptide as a small peptide with a retention time of 79 min.

The initial thermolysin digest showed a reproducible radioactivity profile when separated on the HPLC. Secondary CNBr digest of the [^{125}I]MFZ 2-24 peptides resulted in a shift of the retention time, indicating the presence of methionine in the peptide from the thermolysin digest. Additional information was obtained from the Edman degradation experiment with the labeled peptide produced from the thermolysin digest. The release of radioactivity was monitored for each Edman degradation cycle. The second cycle, corresponding to the second amino acid residue of the labeled peptide, exhibited the largest radioactivity release.

To confirm the results of the radiolabeling experiments, the chemical labeling of small synthetic peptides and amino acids of interest with isothiocyanate analog MFZ 3-37 was performed to evaluate the effect of the label on the peptides and the retention times

of the amino acids. The products of the MFZ 3-37 reaction with synthetic peptides were analyzed by mass spectrometry. The products of the reaction of tritiated amino acids with MFZ 3-37 were detected by the radioactivity trace.

The discovery of the LeuTAa crystal structure in 2005 (Yamashita et al., 2005) suggested that TM1 and TM6 are involved in the cocaine binding site. A question arose regarding how both MFZ 2-24 and MFZ 3-37 can label hDAT. In this research, the importance of the C90 residue located in TM1 was tested by analyzing the X5C and X-A90C hDAT mutants and by using cysteine reactive reagents. The levels of labeling with both MFZ 2-24 and MFZ 3-37 were determined.

The sensitivity of the mass spectrometry method was assessed for detection of hDAT peptides. It demonstrated promising results in detecting hDAT peptides from digests. Several nanoLC-MS analyses allowed detecting a number of hDAT peptides from both the hydrophilic N- , C- terminal, loop regions and hydrophobic transmembrane domain regions. Finally, mass spectrometry was used in an attempt to localize the MFZ 2-24 and MFZ 3-37 labeled amino acid residue of hDAT. However, this attempt encountered several difficulties, such as the instability of the product formed with MFZ 3-37 and low labeling efficiency of MFZ 2-24.

In this chapter, the interpretation of results will be presented and supported by information from the literature and the experimental data. Based on the information obtained from CNBr and thermolysin digests of hDAT, the small labeled peptide will be tentatively identified. The data from the crystal structure identification of the LeuTAa transporter (Yamashita et al., 2005) will be used as the main guide for the three-dimensional localization of the suspected peptide in hDAT. In addition, the

implementation of mass spectrometry in the search for labeled and unlabeled hDAT peptides will be discussed, and the challenges in using MFZ 2-24 and MFZ 3-37 will be explained for all the listed approaches.

Investigation of hDAT Binding Site Using

$[^{125}I]$MFZ 2-24 and $[^{125}I]$MFZ 3-37

WIN 35,428 Protection Experiment

The protection experiment establishes the relationship between the studied ligand and the binding site of the protein of interest. $[^{125}I]$MFZ 2-24 and $[^{125}I]$MFZ 3-37 are the hDAT labels containing the tropane ring (Zou et al., 2001). These labels can compete with cocaine for the same binding site. The cocaine analog WIN 35,428 is a valuable substitute for cocaine in the protection experiment due to its higher affinity (K_i = 43 nM) compared to cocaine (K_i = 278 nM) (Li et al., 2004; Zou et al., 2003). WIN 35,428 binds tightly to the DAT and prevents the binding of other dopamine transporter inhibitors sharing the same or similar binding site. The affinity of MFZ 2-24 and MFZ 3-37 are K_I = 33 nM and K_I = 31.5 nM, respectively (Vaughan et al., 2005). Incubation of hDAT with WIN 35,428 prior to labeling with $[^{125}I]$MFZ 2-24 or $[^{125}I]$MFZ 3-37 resulted in almost complete inhibition of labeling. This effect of the WIN 35,428 analog was visualized by autoradiography of 7.5% SDS-PAGE-separated hDAT, which was labeled with either of the ligands after incubation with the WIN 35,428. The results suggest that MFZ 2-24 and MFZ 3-37 have the same binding site as WIN 35,428 and that the labeling occurs within a close proximity to the cocaine binding site.

Analysis of [¹²⁵I]MFZ 2-24 Labeled Peptide Resulting from CNBr Digest

A previous immunoprecipitation study with antibodies to the N-terminal region of hDAT showed that MFZ 2-24 labels within the TM1-TM2 region (Vaughan et al., 2005). The peptides from the trypsin digest of hDAT were immunoprecipitated with antibodies generated to the 42-59 amino acid residues, suggesting that the [^{125}I] MFZ 2-24 is incorporated in the TM1-TM2 region.

To further localize the site of [^{125}I] MFZ 2-24 incorporation, cyanogen bromide was used to digest [^{125}I]MFZ 2-24 labeled hDAT. The human dopamine transporter has 13 methionines in its sequence (Figure 4.1). There is concern that harsh conditions used in the CNBr digest may decompose the ligand or lead to the proteolysis of the peptide. The control analysis of the possible hDAT proteolysis was performed by Dr. Laura Parnas. [^{125}I]MFZ 2-24 labeled hDAT was incubated in 70% TFA and separated on 7.5% SDS gel simultaneously with non-treated [^{125}I]MFZ 2-24 labeled hDAT. Autoradiography showed that the labeled hDAT remained intact and corresponded to the 80-125 kDa band. The band corresponding to the radioactivity near the front line was excised and submitted to our laboratory for the HPLC separation analysis. The non-treated hDAT and the 70% TFA-incubated hDAT produced identical radioactivity profiles indicating an excess of the free ligand that did not label hDAT. No labeled peptides were detected in either hDAT sample. This stability study alleviates the concern that the hDAT used in this CNBr digest was degraded due to the harsh acidic conditions.
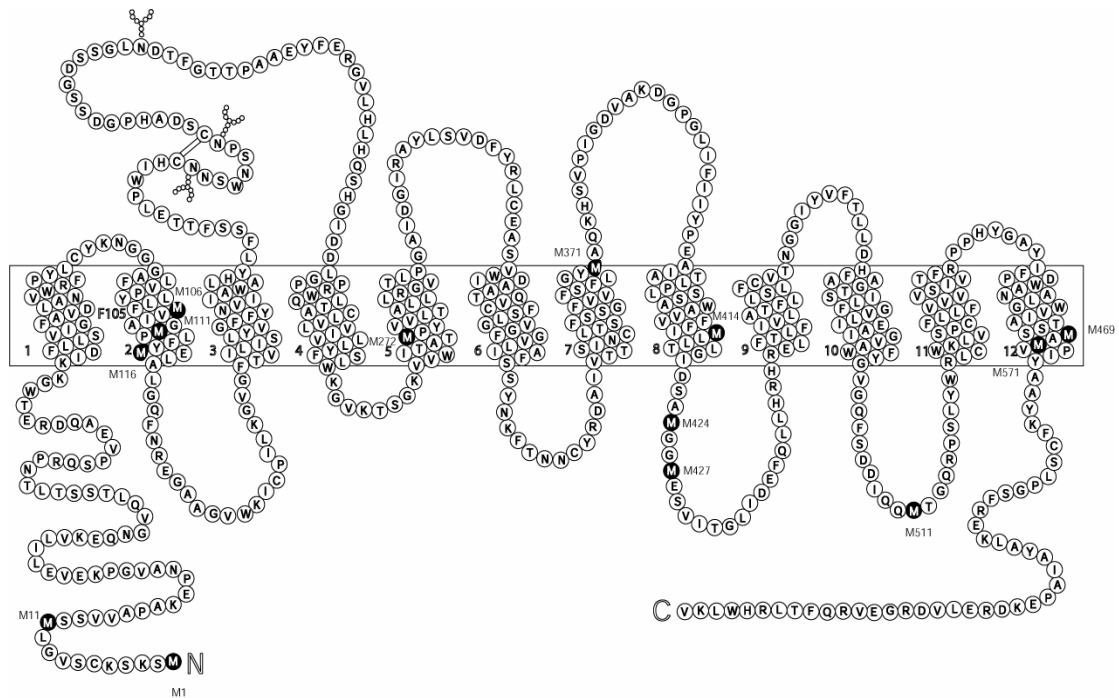
Figure 4.1 CNBr cleavage sites of hDAT

Methionine residues are shown as black circles with white letters. hDAT contains 13 methionines. Six methionines are located in the TM1-TM2 region (adapted from Giros and Caron, 1993).

Another subject of concern was the stability of the MFZ 2-24 ligand in 1M CNBr and 70% TFA. Incubation of the [125I]MFZ 2-24 with 1M CNBr in 70% TFA for 24 hours at room temperature did not result in significant decomposition of the label corresponding to a 63 min. peak. The majority of the label remained intact after the harsh CNBr/TFA conditions. 1M CNBr/70% TFA conditions are widely used for protein digests because of the straightforward interpretation of the results. CNBr is a chemical reagent whose efficiency of bond cleavage exceeds 90% (Kaiser and Metzka, 1999). CNBr is more likely to produce complete digests compared to enzymatic digests therefore, CNBr was used in this experiment.

Cyanogen bromide cleaves a peptide bond between the C-terminal of a methionine and the residue of another amino acid (Gross, 1967). The mechanism of reaction is shown in Figure 4.2. The problematic sites for CNBr cleavage are Met-Ser and Met-Thr due to the hydroxyl-containing side chains of serine and threonine attacking the iminolactone intermediate and resulting in no cleavage. It has also been reported that CNBr can cause unwanted cleavage of the Asp-Pro bond (Kaiser and Metzka, 1999).

The SDS-PAGE gel separation of CNBr-digested [125I]MFZ 2-24 labeled hDAT produced only small labeled peptide(s) corresponding to 2-6 kDa. Subsequent HPLC analysis indicated that only one small labeled peptide with a retention time of 79 min. was produced. hDAT has 13 methionines in its sequence (Figure 4.1). Table 4.1 lists all the hDAT peptides from the CNBr digest as well as their positions in the hDAT. The peptides' HPLC retention times were calculated using GPMAW software (Sakamoto et al., 1988). The predicted retention times match well with the experimental retention times obtained for PLFYM, VIAGM, and M and differ only within 1-3 min.

The addition of the MFZ 2-24 hydrophobic label to a peptide should increase its retention time significantly. Out of fourteen peptides produced from a CNBr digest, only seven small hDAT peptides can have the 79 min. retention time when labeled with MFZ 2-24. The rest of the peptides from a CNBr digest are calculated to have retention times greater than 79 min. even without the label attached. Therefore, attachment of the ligand to the peptides with calculated retention times longer than 95.6 min. should result in even longer retention times. Previous studies indicate that MFZ 2-24 photoincorporates within the TM1-TM2 region (Vaughan et al., 2001; Vaughan et al., 2005) therefore, only two possible matches, VIAGM and PLFYM, both located in TM2, can be identified as the labeled peptides. M1 and SKSKCSVGLM from the N-terminal of hDAT are not possibilities since the antibodies used in the immunoprecipitation study were generated to the 42-59 amino acid residues of hDAT (Vaughan et al., 2001) and the 42-59 amino acid region is separated from M1 and SKSKCSVGLM by a trypsin cut-site at lysine 27.

An *in situ* trypsin digest of hDAT was carried out by Dr. Tamara Henderson to identify whether MFZ 2-24 labels the hDAT part buried in the membrane or labels the loop and the terminal region (Henderson, 2008). Her findings support the immunoprecipitation studies by Vaughan et al. (2001) and point to E61-R125 as the region of MFZ 2-24 photoincorporation (Henderson, 2008). According to the analysis of the leucine transporter crystal structure, the R125 is located right on the border of TM2 and intacellular loop 1 and may be not accessible to tryspin. Therefore, the region of MFZ 2-24 possible incorporation can be extended to E61-K133.
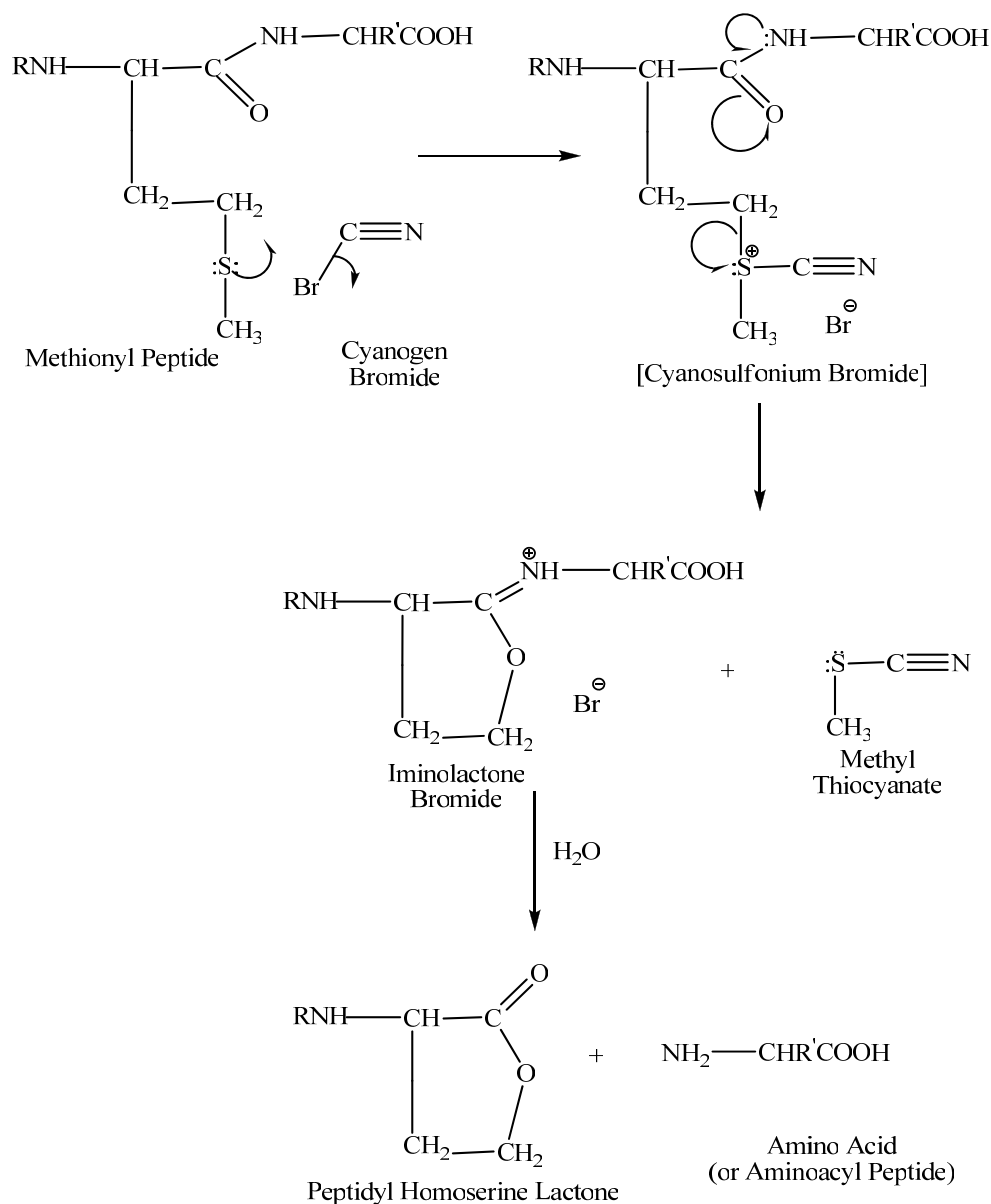
Figure 4.2 Mechanism of CNBr cleavage reaction (adapted from Garrett and Grisham, [1999]; Gross, [1967])

CNBr attacks the nucleophilic sulfur in the methionine side chain. This is followed by the formation of cyanosulfonium intermediate and then by thiocyanate liberation and formation of iminolactone. The iminolactone undergoes Shiff base hydrolysis by water forming peptidyl homoserine lactone and aminoacyl peptide (or amino acid).

The sequence of TM1 and TM2 was also analyzed for the presence of Met-Thr, Met-Ser, and Asp-Pro pairs that can affect CNBr digest. There are no Asp-Pro or Met-Thr sequences in the TM1-TM2 region. Met-Ser is located at the N-terminal part of hDAT, which was eliminated from the suspected regions of MFZ 2-24 photoincorporation sites by immunoprecipitation studies (Vaughan et al., 2001) and an *in situ* digestion study (Henderson, 2008).

A secondary chymotrypsin digest was performed by Dr. Sara Wirtz on the 79 min. peak (Wirtz, 2004). The resulting two new peaks at 47 and 63 min. indicate that the CNBr peptide has chymotrypsin cut-sites (Wirtz, 2004). Chymotrypsin catalyses the hydrolysis of the peptides at the carboxyl side of aromatic amino acid residues tyrosine, tryptophan, phenylalanine, and leucine. Secondary cleavage sites may include methionine glutamine, asparagine, or histidine depending on the digest conditions and the amino acid residues at the P_2' position (Keil, 1992). The presence of proline at the P_2 position prevents cleavage at the X-P site (Keil, 1992). VIAGM does not contain any chymotrypsin cleavage sites. In contrast, PLFYM has phenylalanine, tyrosine, and leucine residues. These residues may be cleaved, indicating that PLFYM is the labeled peptide.

A recent publication (Parnas et al., 2008) proposed that a peptide from TM1 is the site of the [125I]MFZ 2-24 photoincorporation. The researchers reported that CNBr digest of [125I]MFZ 2-24 labeled hDAT produced a 12 kDa band and suggested the long peptide containing the TM1 region and part of the TM2 region (ending at M106) was the labeled peptide (Parnas et al., 2008). Additionally, this study used mutations in the TM1-TM2 region followed by various digests to narrow down the region of label incorporation.

DFLLSVIGFAVDL from TM1 is the sequence of the reported labeled peptide (Parnas et al., 2008).

However, the methodology used by Parnas et al. (2008) has several critical differences from the methods used in this dissertation. In the Parnas et al. (2008) study, the labeled hDAT was electroeluted from the gel and dried down, and CNBr digest was performed on the whole dried protein. Electroelution and drying down of the intact hDAT may lead to strong hydrophobic interactions and aggregation of the protein. Therefore, not all cleavage sites may be accessible to CNBr or enzymes, resulting in difficulties in obtaining the complete digest of such a sample (Speers and Wu, 2007). In our research, labeled hDAT underwent in-gel CNBr digest followed by extraction of smaller-size peptides. Our methodology provides a complete digest of hDAT and decreases the chance of any aggregation problems. According to gels presented in the paper by Parnas et al. (2008), a majority of hDAT was undigested and stayed at the region of the gel corresponding to 85-125 kDa. However, the gel presented as the main evidence of the TM1 labeling lacked the undigested radioactively labeled hDAT in the 85-125 kDa region, which was present on the autoradiographies when other ligands were studied (Parnas et al., 2008; Vaughan et al., 2001). Because of these issues, the TM1 localization of [^{125}I]MFZ 2-24 based on the Parnas et al. (2008) study may be unreliable.

Calculated Unlabeled HPLC RT (min.)	Sequence	From-To	No. of Amino Acids	Location
8.5	M	1-1	1	N-terminus
38.8	SKSKCSVGLM	2-11	10	N-terminus
28.9	VIAGM	107-111	5	TM2
47.8	PLFYM	112-116	5	TM2
50.7	LLTLGIDSAM	415-424	10	TM8-IL4
13.0	GGM	425-427	3	IL4
9.8	AM	570-571	2	TM12
122.7	SSV…LFM	12-106	95	N-terminus–TM2
175.4	ELA…ATM	117-272	156	IL1–TM5
141.1	PYV…GYM	273-371	99	TM5–TM7
96.9	AQK…FIM	372-414	43	EL4–TM8
142.5	ESV…QQM	428-511	84	IL4–IL5
120.9	TGQ…SSM	512-569	58	IL5–TM12
95.8	VPI…LKV	572-620	49	TM12-C-terminus

Table 4.1 List of peptides produced from a CNBr digest of hDAT (from Wirtz, 2004)

The retention times for peptides were predicted using GPMAW software (Sakamoto et al., 1988). Seven peptides that are expected to have retention times less than 51 min. are listed above the line; the peptides eluting in more than 90 min. are listed below the line. According to the results of the CNBr digest, the labeled peptide has a 79 min. retention time. This suggests that only small peptides can be labeled. The peptides with retention times greater than 95 min. are predicted to elute at retention times much greater than 79 min. when labeled with MFZ 2-24. According to the experimental data, methionine,

VIAGM, and PLFYM reacted with the isothiocyanate analog MFZ 3-37 elute at 62 min., 72 min., and 79 min., respectively.

Interpretation of Synthetic VIAGM and PLFYM Reacted with MFZ 3-37

The reaction of synthetic peptides with the MFZ 3-37 containing isothiocyanate group (instead of the azido group of MFZ 2-24) was used to achieve higher yields in the reactions with synthetic peptides. Azido compounds react with proteins or peptide side chains, resulting in ~1% to 22% yields (Schwartz, 1989). However, MFZ 2-24 contains iodine in the ortho position to the azido group on the phenyl ring, diminishing the reactivity of MFZ 2-24, as reported by Watt et al. (1989).

MFZ 3-37 is an isothiocyanate analog. It has the same chemical structure as MFZ 2-24 except the MFZ 2-24 aizdo group is replaced with a highly active isothiocyanate group. Isothiocyanate compounds, such as fluorescenine isothiocyanate (FITC) and phenyl isothiocyanate (PITC), are commonly used to modify amino acids, peptides, and proteins in HPLC analysis by reacting with the free N-terminal amino groups or sulfo and amino side chain groups of the model peptides (Sanchez-Machado et al., 2003; Mora et al., 1988). The reaction is usually conducted under mildly alkaline conditions (pH = 8) (Schnaible and Przybylski, 1999).

The retention times of VIAGM and PLFYM reacted with MFZ 3-37 were estimated. MFZ 3-37 reacted VIAGM was separated on the HPLC with a 72 min. retention time. Dr. Sara Wirtz reacted PLFYM with MFZ 3-37 and obtained a 79 min. retention time for the product (Wirtz, 2004). Knowing from the CNBr digest that the MFZ 2-24 labeled peptide had the 79 min. retention time, the retention time obtained from the reaction of isothiocyanate with PLFYM suggests that PLFYM may be the labeled peptide. Analysis of the fractions corresponding to the MFZ 3-37 reacted peptides was conducted by mass spectrometry to confirm the formed products. The retention time

of PLFYM reacted with MFZ 3-37 matches well with the previous results of the CNBr digest and secondary chymotrypsin digest (Wirtz, 2004), suggesting that the labeled peptide is PLFYM.

Interpretation of the Thermolysin Digest Result

To further investigate the site of [^{125}I]MFZ 2-24 photoincorporation, [^{125}I]MFZ 2-24 labeled hDAT was in-gel digested with 1 mg/ml thermolysin. For our experiments, thermolysin is a much more useful tool than trypsin to study the TM1-TM2 hDAT region. Trypsin is a serine protease that predominantly cleaves peptide chains at the carboxyl side of lysine and arginine residues, except when either is followed by proline (Lin and Brandts, 1985). There are no trypsin cleavage sites in TM2 and produces large hydrophobic peptide starting right after Lys 92 and ending at Arg 125. The large fragment formed in the trypsin digest of TM1 has 18 amino acid residues (Figure 4.3). Thermolysin, on the contrary, has multiple cleavage sites in the TM1-TM2 region and produces smaller peptides that can be easier analyzed by HPLC, Edman degradation, and mass spectrometry.

Thermolysin was used due to the reproducibility of the results obtained from the hDAT digest (personal observation). Furthermore, there are multiple thermolysin cleavage sites in the TM1-TM2 region (Figure 4.3). The shorter labeled peptide produced in the thermolysin digest of a possibly highly hydrophobic region would be easier to separate on the HPLC followed by mass spectrometry analysis. Thermolysin is also a thermostable metallo-endopeptidase that catalyzes the hydrolysis of N-terminal peptide bonds containing hydrophobic amino acids. Thermolysin needs zinc ion for its catalytic

activity and calcium ions for thermostability (Lapointe et al., 2004). Its primary cleavage sites are X-Leu, X-Phe, X-Ile, and X-Val (Heinrikson, 1977; Bark et al., 2001). However, other minor cleavages can take place at X-Met, X-Glu, X-Ala, and X-Tyr (Heinrikson, 1977).

In this research, peptides were extracted from the gel and separated on the HPLC. The initial HPLC separation produced two major peaks at 73 and 78 min. However, it was noticed that re-runs of those peaks resulted in different retention times. These differing results were initially attributed to the incomplete digest; however, the retention times for the labeled peptides shifted to 63 and 72 min., respectively, without any additional re-digestion with thermolysin. The delay in the retention times can be explained by the high load of hydrophobic proteins and peptides on the HPLC column (Parker et al., 1987). Peptides can experience hydrophobic interactions that result in longer retention of peptides on the reverse-phase column (Speers and Wu, 2007). Whereas during the CNBr digest, the peptides were further separated on the 16.5% SDS-PAGE gel and peptides from the low molecular weight band containing the labeled peptide were separated on the HPLC.

To further analyze the 63 min. labeled peptide from the thermolysin digest, a secondary CNBr digest was performed on the 63 min. peak. The retention time of the new labeled peptide shifted to 77 min., suggesting that the 63 min. thermolysin peptide

Trypsin digest:

```
-------------------------------------------N-terminal -------------------------------------------------
₁MSKSKCSVGLMSSVVAPAKEPNAVGPKEVELILVKEQNGVQLTSSTLTNPRQS
```

```
-----------------------_____TM1_____ -------_____
₅₉PVEAQDRETWGKKIDFLLSVIGFAVDLANVWRFPYLCYKNGGGAFLVPYLLF
```

```
___TM2_____-----IL1------
MVIAGMPLFYMELALGQFNREGAAGVWK
```

Thermolysin digest:

```
-------------------------------------------N-terminal -------------------------------------------------
₁MSKSKCSVGLMSSVVAPAKEPNAVGPKEVELILVKEQNGVQLTSSTLTNPRQS
```

```
-----------------------_____TM1_____ -------_____
₅₉PVEAQDRETWGKKIDFLLSVIGFAVDLANVWRFPYLCYKNGGGAFLVPYLLF
```

```
__TM2_____-----IL1-----
MVIAGMPLFYMELALGQFNREGAAGVWK
```
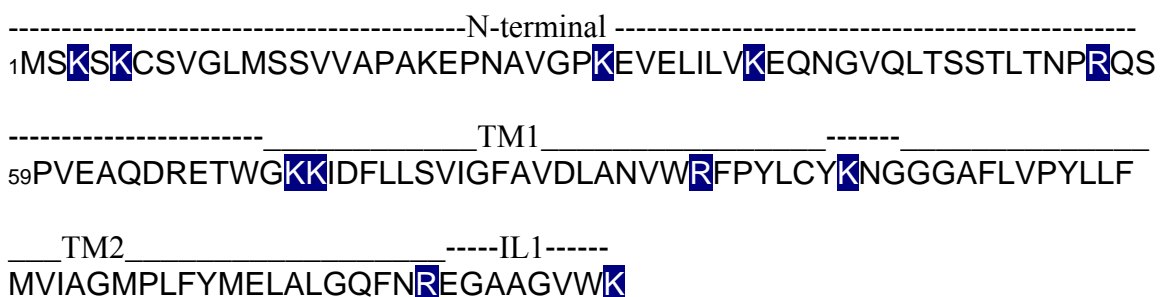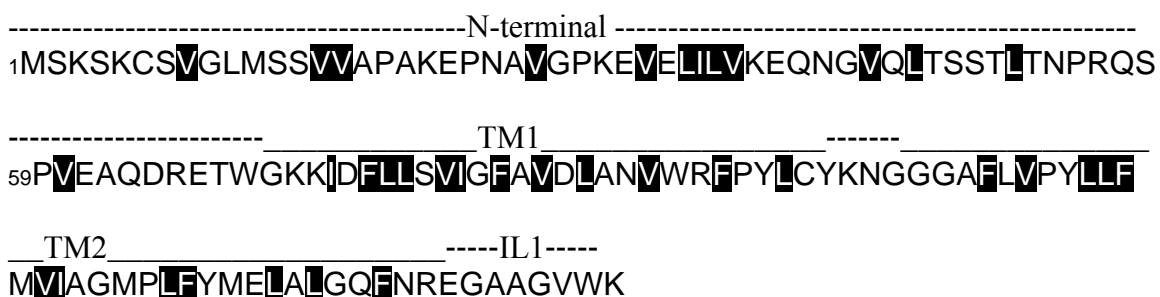
Figure 4.3 Comparison of possible trypsin and thermolysin cleavage sites of the hDAT TM1-TM2 region

There is a much smaller number of trypsin cleavage sites compared to the number of thermolysin cleavage sites in the TM1-TM2 region. The trypsin digest of the transmembrane domains 1 and 2 produces 2149 and 3652 Da hydrophobic peptides. The thermolysin digest of TM1-TM2 produces a number of small peptides, which allow for better HPLC separation and mass spectrometry analysis. Therefore, thermolysin is a more convenient choice of enzyme for HPLC characterization of a labeled peptide.

contained methionine within its sequence. The shift to a longer retention time initially seemed unusual, but additional experiments revealed that this shift can occur in the event of formation of smaller labeled peptide during a digest. Our studies of the influence of the label on the retention time of different synthetic peptides and amino acids are described below. They suggest that smaller peptides experience a more significant influence of the label and therefore their retention times change more compared to the larger peptides (Figure 4.4). The thermolysin digest of the region containing the PLFYM sequence can produce several possible peptides: FYME, FYMELA, LFYME, LFYMELA, FYMELALGQ, or LFYMELALGQ. One of these sequences possibly corresponds to the 63 min. thermolysin peptide.

Interpretation of the Edman Degradation Result

The 63 min. peak from the thermolysin digest was analyzed by Edman degradation. The goal of the experiment was to determine which cycle of the Edman degradation would produce the largest release of radioactivity, which corresponds to the labeled amino acid residue. Edman degradation is widely used to determine the sequence of analyzed peptides (Whitelegge et al., 1992; Kassab et al, 1998).

The following procedure was used to carry out Edman degradation analysis. The peptide from the thermolysin digest was immobilized via the C-terminal on an arylamine-Sequelon disk using ethyl-3-(3-dimethylaminopropyl)carbodiimide. Phenylisothiocyanate was reacted with the N-terminal amino group at mildly basic conditions, and a phenylthiocarbamoyl derivative was formed. The resulting derivative of the N-terminal amino acid was then cleaved as a thiazolinone derivative. The thiazolinone amino acid

was selectively extracted into an organic solvent and measured with a scintillation counter (Bethel et al., 1965; Levy, 1981). The amino acid derivative isomerized into substituted phenylthiohydantoin under acidic conditions (Figure 4.4).

The automated Edman sequencing is a very common technique. HPLC analysis is typically used after each cycle to identify the removed amino acid (Kessler et al., 2006). However, in our case, the peptide was labeled with a radioactive ligand. Due to low amounts of radioactively labeled hDAT peptides, we were not able to submit the sample to a microchemical facility. The amount of hDAT and the labeled peptides were insufficient for UV detection of the cleaved amino acid during the HPLC analysis that followed the Edman degradation. Therefore, manual Edman degradation was used by me and Dr. Tamara Herderson to determine which amino acid residue of the 63 min. peptide from the thermolysin digest was labeled with [125I]MFZ 2-24. Each cycle was performed manually and was followed by measurements of the radioactivity released. The results of the second cycle of the Edman degradation were statistically different from those of the rest of the cycles, which suggests that the second amino acid residue of the 63 min. peptide from the thermolysin digest of [125I]MFZ 2-24 labeled hDAT was modified.

The data from these experiments suggests that the second amino acid residue of the 63 min. peptide from the thermolysin digest of [125I]MFZ 2-24 labeled hDAT—which is Y115 or F114— was modified and is therefore a possible site of the [125I]MFZ 2-24 labeling.

The issue of the reactivity of phenyl azides with various amino acid residues has been addressed in the literature (Vogel, 1992; Schwartz, 1989). Cysteine had the highest reactivity with phenynitrenes among the amino acids and was 166 times more reactive

than the second most reactive amino acid, tryptophan, followed by tyrosine, phenylalanine, hystidine, lysine, and arginine (Schwartz, 1989).

Various amino acid residues have been reported as labeling sites when labels containing a phenylazide structure were used. Tyrosin 345 and Tyr 368 were the sites of photoincorporation of [2'3'-spin labeled]-2-azido-ATP in the mitochondrial F1-ATPase (Vogel, 1992), and Tyr 363 was the attachment site of Gly-Pro-Arg-N-4-azido-2-nitrophenyl-Lys amide at the primary fibrin polymerization site (Yamazumi and Doolittle, 1992). Tyrosines were the sites of incorporation of 8-azido-AMP in transhydrogenase from the bovine heart and the cAMP-dependent protein kinase (Ringheim et al., 1988). Tyr 49 on mouse monoclonal antiestradiol antibodies was modified by the DNA polymerase I Klenow fragment (Rush and Konigsberg, 1990), and 3-(p-azidobenzyl)-4-hydroxycoumarin labeled Tyr 128 of the NAD(P)H:quinine reductase (Myszka and Swenson, 1991). According to the literature, tyrosine seems to be the most often labeled amino acid residue. Cysteine was reported to be a modification site for 2[(4-azido-2-nitrophenyl)amino] ethyl diphosphate of the scallop myosin and in a nicotinic receptor modified with photosensitive snake toxin (Teixeira-Clerc et al., 2003).

Among other reported sites of phenyl azides modifications are Trp (Okamoto and Yount, 1985), Thr (Myszka and Swenson, 1991), Val (Brown et al., 1995), Arg (Kerwin and Yount, 1992), Asp (Moore et al., 1996), Asn, Pro (Tran and Farley, 1996), and Lys (Gibbs and Benkovic, 1991). The variety of amino acids that are labeled is not limited to the amino acids predicted to be most reactive with aryl azides.

The reactivity of tyrosine and phenylalanine was addressed in the recent study when Tyrosine 195 and Methionine 116 of the nicotinic acetylcholine (ACh) receptor

were labeled at the same frequency with azidoepibatidine (Tomizawa et al., 2007). However, the same study showed that substitution of Met 116 to Phe leads to only one site of photoincorporation at Tyr residue due to the insufficient reactivity of Phe suggesting tyrosine being more reactive with arylazides then phenylalanine.

Another indication that the peptides containing the PLFYM sequence are the possible peptides from the CNBr digest is that if VIAGM were the labeled peptide, thermolysin would produce IAGMP, VIAGMP, IAGMP, VIAGMPL, or VIAGMPLFYME peptides, with Ala or Ile as the second amino acid. In addition, aliphatic amino acid residues, Ala and Ile of VIAGM peptide, should react with phenyl azide mainly via formation of triplet nitrenes, and they would require stable intermediate radicals (Kotzyba-Hilbert, 1995). However, the formation of stable intermediates of aliphatic amino acids is unlikely event suggesting that Ile and Ala are unlikely residues for photolabeling (Knorre and Godovikova, 1998).

Analysis of the Influence of MFZ 3-37 on the Retention Time of Synthetic Peptides and Amino Acids

This study was undertaken to further investigate the effect of the label on the HPLC retention times of peptides and amino acids. Previous study has suggested that the effect of the label is a constant of 27 min. for the gradient used in this dissertation (Wirtz, 2004). However, further investigation of MFZ 3-37 reactions with different synthetic peptides and amino acids showed that the effect of the label may significantly vary depending on the size and properties of the peptides or amino acids (Figure 4.4).
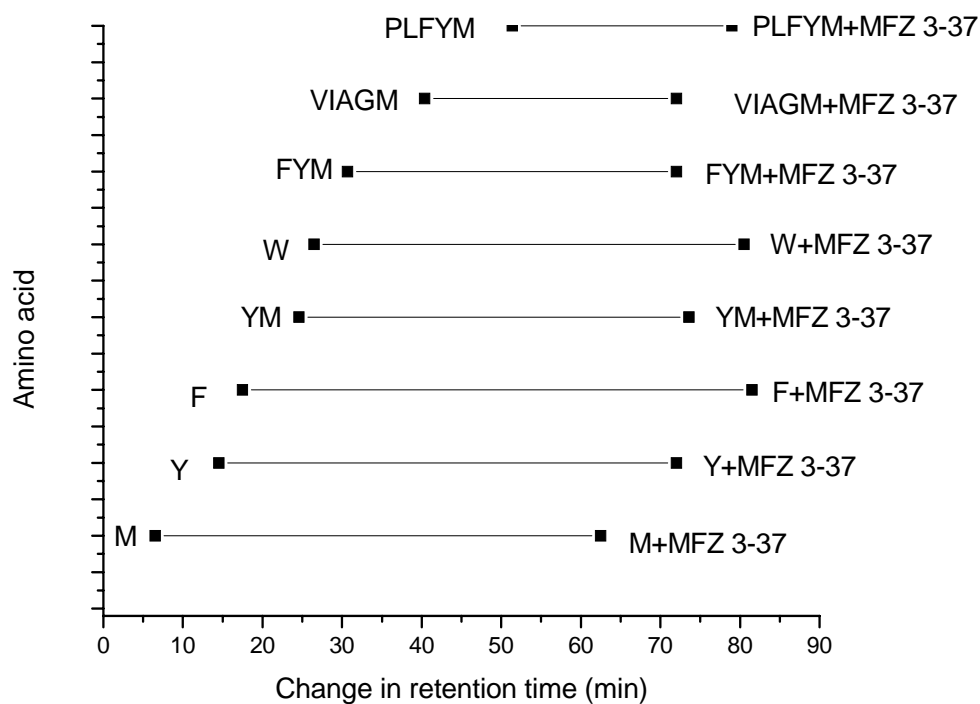
Figure 4.4 Effect of MFZ 3-37 on the retention time of synthetic peptides and amino acids

Several hDAT synthetic peptides and amino acids were reacted with MFZ 3-37. Retention times of the free peptides and amino acids are shown together with retention times of the products of reaction with MFZ 3-37. The label has greater effect on the retention times of amino acids than on those of peptides.

MFZ 3-37 has a retention time of 89 min. The retention times of peptides and amino acids in reverse-phase HPLC separation depend on several factors: the hydrophobicity of the separated molecule, the pH of the mobile phase that may be affected by the charge of the molecule (for example, amino groups from the N-terminal and basic amino acid residues are positively charged at low pH), and the position of the basic amino acid residues within the peptide at acidic pH (Spicer et al., 2007). Numerous studies of the factors contributing to the retention times of peptides in the reverse-phase separation confirmed the effect of amino acid composition, including the hydrophilicity/hydrophobicity of the side chains, the peptides' Van der Waals volumes, the sequence-dependent effect (Tripet et al., 2007), and the sequence-dependent nearest neighbor effects (Shortle, 2002).

The reaction of peptides and amino acids with MFZ 3-37 increases their retention time. As shown in this study, single amino acids exhibit a much larger increase in retention time than do peptides. This result can be attributed to the more significant effect of the label on the properties of the formed product. The product of reaction of a single amino acid with MFZ 3-37 elutes closer to the retention time of the free ligand. However, when a larger peptide is labeled, its properties dominate in the HPLC separation of the MFZ 3-37 product, resulting in a smaller change in the retention time.

Interestingly, PLFYM and FYM reacted with MFZ 3-37 had almost the same retention times—79 and 78.1 min., respectively—even though the retention times of unreacted peptides showed a 9 min. difference. VIAGM, YM, and Y exhibited similar retention times when labeled: 72 min., 73.6 min., and 74 min. Different amino acids within a peptide undoubtedly have different impacts on the retention times. For example,

YM and Y reacted with MFZ 3-37 have similar retention times, suggesting a major influence of the MFZ 3-37 part of the product and possibly a more significant influence of tyrosine compared to methionine. The effect of the MFZ 3-37 part on the model synthetic peptides and amino acids varied from 27.6 min. for PLFYM to 64 min. for phenylalanine (Figure 4.4). The smaller peptides and single amino acids experience larger retention time increases. This explains the increase in the retention time of the [^{125}I]MFZ 2-24 labeled peptide from the thermolysin digest when cleaved with CNBr. Additionally, the information about the retention times of the MFZ 3-37 labeled peptides and amino acids was used to estimate the retention times of the MFZ 2-24 labeled peptides from the CNBr, thermolysin, and chymotrypsin digests discussed previously.

TM1 and TM2 in Light of the LeuT$_{Aa}$ Crystal Structure

Crystal Structure of a Member of the NSS Family, LeuT$_{Aa}$

The most recent information about the structure of the neurotransmitter sodium symporter (NSS) family was obtained from X-ray crystal structure analysis of the bacterial leucine transporter (LeuT$_{Aa}$) (Yamashita et al., 2005). Despite the fact that LeuT$_{Aa}$ has only 25% sequence homology with hDAT, analogies can be made from the structure of LeuT$_{Aa}$ to the possible structure of hDAT (Yamashita et al., 2005). Analysis of the LeuT$_{Aa}$ crystal structure found that TM1 and TM6 of the transporter have a direct contact with the leucine binding site (Yamashita et al., 2005). According to the crystal structure analysis, TM2 does not have a direct contact with the leucine binding site;

instead, it contacts TM1 and TM6 via a pincer-like configuration formed by highly conserved proline residue (Sen et al., 2005).

Inhibitor Binding Site on the LeuT$_{Aa}$

Zhou et al. (2007) expanded the investigation of the leucine transporter by obtaining the crystal structure of LeuT$_{Aa}$ in the presence of the antidepressant desipramine. They confirmed the previously discovered crystal structure of LeuT$_{Aa}$ and located the desipramine binding site. The amino acids found to contact the desipramine molecule were R30 and Q34 from TM1, L400 and D401 from TM10, and A319 and F320 from EL4, along with F253 (the only overlapping residue contacting both the substrate and the inhibitor). Zhou et al. (2007) also showed that desipramine noncompetitively inhibits leucine binding by decreasing its transport activity. Additionally, the authors showed that desipramine binds to the extracellular gate and maintains it in the locked conformation. They also conducted the gain of function mutational studies of hDAT, hSERT, and hNET amino acid residues corresponding to the LeuT$_{Aa}$ binding site. The results suggest the presence of a conserved deziproamine binding site among the NSS family (Zhou et al., 2007). A modified figure from their paper showing the possible molecular contacts of hDAT and bound deziproamine is presented in Figure 4.5.

Singh et al. (2007) determined the structures of LeuT$_{Aa}$ co-crystallized with clomipramine, imipramine, and desipramine. These results confirm the findings of Zhou et al. (2007). Singh et al. (2007) also confirmed the noncompetitive inhibition of the substrate uptake by clomipramine, imipramine, and desipramine by stabilizing the
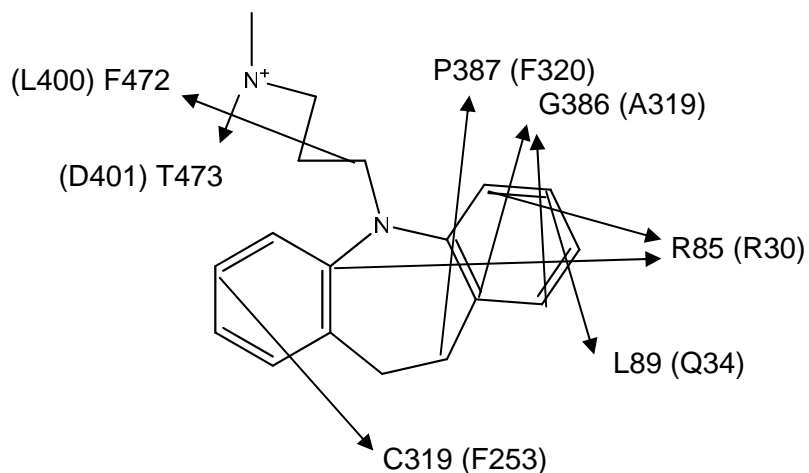
Figure 4.5 Molecular contacts of desipramine with hDAT equivalents of LeuT$_{Aa}$ amino acid residues

hDAT residues equivalent to the LeuT$_{Aa}$ residues from the desipramine binding site are shown. Mutational studies of these hDAT residues indicated that hDAT has the same dezipramine binding site as LeuT$_{Aa}$. LeuT$_{Aa}$ amino acid residues are shown in brackets. (Adapted from Zhou et al. [2007].)

extracellular gate formed by R30 and D404, which in turn stabilizes Y108 and F253, locking the bound substrate.

Indarte et al. (2008) used the sequence alignment of hDAT and LeuT$_{Aa}$ to build a three-dimensional homology model of hDAT based on the LeuT$_{Aa}$ crystal structure template. Docking of the dopamine and d-amphetamine showed two potential binding sites (Indarte et al., 2008). The primary binding site was similar to the binding site in LeuT$_{Aa}$; the proposed secondary binding site was located closer to the outer part of the DAT. Three different sequence alignments of DAT and LeuT$_{Aa}$ pointed to the involvement of A77, V78, and D79 from TM1 and S320 and L321 from TM6 of hDAT, which are in direct interaction with dopamine and amphetamine substrates (Indarte et al., 2007). These results are important for my research because desipramine inhibits hDAT dopamine uptake and may partially share a binding site with cocaine (Zhou et al., 2008). Furthermore, Henry et al. (2006) demonstrated the complete inhibition of the [^{125}I]MFZ 2-24 labeling of hSERT in the presence of imipramine suggesting that MFZ 2-24 and imiparmine binding sites may overlap. However, the desipramine and the cocaine binding sites likely only partially overlap. Mutational studies can facilitate the further identification of the amino acid residues important for the cocaine binding.

Involvement of TM2 in Cocaine Binding

According to the LeuT$_{Aa}$ crystal structure, the TM2 domain is not directly involved in the inhibitor binding site thought to be near the substrate binding site or near the desipramine binding site (Zhou et al., 2007). However, mutational studies suggest three amino acid residues in TM2—L104, F105, and A109—that are either directly or

indirectly involved in the cocaine binding site (Wu and Gu, 2003; Chen et al., 2005). Chen et al. (2005) reported a triple L104V, F105C, and A109V mouse DAT mutant that retains 50% of uptake activity and is 69 times less sensitive to cocaine, suggesting a possible involvement of these residues in the cocaine binding site.

Another study used the substituted cysteine accessibility study method (SCAM), where all the amino acids in TM2 were mutated one by one to cysteines (Sen et al., 2005). TM2 is suggested to be inaccessible to water and is therefore likely to indirectly affect the cocaine binding (Sen et al., 2005). However, Sen et al. (2005) also suggest that cocaine requires the "closed inward" configuration and that TM2 mutations reported by Chen et al. (2005) prevent hDAT from forming the preferable conformation. The required "closed inward" conformation for cocaine binding is questionable in light of other recently published studies suggesting that an "outward" conformation is preferable for cocaine binding (Loland et al., 2008; Loland et al., 2004). Loland et al. (2008) also propose that C159 of the I159C mutant is not water accessible when hDAT is in the "inward" conformation and that C159 is accessible to MTS reagents when cocaine and its analogs are bound in the binding site. The authors also discuss the LeuT$_{Aa}$ crystal structure that represents the closed gate conformation of the transporter and therefore may not fully reflect the hDAT structure in the event of cocaine binding (Loland et al., 2008). Additionally, TM2 was demonstrated to participate in interactions with cocaine and indirectly with the substrate in hNET (Sucic and Bryan-Lluka, 2007). The mutations Q118, Y119, N120, R121, and E122 in TM2 of human NET into cysteine resulted in an increased binding affinity of cocaine due to the improved binding properties of the region (Sucic and Bryan-Lluka, 2007; Sucic et al., 2002). This result suggests the importance of

TM2 for cocaine binding. Furthermore, it was shown that the same mutations did not affect the affinity of desipramine, suggesting that the desipramine and cocaine binding sites are not identical in hNET (Sucic and Bryan-Lluka, 2007).

PLFYM as a Possible Region of hDAT Labeling

To evaluate the possibility that PLFYM is the region labeled with [^{125}I]MFZ 2-24, the LeuT$_{Aa}$ crystal structure was used as a template to visualize the location of the residues of interest (Figure 4.7). P112 and L113 are conserved among the majority of the members of the NSS family (Yamashita et al., 2005). Mutations of P112 and F114 to cysteines deactivate the hDAT (Sen et al., 2005). Amino acid residues at the positions corresponding to F114, Y115, and M116 in the hDAT differ within the family, and these residues are replaced with M59, W60, and I61 in the LeuT$_{Aa}$ structure (Figure 4.6). Although these three residues are not identical throughout the family, the amino acid residues are relatively conservative with respect to their properties (Indarte et al., 2008). In hDAT, F114 corresponds to M59 in LeuT$_{Aa}$, and M116 corresponds to I61. Both pairs are non-polar neutral amino acids with similar hydrophilicity and Van der Waals volumes (Henry et al., 2006). The Y115 position experiences the most significant change due to the replacement of the polar tyrosine with a significantly larger non-polar tryptophane.

TM2 is separated from the desipramine binding site by TM1. PLFYM is located in the middle of TM2. The distances between TM1, TM2, and TM6 are approximately equal, enclosing free space in the shape of a triangle with ~8 Å sides. Therefore, one can speculate that an MFZ 2-24 molecule with a 5 Å pharmacophore and a 10.5 Å arm with

LeuT~Aa~ **P L** M W I

hDAT   **P L** F Y M

rDAT   **P L** F Y M

bDAT   **P L** F Y M

hSERT **P L** F Y M

hNET   **P L** F Y M

GAT1   **P L** F L L

GlyT1b **P L** F F M

ProT   **P L** F L L

ChoX   **P** I F F L

TauT   **P** V F F L

Figure 4.6 Alignment of the amino acid sequences of the NSS family, corresponding to residues 112-116 of the hDAT PLFYM motif

Pro is conserved among all members of the NSS family. Lys is conserved in the majority of the NSS family members. FYM of hDAT is substituted with MWI in LeuT~Aa~. (Adapted from Giros and Caron, 1993.)

reactive nitrene (Wirtz, 2004; Vaughan et al., 2008) can fit in this space, reaching F114 or Y115. Additionally, the previously discussed mutations at L104, F105, and A109 in TM2 may designate a part of the cocaine binding site (Figure 4.8). These three residues important for the cocaine binding are situated within 6.5–13.5 Å from the F114 of PLFYM. This range is comparable to the size of MFZ 2-24, suggesting that PLFYM may be the labeled peptide. Additionally, knowing that the LeuT$_{Aa}$ crystal structure is presented in "inward" conformation (Zhou et al., 2007; Loland et al., 2008) and that cocaine binds to the "outward" conformation (Loland et al., 2008), as it does for hNET (Chen and Justice, 1998), it is possible that the gap between TM1, TM2, and TM6 may be even larger to accommodate MFZ 2-24.

There is also a possibility that cocaine binds at the desipramine binding site region designated by TM1, TM6, and EL4 (Singh et al., 2007). According to the LeuT$_{Aa}$ crystal structure, the distance between the desipramine binding site and the F114 (the amino acid residue closest to the PLFYM sequence facing the desipramine binding site) is 19.8 Å. This distance is slightly greater than the predicted length of MFZ 2-24 (Wirtz, 2004). However, one can argue that even though desipramine and cocaine may partially share the binding site, these two molecules may have a partially different binding pocket, as discussed above (Henry et al., 2005; Zhou et al., 2007). Therefore, MFZ 2-24 may still be within reach of TM2. Interestingly, the PLFYM sequence is situated right next to the unwound region of TM1. Therefore, PLFYM may be accessible to the MFZ 2-24 arm containing a reactive azido group when the pharmacophore is bound to the elements of the dezipramine binding site. Additionally, according to the hDAT model, F114 faces the desipramine and leucine binding sites, while Y115 does not directly face these binding
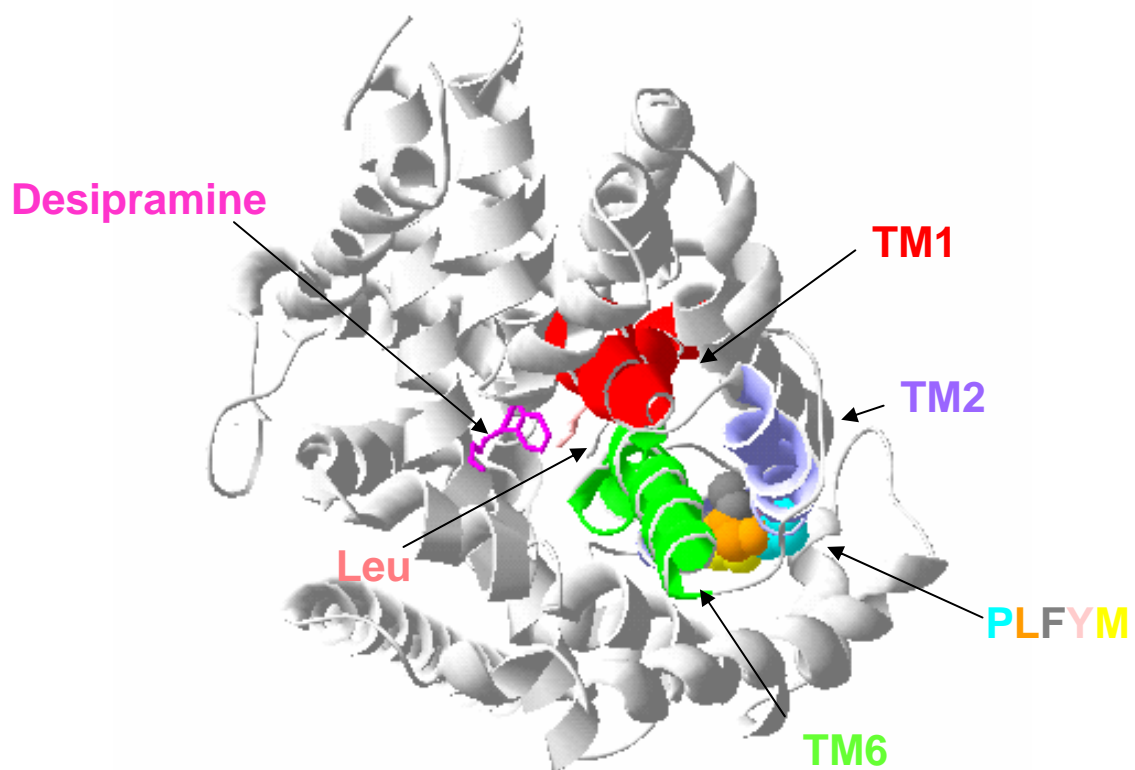
Figure 4.7 Top view of the molecular representation of hDAT using the LeuT$_{Aa}$ crystal structure template

TM1 is shown in red, TM2 is lavender, TM6 is green, the desipramine molecule is magenta, and the leucine molecule is pink. The PLFYM sequence of TM2 is light blue, orange, dark green, pink, and yellow, respectively. The distances between TM1, TM2, and TM6 are approximately equal at 8 Ǻ.
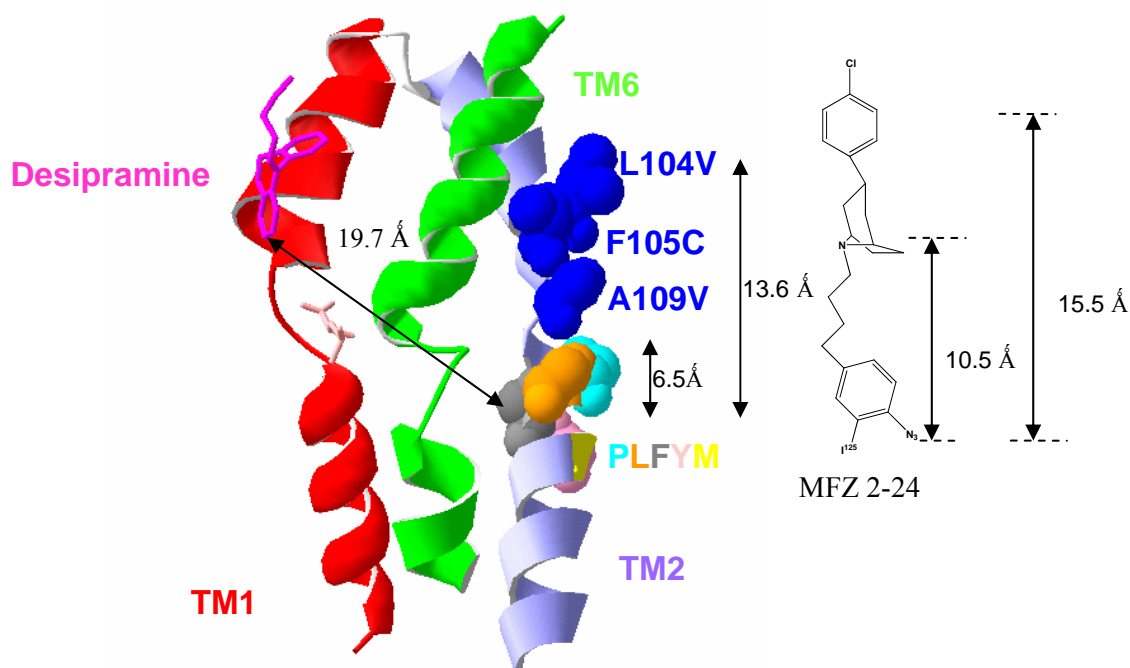
Figure 4.8 A model of TM1, TM2, and TM6 of hDAT using the LeuT$_{Aa}$ crystal structure template

TM1 is shown in red, TM2 is lavender, TM6 is green, the desipramine molecule is magenta, and the leucine molecule is pink. The PLFYM sequence of TM2 is shown in light blue, orange, dark green, pink, and yellow, respectively. The locations of three residues important for cocaine binding, L104, F105, and A109 (Chen et al., 2005) are shown in dark blue. The distance between A109 and F114 is 6.5Å and between L104 and F114 is 13.6 Å. MFZ 2-24 is 15.5Å long when it is in the longest conformation. The distance between the nitrene and the tropane nitrogen is 10.5 Å. The distance between desipramine and F114 is 19.7 Å.

sites. Therefore, if the cocaine binding site is located near the desipramine binding site, F114 has a better chance than Y155 to be labeled. On the other hand, Y115 is proposed to be more reactive with phenyl nitrenes than F114 suggesting that tyrosine is the more likely candidate for labeling (Schwartz, 1998).

Involvement of TM1 in Cocaine Binding

To fully evaluate the possible photoincorporation region, the TM1 domain should be investigated. TM1 is situated next to the leucine and desipramine binding sites of LeuT$_{Aa}$ and is suggested to participate in the desipramine binding site of hDAT (Zhou et al, 2007). Therefore, TM1 may be a region of particular interest.

Kitayama et al. (1992) showed the importance of negatively charged Asp79 situated in the middle of TM1 of DAT. Mutations of Asp79 to Ala, Glu, or Gly decreased the affinity of the mutant DAT to the cocaine analog WIN 35,428 and reduced the dopamine uptake, suggesting that a positively charged amino group may be important for interaction with cocaine analogs and substrate (Kitayama et al., 1992; Chen et al., 2005). Mutation of Phe76 to Ala in rDAT reduced the affinity for WIN 35,428 by a factor of three while the dopamine uptake remained at the wild type level, suggesting a possible contribution to inhibitor recognition via π-π interaction of the aromatic rings of cocaine and phenylalanine (Lin et al., 1999; Uhl and Lin, 2003). The mutational studies and information obtained from the LeuT$_{Aa}$ crystal structure suggest that both TM1 and TM2 may play an important role in cocaine binding directly by interacting with the inhibitor molecule or indirectly by participating in the conformational changes of DAT.

Analysis of Cysteine 90 hDAT Mutant

C90 as a Possible Site of MFZ 2-24 and MFZ 3-37 Labeling

As stated previously, both MFZ 2-24 and MFZ 3-37 label hDAT (Vaughan et al., 2005). The only difference between these two labels is that MFZ 2-24 has an azido group and MFZ 3-37 has an isothiociano group; otherwise, these two compounds share very similar chemical structures, including identical pharmacophores. Therefore it is likely that their sites of label incorporation are identical or situated in close proximity to each other. A previous immunoprecipitation study suggested the TM1-TM2 region as the site of MFZ 2-24 photoincorporation (Vaughan et al., 2005), so in order to evaluate the possible targets for both MFZ 2-24 and MFZ 3-37, the TM1-TM2 region was examined.

As stated previously, the only difference between MFZ 2-24 and MFZ 3-37 is that they have azido and isothiocyano groups, respectively. The reactivities as well as the reaction yields of these two groups are significantly different (Schuster and Platz, 1992; Schwartz, 1989; Conaway et al., 2001). Yet, there are some similarities in the targets of both ligands. For example, the reactivity of arylazides with various aromatic and aliphatic amino acid residues has been previously discussed in this chapter. Schwartz et al. (1989) showed that the reactivity of cysteine residue with phenynitrenes is 166 times higher than its reactivity with the second most reactive amino acid, tryptophan. Multiple photoaffinity studies suggest tyrosine, cysteine, or tryptophan as the most common sites of incorporation (Tomizawa et al, 2007; Knorre and Godovikova, 1998). However, numerous aliphatic residues were reported as labeling sites (Knorre and Godovikova, 1998). Isothiocyanates are reactive with thiols and, to a lesser extent, with amino or

hydroxyl groups due to their electrophilic properties (Drobinica and Augustin, 1965). The main target for isothiocyanates are cysteines and lysines (Breier and Ziegelhoffer, 2000).

There are only one cysteine and four lysines in the TM1-TM2 region that is suggested to be the site of MFZ 2-24 incorporation (Vaughan et al., 2003). The hDAT model using the LeuT$_{Aa}$ crystal structure has been used to identify the location of residues of interest (Yamashita et al., 2005; Zhou et al., 2007). The object of our particular interest for this research was C90, a highly conserved residue situated at the top of TM1. Additionally, only one lysine, K92, is located in the outer part of the hDAT in EL1. We propose that because cysteine was shown to be the most reactive amino residue with both isothiocyanates and phenynitrenes, C90 can be a site of incorporation for MFZ 3-37 and possibly MFZ 2-24.

According to the LeuT$_{Aa}$ crystal structure, the residue corresponding to C90 is situated at the top of TM1 and within close proximity to the desipramine binding site (Figure 4.9). The distance between desipramine and the residue corresponding to C90 in LeuT$_{Aa}$ is 9.3 Å (measured with a DeepView PDB viewer distance measuring tool), which is within the length of the most flexible part of the label (the distance between the nitrene or isothiocyanate group and tropane nitrogen is 10.5 Å) (Vaughan et al., 2005). Therefore, we conclude that C90 is situated within reach of the label.

Interpretation of MFZ 2-24 and MFZ 3-37 Labeling of WT and X5C hDAT

To explore the importance of C90 for MFZ compounds, the X5C hDAT was studied. X5C is a mutant in which five out of thirteen cysteines (C90, C135, C306, C319,
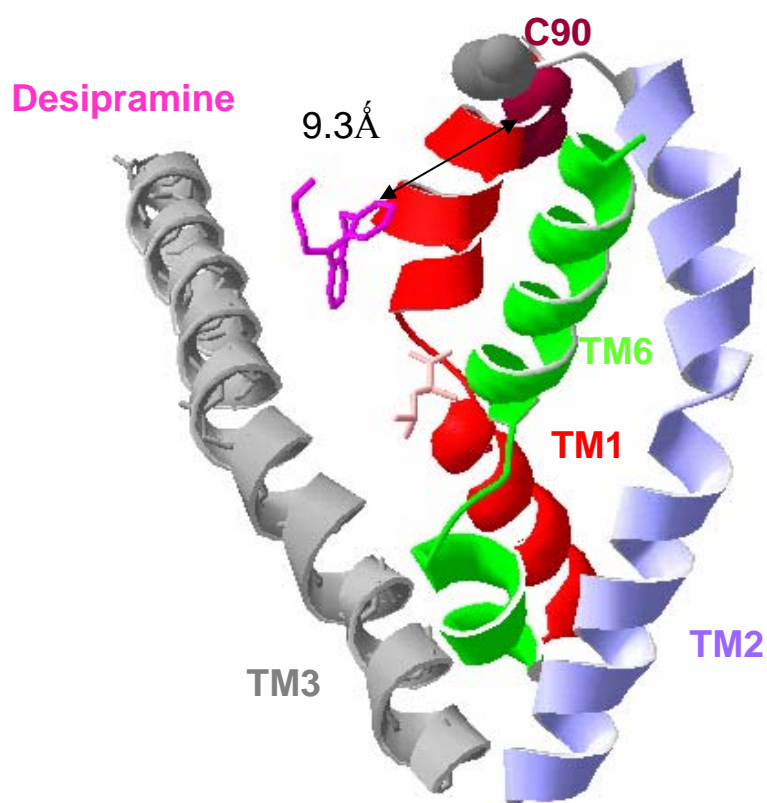
Figure 4.9 A model of TM1, TM2, TM3, and TM6 of hDAT using the LeuT$_{Aa}$ crystal structure template (Zhou et al., 2007)

TM1 is shown in red, TM2 is lavender, TM3 is grey, TM6 is green, the desipramine molecule is magenta, and the leucine molecule is pink. C90 of TM1 is shown in burgundy, and K92 is dark grey. The maximum distance between C90 and desipramine is 9.3 Å. MFZ 2-24 and MFZ 3-37 are 15.5Å long when they are in their longest conformations. The distance between the nitrene or isothiocyanate group and tropane nitrogen is 10.5 Å (Vaughan et al., 2005).

and C342) were mutated to alanines or phenylalanines to create the MTSET-insensitive construct (Ferrer and Javitch, 1998). The X5C mutant was initially constructed by Ferrer and Javitch (1998) to investigate the influence of cocaine analogs on the accessibility and reactivity of endogenous cysteines. Different hDAT inhibitors were tested for their ability to protect hDAT C90, C135, and C342 in order to study conformational changes of hDAT (Reith et al., 2001).

A general labeling procedure was used for our study. Results showed that MFZ 2-24 labels both wild type (WT) hDAT and X5C hDAT at the same level. These data suggest that C90 is not the site of MFZ 2-24 incorporation or it could suggest that in the absence of C90 MFZ 2-24 or MFZ 3-27 could possibly label another amino acid instead of the cysteine. K92 is situated within one amino acid residue from C90 and can possibly react with MFZ 3-37 when C90 is not present. However, the lysine residues are not a favorable target for MFZ 2-24 containing an azido group (Knorre and Godovikova, 1998). Taking into account that X5C and WT hDAT have nearly the same affinity for the WIN 35,428 cocaine analog (Ferrer and Javitch, 2008) and that the rates of labeling with MFZ 3-37 or MFZ 2-24 did not change, we conclude that C90 is not required for MFZ 2-24 or MFZ 3-37 labeling. However, it is unclear whether C90 is not a labeled amino acid residue or whether another residue is labeled when C90 is mutated out. Therefore, to further investigate these uncertainties, cysteine-reactive MTS reagents were used to collect data on the importance of C90 for MFZ 3-37 and MFZ 2-24 labeling.

Analysis of X-A90C hDAT Labeling in the Presence of Cysteine-Reactive MTS Reagents

To further investigate whether C90 is important for MFZ 2-24 and MFZ 3-37 labeling, the X-A90C hDAT mutant was examined along with WT, X5C, and X-A306C. WT, X5C, and X-A306C were used as controls. In X-A90C and X-A306C, the same five cysteines are mutated out and replaced with C90 or C306 in the sequence in order to evaluate the effect of each of cysteine residues on ligand binding (Ferrer and Javitch, 1998).

X-A90C and X-A306C are situated in EL1 and EL3, respectively (Ferrer and Javitich, 1998). It has previously been shown that re-introduction of C90 into the sequence leads to the increased binding affinity of the cocaine analog CFT (Ferrer and Javitch, 1998). The labeling levels of WT, X5C, X-A90C, and X-A306C were determined both in the absence and in the presence of the cysteine-reactive reagents [2-(trimethylammonium)ethyl] methanethiosulfonate bromide (MTSET) or/and benzyl methanethiosulfonate (MTSBn). Probes reacted with MTS reagents were incubated with MTSET or MTSBn prior to incubation with MFZ 2-24. Ferrer and Javitch (1998) showed that pre-incubation of X-A90C, and X-A306C with MTSET leads to increase in WIN 35,428 binding .

Interestingly, WT and X5C exhibited a decrease in labeling in the presence of MTSET, while X-A90C and X-A306C showed significant increases in labeling when reacted with MTSET or even larger-sized neutral MTSBn. This suggests that C90 may be exposed to the cocaine binding site (Ferrer and Javitch, 1998). The change in the binding affinity could be explained by MTS reagents changing the environment of MFZ 2-24 or

MFZ 3-37 binding pockets due to the introduction of positively charged or bulky groups of MTS reagents or just to special rearrangement of the TM1 or TM6 regions and increasing the affinity by allowing more accessibility to the labeling site (Ferrer and Javitch, 1998).

An increase in ligand binding does not necessarily lead to increased labeling when a modified amino acid residue is mutated out. However, the increased labeling of X-A306C, the mutant with increased binding affinity to CFT but that lacks C90, suggests that C90 is not required for increased labeling. Therefore, C90 is likely not the labeled amino acid residue.

There is no definite answer to the question of whether C90 is the target for MFZ 2-24 or MFZ 3-37. However, it has been determined that the presence of C90 is not mandatory for MFZ 2-24 and MFZ 3-37 labeling. This could be explained by the fact that another amino acid is labeled initially or because ligands are not selective and label different amino acid residues (for example, K92) when C90 is missing. However, our results support the findings by Ferrer and Javitch (1998) that C90 may be involved in cocaine binding, directly or indirectly because of the increased hDAT labeling with MFZ 2-24 and MFZ 3-37 when preincubated with MTS reagents.

Mass Spectrometry Approach to the Identification of hDAT Peptides and Labeled hDAT Peptides

Sample Preparation Strategies for Membrane Protein hDAT

hDAT is a membrane protein (Giros and Caron, 1993) and is thus a challenging object for mass spectrometry analysis. The two main problems with α-helical integral membrane proteins are, as in all the membrane proteins, the presence of the hydrophobic transmembrane domains and the low abundance of the protein (Speers and Wu, 2007), which lead to difficulty of solubilization during sample preparation (Grant and Wu, 2007). Wirtz (2004) calculated that 1 plate of HEK 293 cells expressing hDAT contains 2 pmol of the dopamine transporter suggesting that it may be challenging to detect hDAT peptides due to their low amount. Therefore, special approaches to solubilization, separation, purification, and analysis are required.

Nonionic detergent Triton X-100 was selected for solubilization due to its compatibility with enzymatic digests and low ionization suppression effect (Zhang et al., 2008; Peng et al., 2004). Additionally, a solubilization buffer containing Triton X-100 was shown to solubilize $[^{125}I]$MFZ 2-24 labeled hDAT in the experiments described in this chapter. Certain solubilizing agents, such as 90% formic acid and 70% TFA, would not have been suitable in experiments where hDAT labeled with MFZ 3-37 was analyzed because of hydrolysis of the product of reaction of MFZ 3-37 with the protein (Edman, 1950; Sanchez-Machado et al., 2003; Mora et al., 1988).

Another possible problem in mass spectrometric analysis of membrane proteins is sample complexity. Solubilized cell lysate contained a complex protein mixture. Taking

into account the low protein abundance of hDAT, purification steps are necessary to ensure detection of hDAT peptides. Additionally, gel separation lowers the amount of peptides and proteins in the final muli-component sample and prevents ion suppression, which can affect identification of both hydrophilic and hydrophobic peptides when the sample is analyzed by electrospray ionization (Sterner et al., 2000). One-dimensional SDS-PAGE was chosen as a separation method because this separation method is not dependant on pI values of proteins compared to two-dimensional gel electrophoresis. This method is also capable of separating highly hydrophobic peptides and proteins (Speers and Wu, 2007). In addition, Sostaric et al. (2006) demonstrated that the detection of membrane proteins exhibited a six-fold improvement when one-dimensional gel electrophoresis was used instead of two-dimensional separation of solubilyzed proteins from oviductal epithelial cells.

After the SDS-PAGE separation, hDAT was in-gel digested using thermolysin. The commonly used trypsin is not the preferred choice of enzyme for membrane proteins, including hDAT because there are only a few trypsin cleavage sites in transmembrane domains (Speers and Wu, 2007). The digest produces large hydrophobic peptides, which are difficult to extract from a gel (Grant and Wu, 2007), because few Lys and Arg are located in the transmembrane regions. In fact, eight out of twelve TMs lack Arg or Lys residues. HPLC separation using reverse-phase chromatography then becomes complicated due to the inability to elute long hydrophobic peptides from the column (Zhang et al., 2008). As stated previously, TM1 and TM2 are the domains of particular interest in hDAT due to their role as possible incorporation sites for the label (Vaughan et al., 2003). The trypsin digest of the TM1-TM2 region produces the 2-3 kDa peptides.

TM1 can produce the 19 amino acid peptide starting with I67 and ending with R85 and the small 7 amino acid peptide FPTLCYK. The peptide containing the complete TM2 starting with N93 and ending with R125 is also formed (Figure 4.3). The extracted long hydrophobic peptides may aggregate during the extraction and subsequent analysis, failing to elute from the reverse-phase HPLC column (Zhang et al., 2008; Speers and Wu, 2007; Quach et al., 2003). Instead, different approaches to enzymatic digests were taken to obtain small peptides in the membrane protein digests (Wu and Yates, 2003; Nielsen et al., 2005). CNBr/formic acid, Lys-C, a combination of 60% methanol with trypsin, proteinase K, and a combination of chymotrypsin with trypsin are just a few of the conditions used.

The search for hDAT peptides using mass spectrometry analysis did not result in detection of any hDAT peptides after using the CNBr/70% TFA digest. This failure may be attributed to the fact that only 13 methiones are present in hDAT and some of the produced peptides may aggregate or be too long for HPLC separation using the reverse-phase HPLC column. Surprisingly, thermolysin is not one of the commonly used enzymes for mass spectrometry sample preparation despite its ability to cleave hydrophobic regions. Previous experiments showed that thermolysin produces small labeled peptides when MFZ 2-24 labeled hDAT is cleaved. In our mass spectrometry experiments, we utilized thermolysin to obtain small peptides from both hydrophobic TMs as well as the loop and terminal regions.

Before the mass spectrometry analysis, nanoLC separation was introduced to ensure that hDAT peptides were detected despite the low abundance of hDAT. NanoLC was connected in line with a Fourier transform ion cyclotron resonance mass

spectrometer (FT-ICR) to obtain high resolution spectra, followed by secondary-stage MS/MS analysis of the six most intense ions from the initial high resolution mass spectrometry analysis. hDAT peptides do not always produce the strong signal necessary for selection of the top six ions that undergo MS/MS characterization. Therefore, nanoLC separation was used because it is thought to allow the detection of more peptides from low-abundance hDAT. The reverse-phase nanoLC column was selected as the most appropriate choice for separation of hydrophilic peptides from the N-terminus, C-terminus, and loop regions from the hydrophobic peptides of TMs. The columns were packed in-house using a pressure bomb.

In order to process samples faster and avoid the peptide extraction step, during which a significant loss of peptides can occur (Zhang et al., 2008), attempts were made to develop a purification step involving FLAG M2 affinity chromatography of 3XFLAG-6XHis-hDAT or affinity purification using monoclonal antibodies to MFZ 2-24 instead of one-dimensional gel purification. 3XFLAG-6XHis-hDAT was tested for the presence of the Flag-tag using Western blot analysis, and its presence was confirmed; however, despite this, the Flag-column purification allowed only 12% recovery of hDAT. The majority of the protein did not bind to the column, likely due to weak interaction of 3XFLAG-6XHis-hDAT with the anti-FLAG M2 affinity column. Possible reasons for the weak interaction include the hindering of the tag with the hydrophobic parts of hDAT or Flag-tag expression only in part of hDAT (Elhofy and Bost, 1998). Another attempted approach involved purification of only the MFZ-labeled hDAT peptides from the thermolysin digest of hDAT labeled with MFZ 3-37, using monoclonal antibodies to MFZ 2-37 (provided by Dr. Javitch, Columbia University). This approach can provide

the best purification since only labeled peptide is expected to remain in the sample for mass spectrometry. However, this approach was not successful in our experiments due to two major challenges. First, the product of the MFZ 3-37 reaction with peptide is not stable and may hydrolyze during the enzymatic digestion and column purification steps (Conaway et al., 2001; Sanchez-Machado et al., 2003). Second, MFZ 2-24 antibodies have affinity to the free label that is present in the solution. Therefore, free MFZ 3-37 or MFZ 2-24 compete with the labeled peptides. Attempts to eliminate excess free ligand by dialysis were not successful, likely due to the unfavorable properties of the MFZ compounds. Therefore, it was concluded that affinity purification using the MFZ 2-24 antibody column is not a reliable purification method.

Detection Limit for FT-ICR Mass Spectrometer Coupled with NanoLC Chromatography

To evaluate the utility of FT-ICR mass spectrometry coupled with nanoLC chromatography, the sensitivity of the method was measured. FT-ICR is a very powerful technique whose reported detection limit can be as low as 10 fmol for the digest of casein (Choudhary et al., 2004). Several studies also report detection of protein mixtures in the low femtomolar range (Peng and Gygi, 2001; Witt et al., 2003). For example, separation and detection of low femtomolar amounts of peptides from bovine serum albumin (BSA) tryptic digest were reported by Witt et al. (2003); however, the BSA sequence coverage at such a low amount was only 7% suggesting the inability to detect the majority of peptides.

To estimate the amount of hDAT sufficient for mass spectrometry identification of labeled peptides, the detection limit for MFZ 2-24 and synthetic FYMELAL were determined in FT and ion trap modes. Synthetic FYMELAL was chosen because it has the same sequence as a peptide from the hydrophobic TM2 region. The amount of MFZ 2-24 detectable in both FT and ion trap was 5 fmoles when the in-house packed nanoLC connected to standard nanospray source was used; the limit of detection for synthetic peptide FYMELAL was 10 fmoles. It was determined that 1 plate of HEK cells contained 2 pmols of hDAT (Wirtz, 2004). Even though this amount of hDAT decreases during the processing and purification steps, detection limits for MFZ 2-24 and FYMELAL are very promising compared to the amounts of hDAT from 48 plates, which is the amount typically used in experiments.

The detection limit for FT-ICR mass spectrometry coupled with nanoLC chromatography is comparable to the amount of MFZ 2-24 labeled hDAT peptides obtained from CNBr and thermolysin digests. Vaughan et al. (2005) reported that only 1 fmol of labeled peptide was obtained from 100 plates of HEK 293 cells expressing hDAT. The amount of $[^{125}I]$MFZ 2-24 labeled peptides obtained from HPLC separation can be calculated using $[^{125}I]$MFZ 2-24 specific radioactivity. According to the calculations determined from this research, 100 plates of HEK 293 cells expressing hDAT yield 11 fmol of $[^{125}I]$MFZ 2-24 labeled hDAT peptide after the gel separation, in-gel digestion, extraction, and HPLC separation steps. This amount is comparable to the detection limits of the instruments and may be difficult to detect due to the complexity of the analyzed sample. Such a low amount of MFZ 2-24 peptides can be attributed to the low efficiency of label photoincorporation (less than 1%) containing iodine in the ortho-

position in the aryl azide moiety (Watt et al., 1989; Schuster and Platz, 1992) and multi-step processing of the sample containing hydrophobic peptides (Speers and Wu, 2007).

A new Axial Desolvation Vacuum Assisted Nano Capillary Electrospray source (ADVANCE) was tested for future application to detect low-abundance peptides and proteins, including hDAT. C18 microcolumn was coupled with ADVANCE source of the high resolution LTQ-FT to facilitate separation of a sample. This source allows higher flow rates for HPLC separation (5 µl/min. compared to 250 nl/min. when using the standard nanospray source connected to the in-house fabricated nanoLC column). A sensitivity study showed that the detection limit for synthetic FYMELAL was 5 fmol, which is two times lower than the detection limit of the standard source. Additionally it was noticed that the ADVANCE source provides eight times higher sensitivity than the standard source at higher femtomolar range (100 fmol), probably due to decreased loss of ions. The ADVANCE source was found to be a valuable tool for detection of small amounts of peptides and proteins.

Identification of hDAT Peptides from the Thermolysin Digest

hDAT peptides were identified using a high-resolution Fourier transform ion cyclotron resonance mass spectrometer (FT-ICR-MS). FT-ICR allows detection of medium- and low-abundance proteins with an accuracy within 5 ppm (Barrow et al., 2004; Lu et al., 2008). Two different methodologies were used to search for the detected hDAT peptides. The first approach employed the detection of the peptide based on the accurate mass, which started to be employed often due to the high-resolution instrumentation availability (Lu et al., 2008), using PepMap (Thermo Electron, San Jose)

software. PepMap matches the masses from acquired spectra of the hDAT digest to the masses from the predicted digest. The peptides were detected based on high-resolution FT-MS data with 5 ppm mass tolerance. The program also yields the retention times at which the detected peptides were eluted. Only 3% false positive identification was reported for this approach (Lu et al., 2008).

The second approach to detection of hDAT peptides involved the TurboSequest (Thermo Scientific, San Jose, CA) search algorithm, which allowed the search of acquired first stage MS and second stage MS/MS data in the protein FASTA database (Falkner, 2008). The program correlates the tandem MS/MS mass spectra with theoretical MS/MS spectra. The MS scan is followed by six data-dependent MS/MS scans of the top six most intense ions. This approach can be disadvantageous for low-abundance proteins because the hDAT peptide may not be one of the top six most intense ions and therefore, the data-dependent scans of hDAT peptides can be omitted and the hDAT peptide may not be identified (Lu et al., 2008).

Miranda et al. (2005) reported identification of ubiquitylation sites of hDAT using mass spectrometry. In their research, a trypsin digest of hDAT was analyzed for the presence of ubiquitin modifications, and four overlapping N-terminal hDAT peptides and one C-terminal peptide were detected with only 7.2% hDAT sequence coverage (Miranda et al., 2005).

In our study, mass spectrometry detection of hDAT peptides from the thermolysin digest resulted in 37% coverage. The peptides were detected using PepMap and TurboSEQUEST approaches and are shown in Figure 4.10. The hydropathy plot (Giros et al., 1992) was updated based on the recent LeuT$_{Aa}$ crystal structure information

(Yamashita et al., 2005) and structure-based alignment of prokaryotic and eukaryotic neurotransmitter symporters (Beuming et al., 2006). In the research reported in this dissertation, six detected peptides are situated in the C- and N-termini, two peptides are from EL4 and IL5, and the rest of the peptides are from transmembrane domains or are localized in both the loop and domain regions. We were able to identify peptides from both transmembrane domains and loop and terminal regions, but peptides from the TM1-TM2 region of interest were not detected.

Approach to Detect Labeled Peptides using NanoLC Nanospray FT-ICR Mass Spectrometer

MFZ 2-24 labels less than 1% of the hDAT (Vaughan et al., 2005; Watt et al., 1989). According to our calculations, MFZ 2-24 is not a suitable label for mass spectrometry analysis due to the low yields of labeled hDAT peptides. Several attempts to identify MFZ 2-24 labeled peptide from the CNBr digest of 100 plates of hDAT were not successful. Therefore, MFZ 3-37 was used to chemically label hDAT. The product of the reaction of MFZ 3-37 with a peptide produced the 595 m/z ion corresponding to the detached label in the second-stage MS. Thus, 595 m/z was used for the search of the labeled peptide.

The labeled hDAT was in-gel digested and processed using standard procedure of mass spectrometry sample preparation. The peptides were separated on a nanoLC connected to a nanoelectrospray source of a ThermoFinnigan LTQ-FT high-resolution mass spectrometer. The instrument was operated in MS and MS/MS modes. The six most intense ions of each MS scan were examined in the second stage for the presence of MFZ

3-37 by monitoring the 595 m/z ion in the ion trap. The parent ions were ranked by a scoring algorithm for spectral analysis (SALSA), (Thermo Scientific, San Jose,CA), and the highest-ranking ions were compared to a theoretical thermolysin digest of hDAT (Zhang and Bartels, 2004; Schiewe et al., 2004). Parent ions matching hDAT sequences were observed. However, detected peptides did not contain cysteine or lysine resides and, therefore, the detected labeled peptides were likely to be false positives or formed due to nonspecific labeling. It is possible that due to the complexity of the analyzed sample, MFZ 3-37 labeled peptides were not within the top six most intense ions during the analysis, causing the secondary stage analysis of labeled hDAT peptides not to be performed. However, MFZ 3-37 showed high reactivity when reacted with synthetic peptides. Therefore, a stability study was performed.

The stability study was conducted to evaluate the stability of MFZ 3-37 product with a peptide. Incubation at 37°C for 24 hrs. led to decomposition of 90% of the product determined by HPLC separation. This suggests that the product of isothiocyanate MFZ 3-37 with hDAT hydrolyses during enzymatic digest and processing. Several studies confirm the instability of isothiocyanate products with amino acids. Sanchez-Machado et al. (2003), for example, report derivatization of amino acids with phenyl isothiocyanate at low temperatures under vacuum to minimize degradation of the product. They report only 48 h stability of the derivatized amino acids when stored dry at +4°C. Conaway et al. (2001) determined the decomposition rate for cysteine derivatized with 6-phenylhexyl isothiocyanate and showed that the half-life of the product was 45 min. at 37°C, pH 7.4.
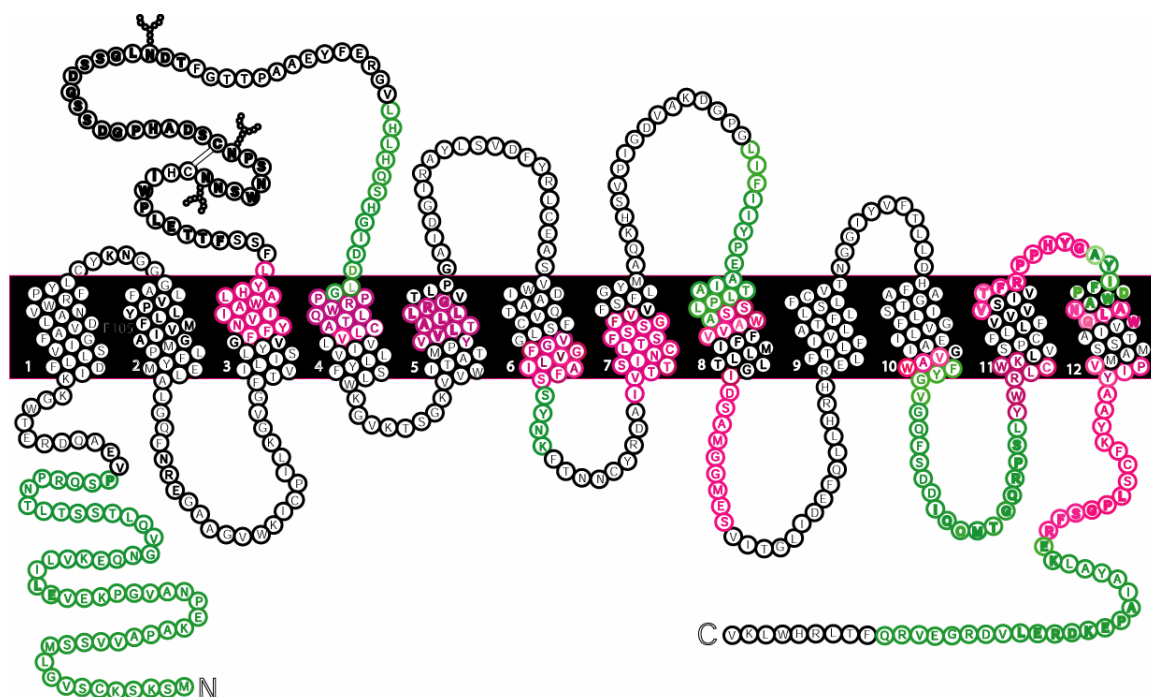
Figure 4.10 hDAT peptides found in thermolysin digest

Amino acid residues that are located within the transmembrane domains are shown in red. The residues from loop/termini regions are shown in green. Approximately equal amounts of peptides from the TM domains and the loop/termini regions were detected. The sequence converge is 37%. Interestingly, the hydropathy plot of hDAT was predicted very accurately for TM1-TM7 (Giros et al., 1992). Peptides from TM1-TM2 region were not detected.

The mass spectrometry method demonstrated sufficient sensitivity to identify hDAT peptides in a relatively small preparation. Of more relevance to the cocaine binding site, the sensitivity needed to detect the lower amounts of irreversibly labeled peptides was demonstrated. The selection of different hDAT affinity labels can possibly result in identification of labeled amino acid residue.

References

Annesley R. (2003) Ion Suppression in Mass Spectrometry. *Clin. Chem.*, **49**, 1041-1044.

Alqwai O., Poelarends G., Konings W., and Georges E., (2003) Photoaffinity Labeling under Non-energized Conditions of a Specific Drug-binding Site of the ABC Multidrug Transporter LmrA from Lactococcus lactis. *Biochem. Biophys. Res. Comm.,* **311**, 696-701.

Appell, M., Berfield, J. L., Wang, L. C., Dunn, W. J. , Chen, N., and Reith, M .E., (2004) Structure-Activity Relationships for Substrate Recognition by the Human Dopamine Transporter. *Biochem. Pharmacol.*, **67**, 293-302.

Bannon M.J., (2005) The Dopamine Transporter: Role in Neurotoxicity and Human Disease. *Toxicol. Appl. Pharmacol*., **204**, 355-360.

Bakalarski C. E., Haas W., Dephoure N. E., and Gygi S. P., (2007) The Effects of Mass Accuracy, Data Acquisition Speed, and Search Algorithm Choice on Peptide Identification Rates in Phosphoproteomics. *Anal. Bioanal.Chem*., **389**, 1409-1419.

Barlow D. J., and Thornton J. M., (1988) Helix Geometry in Proteins. *J. Mol. Biol*., **201**, 601-619.

Barrow M. P., Headley J. V., Peru K. M., and Derrick P. J., (2004) Fourier Transform Ion Cyclotron Resonance Mass Spectrometry of Principal Components in Oilsands Naphthenic Acids. *J. Chromatogr. A*, **1058**, 51-59.

Badghisi H., and Liebler D.C., (2002) Sequence Mapping of Epoxide Adducts in Human Hemoglobin with LC-Tandem MS and the SALSA Algorithm. *Chemical Research in Toxicology,* **15**, 799-805.

Bayley H., (1983) Photogenerated Reagents in Biochemistry and Molecular Biology. In *Laboratory Techniques in Biochemistry and Molecular Biology*, 2nd ed.; Work, T., Burdon, R., Eds., Vol.12; Elsevier: Amsterdam•New York• Oxford.

Bayley H., and Knowles J., (1977) Photoaffinity Labeling. *Method. Enzymol.*, **26**, 69-144

Bayley H., and Staros J., (1984) *Photoaffinity Labeling and Related Techniques. Azides and Nitrenes. Reactivity and Stability*; Academic Press: New York.

Bark S J., Muster N., Yates J. R., and Siuzdak G., (2001) High-temperature Protein Mass Mapping using a Thermophilic Protease. *J. Am. Chem. Soc.,* **123,** 1774-1775.

Beuming T., Shi L., Javitch J.A., and Weinstein H., (2006) A Comprehensive Structure-Based Alignment of Prokaryotic and Eukaryotic Neurotransmitter/Na Symporters (NSS)

Aids in the Use of the LeuT Structure to Probe NSS Structure and Function. *Mol. Pharmacol.*, **70,** 1630-1642.

Bogen I. L., Boulland J., Mariussen E., Wright M. S., Fonnum F., Kao H., and Walaas, S. I., (2006) Absence of Synapsin I and II is Accompanied by Decreases in Vesicular Transport of Specific Neurotransmitters. *J. Neurochem.*, **96,** 1458-1466.

Bouchet M., and Goeldner M., (1997) Photochemical Labeling: Can Photoaffinity Labeling be Differentiated from Site-directed Photochemical Coupling? *Photochem. Photobiol.*, **65**, 195-200.

Brecklin C. S., and Bauman J. L., (1999) Cardiovascular Effects of Cocaine: Focus on Hypertension. *J. Clinical Hypertension,* **1,** 212-217.

Brecht M., Huang D., Evans E., and Hser Y., (2008) Polydrug Use and Implications for Longitudinal Research: Ten-year Trajectories for Heroin, Cocaine, and Methamphetamine Users.   *Drug Alcohol Depend.*, **96**, 193-201.

Breier, A., Ziegelhoffer A., Famulsky K., Michalak M., and Slezak J., (1996) Is Cysteine Residue Important in FITC-sensitive ATP-binding Site of P-type ATPases? A Commentary to the State of the Art. *Mol. Cell. Biochem.*, **160**, 89-93.

Breier A., and Ziegelhoffer A., (2000) "Lysine is the Lord", Thought Some Scientists in Regard to the Group Interacting with Fluorescein Isothiocyanate in ATP-binding Sites of P-type ATPases But, is it not Cysteine? *Gen. Physiol. Biophys.,* **19**, 253-263.

Brooks D.J., (2005) Imaging Studies in Drug Development: Parkinson's Disease. *Drug Discovery Today: Technologies*, **2**, 317-321.

Budyka M. F., Kantor M. M., and Alfimov M. V., (1992) Photochemistry of Phenyl Azide. *Uspekhi Khimii,* **61**, 48-74.

Cammack J. N., and Schwartz E. A., (1996) Channel Behavior in a Gamma - Aminobutyrate Transporter. *Proc. Nat. Acad. Sci. U.S.A.*, **93**, 723-727.

Cao J., Husbands S. M., Kopajtic T., Katz J. L., Newman A. H., (2001) [3-cis-3,5-Dimethyl-(1-piperazinyl)alkyl]-bis-(4'-fluorophenyl)amine Analogues as Novel Probes for the Dopamine Transporter. *Bioorg. Med. Chem. Lett.*, **11,** 3169-3173.

Chao C., C., Wu, S.L., and Ching, W.M., (2004) Using LC-MS with de Novo Software to fully Characterize the Multiple Methylations of Lysine Residues in a Recombinant Fagment of an Outer Membrane Protein from a Virulent Strain of Rickettsia Prowazekii. *Biochim. Biophys. Acta - Proteins Proteom.*, **1702**, 145-152.

Carneiro A.M., Ingram S.L., Beaulieu J.M., Sweeney A., Amara S.G., Thomas S.M., Caron M.G., and Torres G.E., (2002) The Multiple LIM Domain-Containing Adaptor Protein Hic-5 Synaptically Colocalizes and Interacts with the Dopamine Transporter. *J. Neurosci.*, **22**, 7045-7054.

Carroll F.I, Gao Y., Rahman M.A., Abraham P., Parham K., Lewin A.H, Boja J.W., and Kuhar M.J., (1991) Synthesis, Ligand Binding, QSAR, and CoMFA Study of 3β-(p-Substituted phenyl)tropane-2β-carboxylic Acid Methyl Esters. *J. Med. Chem.*, **34**, 2719-2725.

Carroll F.I., Lewin A.H., Boja J.W., and Kuhar M.J., (1992) Cocaine Receptor: Biochemical Characterization and Structure-Activity Relationships of Cocaine Analogues at the Dopamine Transporter. *J. Med. Chem.*, **35**, 969-981.

Carroll F., Howell L., and Kuhar M.J., (1999) Pharmacotherapies for Treatment of Cocaine Abuse: Preclinical Aspects. *J. Med. Chem.*, **42**, 2721-2736.

Carvelli L., McDonald P.W., Blakely R.D., and DeFelice L.J., (2004) Dopamine Transporters Depolarize Neurons by a Channel Mechanism. *Proc. Nat. Acad. Sci. U.S.A.*, **101**, 16046-16051.

Chen R., Han D.D., and Gu H.H., (2005) A Triple Mutant in the Second Transmembrane Domain of Mouse Dopamine Transporter Markedly Decreases Sensitivity to Cocaine and Methylphenidate. *J. Neurochem.*, **94**, 352-359.

Chen N., Vaughan R.A., and Reith M.E.A., (2001) The Role of Conserved Tryptophan and Acidic Residues in the Human Dopamine Transporter as Characterized by Site-Directed Mutagenesis. *J Neurochem.*, **77**, 1116-1127.

Chen N. and Justice J.B. Jr (1998) Voltammetric Studies on Mechanisms of Dopamine Efflux in the Presence of Substrates and Cocaine from Cells Expressing Human Norepinephrine Transporter. *J Neurochem.*, **71**, 653-65.

Chen N., and Justice J. B., (2000) Differential Effect of Structural Modification of Human Dopamine Transporter on the Inward and Outward Transport of Dopamine. *Mol. Brain Res.*, **75**, 208-215.

Chen, Nian-Hang; Reith, Maarten E. A., (2002) Structure-function Relationships for Biogenic Amine Neurotransmitter Transporters. *Neurotransmitter Transporters (2nd Edition)*, 53-109.

Chen N., and Reith M. E. A., (2008) Substrates Dissociate Dopamine Transporter Oligomers. *J. Neurochem.*, **105**, 910-920.

Chen N., Vaughan R.A., and Reith M.E.A., (2001) The Role of Conserved Tryptophan and Acidic Residues in the Human Dopamine Transporter as Characterized by Site-Directed Mutagenesis. *J Neurochem.*, **77**, 1116-1127.

Chen N., Zhen J., and Reith M.E.A., (2004) Mutation of Trp84 and Asp313 of the Dopamine Transporter Reveals Similar Mode of Binding Interaction for GBR12909 and Benztropine as Opposed to Cocaine. *J Neurochem.*, **89**, 853-864.

Chen R., Wei H., Hill E. R.,Chen L., Jiang L., Han D. D., and Gu H. H., (2007) Direct Evidence that Two Cysteines in the Dopamine Transporter Form a Disulfide Bond. *Mol. Cell. Biochem.*, **298**, 41-48.

Chen Y., Ali T., Todorovic V., O'Leary, J. M., Downing, K. A.., and Rifkin D.B., (2004) Amino Acid Requirements for Formation of the TGF-Latent TGF-Binding Protein Complexes. *J. Mol. Biol.*, **345**, 175-186.

Choudhary G., Hemenway E., Schwartz J., and Cho D., (2004) Capillary LC-MS/MS identification of phosphorylated peptides from data dependent neutral loss scans on the Finnigan LTQ ion trap mass spectrometer. *LC-GC Europe*, **17**, 49-50.

Coic Y., Vincent M., Gallay J; Baleux F., Mousson F., Beswick V., Neumann J., and de Foresta B., (2005) Single-spanning Membrane Protein Insertion in Membrane

Mimetic Systems: Role and Localization of Aromatic Residues. *Eur. Biophys. J.*, **35**, 27-39.

Conaway C. C., Krzeminski J., Amin S., and Chung F.L., (2001) Decomposition Rates of Isothiocyanate Conjugates Determine their Activity as Inhibitors of Cytochrome p450 Enzymes. *Chem. Res. Toxicol.*, **14**, 1170-1176.

Dackis C.A., (2005) New Treatment for Cocaine abuse. *Drug Discov. Today,* **2**, 79-86.

Dackis C.A. and O'Brien C. P., (2001) Cocaine Dependence: a Disease of the Brain's Reward Centers. *J. Subst. Abuse Treat.*, **21**, 111-117.

Daniels G.M. and Amara S.G., (1999) Regulated Trafficking of the Human Dopamine Transporter. Clathrin-mediated Internalization and Lysosomal Degradation in Response to Phorbol Esters. *J. Biol. Chem.*, **274**, 35794–35801.

Dar D. E., Metzger T.G., Vandenbergh D. J.,and Uhl G. R., (2006) Dopamine uptake and cocaine binding mechanisms: The involvement of charged amino acids from the transmembrane domains of the human dopamine transporter. *Eur. J. Pharmacol.*, **538**, 43-47.

DeFelice L. J., and Goswami T., (2007) Transporters as channels. *Annu. Rev. Physiol.*, **69**, 87-112.

Deken S. L., Beckman M. L., Boos L., and Quick M. W., (2000) Transport Rates of GABA Transporters: Regulation by the N-terminal Domain and Syntaxin 1A. *Nat. Neurosci.*, **3**, 998-1003.

Desai R.I., Kopajtic T.A., French D., Newman A.H., and Katz J.L., (2005) Relationship Between in Vivo Occupancy at the Dopamine Transporter and Behavioral Effects of Cocaine, GBR 12909 [1-{2-[bis-(4-fluorophenyl)methoxy]ethyl}-4-(3-phenylpropyl)piperazine], and Benztropine Analogs. *J. Pharmacol. Exp. Ther.*, **315**, 397-404

DiMaio S., Grizenko N., and Joober R., (2003) Dopamine Genes and Attention-deficit Hyperactivity Disorder: a Review. *J. Psychiat. Neurosci.*, **28**, 27-38.

Dorman G. and Prestwich G.D., (2000) Using Photolabile Ligands in Drug Discovery and Development. *TIBTECH*, **18**, 64-77.

Drobnica L., and Augustin J., (1965) Reactions of Isothiocyanates with Amino Acids, Peptides, and Proteins. II. Kinetics of the Reaction of Aromatic Isothiocyanates with Amino Acids and Cyclization of the Addition Products. *Collect. Czech. Chem. Commun.*, **30**, 1221-1228.

Drobnica L., Podhradsky D., and Gemeiner P., (1975) Kinetics of the Reaction of Isothiocyanates with Sodium Sulfide and Some Thiols. *Collect. Czech. Chem. Commun.*, **40**, 3688-97.

Dutta A.K., Zhang S., Kolhatkar R., and Reith M.E.A., (2003) Dopamine Transporter as a Target for Drug Development of Cocaine Dependence Medications. *Eur. J. Pharm.*, **479**, 93-106.

Elhofy A., and Bost K. L., (1998) Limitations for Purification of Murine Interleukin-18 When Expressed as a Fusion Protein Containing the FLAG Peptide. *BioTechniques*, **25**, 425-432.

Falkner J.A., Hill J. A., Andrews P. C., (2008) Proteomics FASTA Archive and Reference Resource. *Proteomics*, **8**, 1756-1757.

Ferrer J.V. and Javitch J.A., (1998) Cocaine Alters the Accessibility of Endogenous Cysteines in Putative Extracellular and Intracellular Loops of the Human Dopamine Transporter. *Proc. Natl. Acad. Sci.U.S.A.*, **95**, 9238- 9243.

Flippen-Anderson J. L., George C., and Deschamps J. R., (2003) Molecular Approaches to Treatments for Cocaine Abuse. *J. Mol. Struct.*, **647**, 259-267.

Foster J.D., Pananusorn B., and Vaughan R.A., (2002) Dopamine Transporters are Phosphorylated on N-terminal Serines in Rat Striatum. *J. Biol. Chem.*, **277**, 25178–25186.

Galli A., Blakely R. D., and DeFelice L. J., (1996) Norepinephrine Transporters have Channel Modes of Conduction. *Proc. Nat. Acad. Sci. U.S.A.*, **93**, 8671-8676.

Gether U., Norregaard L.,and Loland C. J., (2001) Delineating Structure-Function Relationships in the Dopamine Transporter from Natural and Engineered Zn^{2+} Binding Sites. *Life Sci.*, **68**, 2187-2198.

Gibbs B.S., and Benkovic S. J., (1991) Affinity Labeling of the Active Site and the Reactive Sulfhydryl Associated with Ativation of Rat Liver Phenylalanine Hydroxylase. *Biochemistry*, **30**, 6795-802.

Gilbert K. M., Boos T. L., Dersch C. M., Greiner E., Jacobson A. E. Lewis D.. Matecka D., Prisinzano T. E., Zhang Y., Rothman R. B., Rice K. C., and Venanzi, C. A., (2007) DAT/SERT Selectivity of Flexible GBR 12909 Analogs Modeled using 3D-QSAR Methods. *Bioorg. Med. Chem.*,**15** , 1146-1159.

Giros B., el Mestikawy, Godinot N., Zheng K., Han H., Yang-Feng T., and Caron M. G., (1992)   Cloning, Pharmacological Characterization, and Chromosome Assignment of the Human Dopamine Transporter. *Mol. Pharmacol.*, **42**, 383-390.

Giros B. and Caron M., (1993) Molecular Characterization of the Dopamine Transporter. *Trends Pharmacol. Sci.*, **14**, 43-49.

Gold L. H., and Balster R. L., (1996) Evaluation of the Cocaine-like Discriminative Stimulus Effects and Reinforcing Effects of Modafinil. *Psychopharmacology*, **126**, 286-292.

Granas C., Ferrer J., Loland C.J., Javitch J.A., and Gether U., (2003) N-terminal Truncation of the Dopamine Transporter Abolishes Phorbol Ester- and Substance P Receptor-stimulated Phosphorylation without Impairing Transporter Internalization. *J. Biol. Chem.*, **278**, 4990-5000.

Grant K.J., and Wu C. C., (2007) Advances in Neuromembrane Proteomics: Efforts Towards a Comprehensive Analysis of Membrane Proteins in the Brain. *Brief. Funct. Genomic. Proteomic.*, **6**, 59-69.

Gross E., (1967) The Cyanogen Bromide Reaction in *Method. Enzymol.*, **11**, 238-255.

Grutter T., Bertrand, S., Kotzyba-Hilbert F., Bertrand D., and Goeldner M., (2002) Structural Reorganization of the Acetylcholine Binding Site of the Torpedo Nicotinic Receptor as Revealed by Dynamic Photoaffinity Labeling. *ChemBioChem.*, **3**, 652-658.

Gulley, J. M., and Zahniser, N. R., (2003) Rapid regulation of dopamine transporter function by substrates, blockers and presynaptic receptor ligands. *Eur. J. Pharmacol.*, **479**, 139-152.

Haas W., Faherty B. K., Gerber S. A., Elias J. E., Beausoleil S. A., Bakalarski C. E., Li X.; Villen J., and Gygi S.P., (2006) Optimization and Use of Peptide Mass Measurement Accuracy in Shotgun Proteomics. *Mol. Cell. Proteomics*, **5**, 1326-1337.

Hakansson K., Cooper H. J., Hudgins R. R., and Nilsson C. L., (2003) High Resolution Tandem Mass Spectrometry for Structural Biochemistry. *Curr. Org. Chem.*, **7**, 1503-1525.

Harder T., Stoser R., Wessig P., and Bendig J., (1997) Low-temperature Photochemistry of Nitro-substituted Aromatic Azides; Subsequent Reactions of Intermediates. *J. Photochem. Photobiol.*, **103**, 105-113.

Harrington K. A., Augood S. J. Kingsbury A. E., Foster O. J. F., and Emson P. C., (1996) Dopamine Transporter (DAT) and Synaptic Vesicle Amine Transporter (VMAT2) Gene Expression in the Substantia Nigra of Control and Parkinson's Disease. *Mol. Brain Res.*, **36**, 157-62.

Hastrup H., Karlin A., and Javitch, J. A., (2001) Symmetrical Dimer of the Human Dopamine Transporter Revealed by Cross-linking Cys-306 at the Extracellular End of the Sixth Transmembrane Segment. *Proc. Nat. Acad. Sci. U.S.A.*, **98**, 10055-10060.

Hawkes C., Amritraj A., MacDonald R. G., Jhamandas J. H., and Kar S., (2007) Heterotrimeric G Proteins and the Single-transmembrane Domain IGF -II/M6P Receptor: Functional Interaction and Relevance to Cell Signaling. *Mol. Neurobiol.*, **35**, 329-345.

Heinrikson R.L., (1977) Applications of Thermolysin in Protein Structural Analysis. *Method. Enzymol.*, **47**, 175-189.

Helenius A., and Aebi M., (2004) Roles of N-linked Glycans in the Endoplasmic Reticulum. *Annu. Rev. Biochem.*, **73**, 1019-1049.

Henderson T., (2008) Photoaffinity Labeling of the Human Dopamine Transporter using Cocaine Analogs, *Ph.D. Dissertation*, Emory University.

Henry L.K., Field J.R., Adkins E.M., Parnas M.L., Vaughan R.A., Zou M.F., Newman A.H., and Blakely R.D., (2006) Tyr-95 and Ile-172 in Transmembrane Segments 1 and 3 of Human Serotonin Transporter Interact to Establish High Affinity Recognition of Antidepressants. *J. Biol. Chem.*, **281**, 2012-2023.

Huang X., and Zhan C., (2007) How Dopamine Transporter Interacts with Dopamine: Insights from Molecular Modeling and Simulation. *Biophys. J.*, **93**, 3627-3639.

Huq, F., (2007) Molecular Modeling Analysis of the Metabolism of Cocaine. *J. Pharmacol. Toxicol.*, **2**, 114-130.

Indarte M. Madura J. D. and Surratt C.K., (2008) Dopamine Transporter Comparative Molecular Modeling and Binding Site Prediction using the LeuTAa Leucine Transporter as a Template. *Proteins: Structure, Function, and Bioinformatics*, **70**, 1033-1046.

Javitch J.A., (1998) Probing Structure of Neurotransmitter Transporters by Substituted-Cysteine Accessibility Method. *Method. Enzymol.*, **296**, 331-346

Kaiser R. and Metzka L., (1999) Enhancement of Cyanogen Bromide Cleavage Yields for Methionyl-Serine and Methionyl-Threonine Peptide Bonds. *Anal. Biochem.*, **266**, 1-8.

Kampman K. M., Dackis C., Lynch K.G., Pettinati H., Tirado C., Gariti P., Sparkman T., Atzram Mi., and O'Brien C.P., (2006) A Double-blind, Placebo-controlled Trial of Amantadine, Propranolol, and Their Combination for the Treatment of Cocaine Dependence in Patients with Severe Cocaine Withdrawal Symptoms. *Drug Alcohol Depend.*, **85**, 129-137.

Kanner B., I., and Zomot E., (2008) Sodium-Coupled Neurotransmitter Transporters. *Chem. Rev.*, **108**, 1654-1668.

Kassab D., Pichat S., Chambon C., Blachere T., Rolland M., de Ravel M.R., Mappus E., Grenot C., and Cuilleron C., (1998) *Biochemistry*, **37**, 14088-14097.

Keil B., (1992) Specificity of Proteolysis. Springer-Verlag, New York.

Kerwin B.A., and Yount, R. G., (1992) Photoaffinity Labeling of Scallop Myosin with 2-[(4-azido-2-nitrophenyl)amino]ethyl Diphosphate: Identification of an Active Site Arginine Analogous to Tryptophan-130 in Skeletal Muscle Myosin. *Bioconjugate Chem.*, **3**, 328-336.

Kessler P., Thai R., Beau F., and Menez A., (2006) Photocrosslinking/Label Transfer: A Key Step in Mapping Short Neurotoxin Binding Site on Nicotinic Acetylcholine Receptor. *Bioconjugate Chem.*, **17**, 1482-1491.

Kitayama S., Shimada S., Xu H., Markham L., Donovan D.M., and Uhl G.R., (1992) Dopamine Transporter Sited-Directed Mutations Differentially Alter Substrate Transport and Cocaine Binding. *Proc. Nat. Acad. Sci. U.S.A.*, **89**, 7782-7785.

176

Knorre D, G., Godovikova T. S., (1998) Photoaffinity Labeling as an Approach to Study Supramolecular Nucleoprotein Complexes. *FEBS Lett.*, **433**, 9-14.

Koike K., Conseil G., Leslie E. M., Deeley R. G., and Cole S. P., (2004) Identification of Proline Residues in the Core Cytoplasmic and Transmembrane Regions of Multidrug Resistance Protein 1 (MRP1/ABCC1) Important for Transport Function, Substrate Specificity, and Nucleotide Interactions. *J. Biol. Chem.*, **279**, 12325-12336.

Kotzyba-Hibert F., Kapfer I., and Goeldner M., (1995) Recent Trends in Photoaffinity Labeling. *Angew. Chem. Int. Ed. Engl.*, **34**, 1296-1312.

Krause J., (2008) SPECT and PET of the Dopamine Transporter in Attention-Deficit/Hyperactivity Disorder. *Expert Rev. Neurother.*, **8**, 611-625.

Kuehl D, and Wang Y., (2007) The Role of Spectral Accuracy in Mass Spectrometry. *LCGC North America*, **10**, 12-16.

Kuhar M.J., Ritz M.C., and Boja J.W., (1991) The Dopamine Hypothesis of the Reinforcing Properties of Cocaine. *Trends Neurosci.*, **14**, 299-302.

Laemmli U.K., (1970) Cleavage of Structural Proteins During the Assembly of the Head of Bacteriophage T4. *Nature*, **227**, 680-685.

Lapointe J.F., Molle D., Gauthier S. F., and Pouliot Y., (2004) Effect of Calcium on Thermolysin Hydrolysis of β -Casein Tryptic Peptides. *Int. Dairy J.*, **4**, 185-193

Li L. B., Chen N., Ramamoorthy S., Chi L., Cui X. N., Wang L. C., and Reith M. E., (2004) The role of N-glycosylation in Function and Surface Trafficking of the Human Dopamine Transporter. *J. Biol. Chem.*, **279**, 21012-21020.

Lin F., Lester H.A., and Mager S., (1996) Single- channel Currents Produced by the Serotonin Transporter and Analysis of a Mutation Affecting Ion Permeation. *Biophys. J.*, **71**, 3126-3135.

Lin L. N., and Brandts J. F., (1985) Isomer-specific Proteolysis of Model Substrates: Influence that the Location of the Proline Residue Exerts on Cis Trans Specificity. *Biochemistry*, **24**, 6533-6538.

Lin, Z., Wang, W., Kopajtic, T., Revay, R. S., and Uhl, G. R., (1999) Dopamine Transporter: Transmembrane Phenylalanine Mutations Can Selectively Influence Dopamine Uptake and Cocaine Analog Recognition. *Mol. Pharmacol.*, **56**, 434-447.

Liu J. and Rost B., (2001) Comparing Function and Structure Between Entire Proteomes. *Protein Sci.*, **10**, 1970-1979.

Lin, Z., and Uhl R.R. (2002) Dopamine Transporter Mutants with Cocaine Resistance and Normal Dopamine Uptake Provide Rargets for Cocaine Antagonism. *Mol. Pharmacol.*, **61**, 885-891.

Loland C., Graanas C., Javitch J., and Gether U., (2004) Identification of Intracellular Residues in the Dopamine Transporter Critical for Regulation of Transporter and Cocaine Binding. *J. Biol. Chem.*, **279**, 3228-38.

Loland, C. J., Norregaard, L., and Gether, U., (1999) Defining Proximity Relationships in the Tertiary Structure of the Dopamine Transporter. Identification of a Conserved Glutamic Acid as a Third Coordinate in the Endogenous $Zn(^{2+})$-Binding Site. *J. Biol. Chem.*, **274**, 36928-36934.

Loland C. J., Desai R. I., Zou M.F., Cao J., Grundt P., Gerstbrein K., Sitte H. H., Newman A.H., Katz J. L., and Gether U., (2008) Relationship Between Conformational Changes in The Dopamine Transporter and Cocaine-like Subjective Effects of Uptake Inhibitors. *Mol. Pharmacol.*, **73**, 813-823.

Loo R. R., Ogorzalek S., and Richard D., (1994) Investigation of the Gas-Phase Structure of Electrosprayed Proteins using Ion-molecule reactions. *J. Am. Soc. Mass Spectr.*, **5**, 207-20.

Lu B., Motoyama A., Ruse C., Venable J., and Yates J. R., (2008) Improving Protein Identification Sensitivity by Combining MS and MS/MS Information for Shotgun Proteomics Using LTQ-Orbitrap High Mass Accuracy Data. *Anal. Chem.*, **80**, 2018-2025.

Matthews E. E., Zoonens M., and Engelman D. M., (2006) Dynamic Helix Interactions in Transmembrane Signaling. *Cell* , **127**, 447-450.

Maiya R., Ponomarev I., Linse K. D., Harris R. A., and Mayfield R. D., (2007) Defining the Dopamine Transporter Proteome by Convergent Biochemical and in Silico Analyses. *Genes Brain Behav.*, **6**, 97-106.

Melen K., Krogh A.,and von Heijne G., (2003) Reliability Measures for Membrane Protein Topology Prediction Algorithms. *J. Mol. Biol.*, **327**, 735-744.

Midgett C, R., and Madden D. R., (2007) Breaking the Bottleneck: Eukaryotic Membrane Protein Expression for High-Resolution Structural Studies. *J. Struct. Biol.*, **160**, 265-274.

Miranda M., Wu C. C., Sorkina T., Korstjens D.R., and Sorkin A., (2005) Enhanced Ubiquitylation and Accelerated Degradation of the Dopamine Transporter Mediated by Protein Kinase. *J. Biol. Chem.*, **280**, 35617-35624.

Moore B. M., Jalluri R. K. and Doughty M. B., (1996) DNA Polymerase Photoprobe 2-[(4-azidophenacyl)thio]-2'-deoxyadenosine 5'-triphosphate Labels an Escherichia Coli DNA Polymerase I Klenow Fragment Substrate Binding Site. *Biochemistry*, **35**, 11642-11651.

Mora R., Berndt K.D., Tsai H., and Meredith S.C., (1988) Quantitation of Aspartate and Glutamate in HPLC Analysis of Phenylthiocarbamyl Amino Acids. *Anal. Biochem.*, **172**, 368-376.

Mortensen O. V., and Amara S. G., (2003) Dynamic Regulation of the Dopamine Transporter. *Eur. J. Pharmacol.*, **479**, 159-170.

Mousson F.,Beswick V., Coiec Y. Baleux F., Huynh-Dinh T., Sanson A., and Neumann J., (2001) Concerted Influence of Key Amino Acids on the Lipid Linding Properties of a Single-Spanning Membrane Protein: NMR and Mutational Analysis. *Biochemistry*, **40**, 9993-10000.

Muller D. J., Wu N., and Palczewski K., (2008) Vertebrate Membrane Proteins : Structure, Function, and Insights from Biophysical Approaches. *Pharmacol. Rev.*, **60**, 43-78.

Myszka D. G., and Swenson R. P., (1991) Synthesis of the Photoaffinity Probe 3-(p-azidobenzyl)-4-hydroxycoumarin and Identification of the Dicoumarol Binding Site

in Rat Liver NAD(P)H:Quinone Reductase (EC 1.6.99.2). *J. Biol. Chem.*, 266, 4789-4797.

National Institute on Drug Abuse: InfoFacts 2005. National Institutes of Health; Washington D.C., 2006

National Survey on Drug Use and Health : Main Findings 2004. Department of Health and Human Services: Washington D.C., 2005.

Newman A.H., (1998) Novel Dopamine Transporter Ligands: the State of the Art. *Med. Chem. Res.*, **8**, 1-11.

Newman A.H. and Kulkarni S., (2002) Probes for the Dopamine Transporter: New Leads Toward a Cocaine-Abuse Therapeutic-A Focus on Analogues of Benztropine and Rimcazole. *Med. Res. Rev.*, **22**, 429-464.

Nielsen P.A., Olsen J. V., Podtelejnikov A. V., Andersen J. R., Mann M., and Wisniewski J. R., (2005) Proteomic Mapping of Brain Plasma Membrane Proteins. *Mol. Cell. Proteomics*, **4**, 402-408.

Nilsson C. L., Cooper H. J., Hakansson K., Marshall A. G., Ostberg Y.,; Lavrinovicha M., and Bergstrom S., (2002) Characterization of the p13 Membrane

Protein of Borrelia Burgdorferi by Mass Spectrometry. *J. Am. Soc. Mass Spectr.*, **13**, 295-299.

Nirenberg M. J., Chan J., Vaughan R. A., Uhl G. R., Kuhar M. J., and Pickel V. M., (1997) Immunogold Localization of the Dopamine Transporter: an Ultrastructural Study of the Rat Ventral Tegmental Area. *J. Neurosci.*, **17**, 5255-5262.

Norregaard L., Frederiksen D., Nielsen E.O., and Gether U., (1998) Delination of an Endogenous Zinc-Binding Site in the Human Dopamine Transporter. *EMBO J.*, **17**, 4266-4273.

Norregaard L., Loland C.J., and Gether U., (2003) Evidence for Distinct Sodium-, Dopamine-, and Cocaine-Dependent Conformational Changes in Transmembrane Segments 7 and 8 of the Dopamine Transporter. *J. Bio. Chem.*, **278**, 30587-30596.

Oesterhelt F., and Scheuring S., (2006) High-resolution Imaging and Force Measurement of Individual Membrane Proteins by AFM. *Curr. Nanosci.*, **2**, 329-335.

Okamoto Y., and Yount R. G., (1985) Identification of an Active Site Peptide of Skeletal Myosin after Photoaffinity Labeling with N-(4-azido-2-nitrophenyl)-2-aminoethyl Diphosphate. *Proc. Nat. Acad. Sci. U.S.A.,* **82**, 1575-1579.

Parker J. M., Mant C. T., and Hodges R. S., (1987) A Practical Approach to the Preparative Purification of Peptides using Analytical Instrumentation with Analytical and Semipreparative Columns. *Chromatographia*, **24**, 832-838.

Parnas M.L., Gaffaney J.D., Zou M.F., Lever J.R., Newman A.H., and Vaughan R.A., (2008) Labeling of Dopamine Transporter Transmembrane Domain 1 with the Tropane Ligan N-[4-(4-Azido-3-[^{125}I]iodophenyl)butyl]-2β-carbomethoxy-3-β-(4-chlorophenyl)tropane Implicates Proximity of Cocaine and Substrate Actives. *Mol. Pharmacol.*, **73**, 1141-1150.

Peng J., and Gygi S. P., (2001) Proteomics: the Move to Mixtures. *J. Mass Spectrom.*, **36**, 1083-1091.

Peng J., Kim M. J., Cheng D., Duong D. M., Gygi S. P., and Sheng M., (2004) Semiquantitative Proteomic Analysis of Rat Forebrain Postsynaptic Density Fractions by Mass Spectrometry. *J. Biol. Chem.*, **279**, 21003-21011.

Peterman S. M., and Mulholland J. J., (2006) A Novel Approach for Identification and Characterization of Glycoproteins Using a Hybrid Linear Ion Trap/ FT - ICR Mass Spectrometer. *J. Am. Soc. Mass Spectr.*, **17**, 168-179.

Philapou, S.; Seyer R.; Cotte N., Breton C., Barberis C., Hilbert M., anf Mouillac B., (1999) Docking of Linear Peptide Antagonists into the human V Vasopressin Receptor. *J. Biol. Chem.*, **274**, 23316-23327.

Platz M., (1997) Photoaffinity Labeling Introduction. *Photochem. Photobiol.*, **65**, 193-194.

Preti, A., (2007) New Developments in the Pharmacotherapy of Cocaine Abuse. *Addict. Biol.*, **12**, 133-151.

Quenzer T. L., Emmett M. R., Hendrickson C. L., Kelly P. H., and Marshall A. G., (2001) High sensitivity Fourier Transform Ion Cyclotron Resonance Mass Spectrometry for Biological Analysis with Nano-LC and Microelectrospray Ionization. *Anal. Chem.*, **73**, 1721-1725.

Reith, M.E.A, Berfield, J.L., Wang, L.C., Ferrer, J.V., and Javitch, J.A., (2001) The Uptake Inhibitors Cocaine and Benztropine Differentially Alter the Conformation of the Human Dopamine Transporter. *J. Biol. Chem.*, **276**, 29012-29018.

Riddle E. L., Fleckenstein A. E., and Hanson G. R., (2005) Role of Monoamine Transporters in Mediating Psychostimulant Effects. *AAPS J.*, **7,** 47-851.

Ringheim G. E., Saraswat L. D., Bubis J., and Taylor S. S., (1988) Deletion of cAMP-binding Site B in the Regulatory Subunit of cAMP-dependent Protein Kinase Alters the Photoaffinity Labeling of Site A. *J. Biol. Chem.*, **263**, 18247-18252.

Rush J., and Konigsberg W. H., (1990) Photoaffinity Labeling of the Klenow Fragment with 8-Azido-dATP. *J. Biol. Chem.*, **265**, 4821-4827.

Ritz M. C., Lamb R. J., Goldberg R., and Kuhar M. J., (1987) Cocaine Receptors on Dopamine Transporters are Related to Self-Administration of Cocaine. *Science*, **237**, 1219-1223.

Rothman R. B., and Glowa J. R., (1995) A Review of the Effects of Dopaminergic Agents on Humans, Animals, and Drug-seeking Behavior, and its Implications for Medication Development. Focus on GBR 12909. *Mol. Neurobiol.*, **11**, 1-19.

Rudnick Gary., (2007) What Is an Antidepressant Binding Site Doing in a Bacterial Transporter? *ACS Chem. Biol.*, **2**, 606-609.

Sakamoto Y., Kawakami N., and Sasagawa T., (1988) Prediction of Peptide Retention Times. *J. Chromatogr.,* **442**, 69-79.

Sanchez-Machado D. I., Lopez-Cervantes J., Lopez-Hernandez J., Paseiro-Losada P., and Simal-Lozano J., (2003) High-performance Liquid Chromatographic Analysis of

Amino Acids in Edible Seaweeds after Derivatization with Phenyl Isothiocyanate. *Chromatographia*, **58**, 159-163.

Schnaible V., and Przybylski M., (1999) Identification of Fluorescein-5'-Isothiocyanate-Modification Sites in Proteins by Electrospray-Ionization Mass Spectrometry. *Bioconjugate Chem.*, **10**, 861-866.

Schiewe A. J., Margol L., Soreghan B. A., Thomas S.N., and Yang A. J., (2004) Rapid Characterization of Amyloid-β Side-Chain Oxidation by Tandem Mass Spectrometry and the Scoring Algorithm for Spectral Analysis. *Pharm. Res.*, **21**, 1094-1102.

Schuster G., and Platz M., (1992) Photochemistry of Phenyl Azide. *Adv. Photochem.*, **17**, 69-143.

Schwartz M. A., (1989) Studying the Cytoskeleton By Label Transter Crosslinking: Uses and Limitations. *Photochem. Probes Biochem.*, **189**, 157-168.

Seiwert B. and Karst U., (2007) Analysis of Cysteine -Containing Proteins using Precolumn Derivatization with N-(2-ferroceneethyl)maleimide and Liquid Chromatography/Electrochemistry/ Mass spectrometry. *Anal. Bioanal. Chem.*, **388**, 1633-1642.

Sen N., Shi L., Beuming T., Weinstein H., and Javitch J.A., (2005) A Pincer-Like Configuration of TM2 in the Human Dopamine Transporter is Responsible for Indirect Effects on Cocaine Binding. *Neuropharm.*, **49**, 780-790.

Shortle D., (2002) Composites of Local Structure Propensities: Evidence for Local Encoding of Long-Range Structure. *Protein Sci.*, 111, 18-26.

Tamm L. K., Arora A., and Kleinschmidt, J. H., (2001) Structure and Assembly of β-Barrel Membrane Proteins. *J. Biol. Chem.*, **276**, 32399-32402.

Singh S. K.,Yamashita A., and; Gouaux E., (2007) Antidepressant Binding Site in a Bacterial Homologue of Neurotransmitter Transporters. *Nature*, **448**, 952-956.

Sonders M. S., Quick M., and Javitch J. A., (2005) How did the Neurotransmitter Cross the Bilayer? A Closer View. *Curr. Opin. Neurobiol.*, **15(3)**, 296-304.

Sorkina T., Doolen S., Galperin E., Zahniser N. R., and Sorkin, A., (2003) Oligomerization of Dopamine Transporters Visualized in Living Cells by Fluorescence Resonance Energy Transfer Microscopy. *J. Biol. Chem.*, **278**, 28274-28283.

Sorkina T., Hoover B. R., Zahniser N. R., and Sorkin A.., (2005) Constitutive and Protein Kinase C-induced Internalization of the Dopamine Transporter is Mediated by a Clathrin-Dependent Mechanism. *Traffic*, **6**, 157-170.

Sotnikova T, D., Beaulieu J.; Gainetdinov R. R., and Caron M. G., (2006) Molecular Biology, Pharmacology and Functional Role of the Plasma Membrane Dopamine Transporter. *CNS Neurol. Disord. Drug Targets*, **5**, 45-56.

Sostaric E., Georgiou A. S., Wong C. H..,Watson P. F., Holt W. V., and Fazeli Al., (2006) Global Profiling of Surface Plasma Membrane Proteome of Oviductal Epithelial Cells. *J. Proteome Res.*, **5**, 3029-3037.

Speers A. E., and Wu, C. C., (2007) Proteomics of Integral Membrane Proteins - Theory and Application. *Chem. Rev.*, **107**, 3687-3714.

Speers A. E., Blackler A.E., and Wu, C. C., (2007) Shotgun Analysis of Integral Membrane Proteins Facilitated by Elevated Temperature. *Anal. Chem.*, **79**, 4613-4620.

Spicer V., Yamchuk A., Cortens J.,Sousa S., Ens W., Standing K. G.,Wilkins J. A., and Krokhin O.V., (2007) Sequence-Specific Retention Calculator. A Family of Peptide Retention Time Prediction Algorithms in Reversed-Phase HPLC :

Applicability to Various Chromatographic Conditions and Columns. *Anal. Chem.*, **79**, 8762-8768.

Sterner J. L., Johnston M. V., Nicol G. R., and Ridge D. P., (2000) Signal Suppression in Electrospray Ionization Fourier transform Mass Spectrometry of Multi-component Samples. *J. Mass Spectrom.*, **35**, 385-391.

Sucic S., Paczkowski F.A., Runkel F., Bonisch H., and Bryan-Lluka L.J., (2002) Functional Significance of a Highly Conserved Glutamate Residue of the Human Noradrenaline Transporter. *J. Neurochem.*, **81**, 344-354.

Sucic B. L., Lesley J., (2007) Investigation of the Functional Roles of the MELAL and GQXXRXG Motifs of the Human Noradrenaline Transporter using Cysteine Mutants. *Eur. J. Pharmacol.*, **556**, 27-35.

Tanaka Y., Ikuya C., Kosaka I., Ikeda T., Toshihiko C., and Nakamura T., (2001) Identification of Human Liver Diacetyl Reductases by Nano-Liquid Chromatography/Fourier Transform Ion Cyclotron Resonance Mass Spectrometry. *Anal. Biochem.*, **293**, 157-168.

Tate C. G., (2001) Overexpression of Mammalian Integral Membrane Proteins for Structural Studies. *FEBS Lett.*, **504**, 94-98.

Teixeira-Clerc F. Michalet S., Menez A., and Kessler P., (2003) A Cysteine-Linkable, Short Cleavable Photoprobe with Dual Functionality To Explore Protein-Protein Interfaces. *Bioconjugate Chem.*, **14**, 554-562.

Tomizawa M., Maltby D., Medzihradszky K.F., Zhang N., Durkin K. A., Presley J., Talley T. T., Taylor P., Burlingame A. L., and Casida J. E., (2007) Defining Nicotinic Agonist Binding Surfaces through Photoaffinity Labeling. *Biochemistry*, **46**, 8798-8806.

Tomlinson I., Mason J., Burton J., Blakely R., and Rosenthal S., (2003) The Design and Synthesis of Novel Derivatives of the Dopamine Uptake Inhibitors GBR 12909 and GBR 12935. High-affinity Dopaminergic Ligands for Conjugation with Highly Fluorescent Cadmium Selenide/Zinc Sulfide Core/Shell Nanocrystals. *Tetrahedron*, **59**, 8035-8047.

Torres G.E., (2006) The Dopamine Transporter Proteome. *J. Neurochem.,* **97**, 3-10.

Torres G. E., Yao W, D., Mohn A. R., Quan H., Kim K. M., Levey A. I., Staudinger J., and Caron M.G., (2001) Functional Interaction Between Monoamine Plasma Membrane Transporters and the Synaptic PDZ Domain-containing Protein PICK1. *Neuron*, **30**, 121-34.

Torres G. E., and Amara S. G., (2007) Glutamate and Monoamine Transporters: New Visions of Form and Function. *Curr. Opin. Neurobiol.*, **17**, 304-312.

Torres G. E., and Caron M. G., (2005) Approaches to Identify Monoamine Transporter Interacting Proteins. *J. Neurosci. Meth.*, **143**, 63-68.

Torres G. E., Gainetdinov R.R., and Caron M.G., (2003) Plasma Membrane Monoamine Transporters: Structure, Regulation, and Function. *Nature Review; Neuro.*, **4**, 13-25.

Tran C. M., and Farley R. A., (1996) Photoaffinity Labeling of the Active Site of the Na+/K+-ATPase with 4-Azido-2-nitrophenyl Phosphate. *Biochemistry*, **35**, 47-55.

Tripet B., Cepeniene D., Kovacs J. M. Mant C. T., Krokhin O. V., and Hodges R. S., (2007) Requirements for Prediction of Peptide Retention Time in Reversed-Phase High - Performance Liquid Chromatography: Hydrophilicity/hydrophobicity of Side-Chains at the N- and C -termini of Peptides are Dramatically Affected by the End-groups and Location. *J. Chromatogr. A*, **1141**, 212-225.

Uhl G.R. and Lin Z., (2003) The Top 20 Dopamine Transporters Mutants: Structure-Function Relationships and Cocaine Actions. *Eur. J. Pharm.*, **479**, 71-82.

Unwin N., (2005) Refined Structure of the Nicotinic Acetylcholine Receptor at 4.ANG. Resolution. *J. Mol. Biol.*, **346**, 967-989.

Vaughan, R. A., (1998) Cocaine and GBR photoaffinity Labels as Probes of Dopamine Transporter Structure. *Method. Enzymol.*, **296**, 219-230.

Vaughan R.A., Gaffaney J.D., Lever J.R., Reith M., and Dutta A., (2001) Dual Incorporation of Photoaffinity Ligands on Dopamine Transporters Implicates Proximity of Labeled Domains. *Mol. Pharmacol.*, **59**, 1157-1164.

Vaughan R. A., Parnas M. L., Gaffaney J. D., Lowe M. J., Wirtz S., Pham A., Reed B., Dutta S. M., Murray K. K., and Justice J. B., (2005) Affinity labeling the Dopamine Transporter Ligand Binding Site. *J. Neurosci. Meth.*, **143**, 33-40.

Vaughan R.A., Sakrikar D.S., Parnas M.L., Adkins S., Foster J.D., Duval R.A., Lever J.R., Kulkarni S.S., and Hauck-Newman A., (2007) Localization of Cocaine Analog [^{125}I]RTI-82 Irreversible Binding to Transmembrane Domain Six of the Dopamine Transporter. *J. Biol. Chem.*, **282**, 8915-25.

Wagner S., Bader M. L., Drew D., and De Gier J.W., (2006) Rationalizing Membrane Protein Overexpression. *Trends Biotechnol.*, **24**, 364-371.

Watt D.S., Kawada K., Leyva E., and Platz M.S., (1989) Exploratory Photochemistry of Iodinated Aromatic Azides. *Tetrahedron Lett.*, **30**, 899-902.

Whitelegge J., Halgand F., Souda P., and Zabrouskov V., (2006) Top-Down Mass Spectrometry of Integral Membrane Proteins. *Expert Rev. Proteomic.*, **3**, 585-596.

Whitelegge J.P, Jewess P., Pickering M.G., Gerrish C., Camilleri P., and Bowyer J.R., (1992) Sequence Analysis of Photoaffinity-labelled Peptides Derived by Proteolysis of Photosystem-2 Reaction Centres from Thylakoid Membranes Treated with [^{14}C]azidoatrazine. *Eur. J. Biochem.*, **207**, 1077-1084.

Wirtz S., (2004) Identification of an MFZ 2-24 Affinity Labeling Site on the Human Dopamine Transporter, *Ph.D. Dissertation*, Emory University.

Witt M., Fuchser J., and Baykut G., (2003) Fourier Transform Ion Cyclotron Resonance Mass Spectrometry with NanoLC/Microelectrospray Ionization and Matrix-assisted Laser Desorption/ionization: Analytical Performance in Peptide Mass Fingerprint Analysis. *J. Am. Soc, Mass Spectr.*, **14**, 553-561.

Wu X. and Gu H.H., (2003) Cocaine Affinity Decreased by Mutations of Aromatic Residue Phenylalanine 105 in the Transmembrane Domain 2 of Dopamine Transporter. *Mol. Pharm.,* **63**, 653-658.

Wu C. and Yates J R., (2003) The Application of Mass Spectrometry to Membrane Proteomics. *Nat. Biotechnol.*, **21**, 262-267.

Emmet M., (2003) Determination of Post-translational Modifications of Proteins by High-Sensitivity, High-Resolution Fourier Transform Ion Cyclotron Resonance Mass Spectrometry. *J. Chromatogr.*, **1013**, 203-213.

Yamashita A., Singh S.K., Kawate T., Jin Y., and Gouaux E., (2005) Crystal Structure of a Bacterial Homologue of Na^+/Cl^--Dependent Neurotransmitter Transporters. *Nature*, **437**, 215-222.

Yamazumi K., and Doolittle R. F., (1992) Photoaffinity Labeling of the Primary Fibrin Polymerization Site: Localization of the Label to α -chain Tyr-363. *Proc. Nat. Acad. Sci. U.S.A.*, **89**, 2893-2896.

Zahniser N. R., and Sorkin A., (2004) Rapid Regulation of the Dopamine Transporter: Role in Stimulant Addiction? *Neuropharmacology*, **47**, 80-91.

Zabrouskov V., and Whitelegge J. P., (2007) Increased Coverage in the Transmembrane Domain with Activated-Ion Electron Capture Dissociation for Top-Down Fourier-Transform Mass Spectrometry of Integral Membrane Proteins. *J. Proteome Res.*, **6**, 2205-2210.

Zhang J., Li J., Xe H.,; Zhu Y., and He F., (2007) A New Strategy to Filter out False Positive Identifications of Peptides in SEQUEST Database Search Results. *Proteomics*, **7**, 4036-4044.

Zhang F., and Bartels M. J., (2004) Structural Analysis of Naphthoquinone Protein Adducts with Liquid Chromatography/Tandem Mass Spectrometry and the Scoring Algorithm for Spectral Analysis (SALSA). *Rapid Commun. Mass Spectrom.*, **18**, 1809-1816.

Zhang J., Li J., Xie H. Zhu Y., and He F. (2007) A New Strategy to Filter Out False Positive Identifications of Peptides in SEQUEST Database Search Results. *Proteomics*, **7**, 4036-4044.

Zhou Z., Zhen J., Karpowich N.K., Goetz R.M., Law C.J., Reith M.E., and Wang D., (2007) LeuT-Desipramine Structure Reveals How Antidepressants Block Neurotransmitter Reuptake. *Science*, **317**, 1390-1393.

Zhu N., Harrison A., Trudell M. L., and Klein-Stevens C. L., (1999) QSAR and CoMFA Study of Cocaine Analogs: Crystal and Molecular Structure of (-)-Cocaine Hydrochloride and N-methyl-3β -(p-fluorophenyl)tropane-2β-carboxylic Acid Methyl Ester. *Struct. Chem.*, **10**, 91-103.

Zou M.Z., Kopajtic T., Katz J.L., Wirtz S., Justice J.B., and Newman A.H., (2001) Novel Tropane-Based Irreversible Ligands for the Dopamine Transporter. *J. Med. Chem.*, **44**, 4453-4461.

Zou M.Z., Kopajtic T.m and Newman A.H., (2003) Substituted 3 -(Bis[4-fluorophenyl]methoxy)tropanes and (R)-2-Substituted 3-(3,4-Dichlorophenyl)tropanes at the Dopamine Transporter. *J. Med. Chem.*, **46**, 2908-2916.